All Master's Theses   Master's Theses

Fall 2020

Selective Synthesis of Trans-fused Lactam-Lactones by Vicinal Difunctionalization of Readily Affordable Allylic Lactams

Morgan J. Rodriguez
Central Washington University, morgan0714@yahoo.com

Follow this and additional works at: https://digitalcommons.cwu.edu/etd

Part of the Organic Chemistry Commons

Recommended Citation

SELECTIVE SYNTHESIS OF *TRANS*-FUSED LACTAM-LACTONES BY VICINAL

DIFUNCTIONALIZATION OF READILY AFFORDABLE ALLYLIC LACTAMS

_____

A Thesis

Presented to

The Graduate Faculty

Central Washington University

_____

In Partial Fulfillment

of the Requirements for the Degree

Master of Science

Chemistry

_____

by

Morgan J. Rodriguez

October 2020

CENTRAL WASHINGTON UNIVERSITY

Graduate Studies

We hereby approve the thesis of

Morgan J. Rodriguez

Candidate for the degree of Master of Science

APPROVED FOR THE GRADUATE FACULTY

11/01/2020

_____
Dr. Timothy Beng, Committee Chair

11/01/2020

_____
Dr. Levente Fabry

11/5/2020

_____
Dr. Carin Thomas-Bradley

_____

_____
Dean of Graduate Studies

ABSTRACT

SELECTIVE SYNTHESIS OF *TRANS*-FUSED LACTAM-LACTONES BY VICINAL

DIFUNCTIONALIZATION OF READILY AFFORDABLE ALLYLIC LACTAMS

by

Morgan J. Rodriguez

October 2020

With intrinsic versatility and an overwhelming presence in natural products, nitrogen- and oxygen-containing heterocycles boast a plethora of medicinal properties. Specifically, lactams and lactones are the respective luminaries of the antibiotic and flavor worlds. However, the synthesis of fused lactams-lactones, especially those bearing *trans*-fusion, is challenging from the standpoints of chemoselectivity, stereoselectivity, and regioselectivity. In this thesis, the highly-selective, cost-effective, and high-yielding conversion of readily affordable allylic lactams into *trans*-fused lactam-lactones by intramolecular vicinal difunctionalization is explored. The approach is highly divergent and requires only two steps, which bodes well for the construction of medicinally pertinent fragments. It is anticipated that the aforementioned merits of the methodology will endear it to both the medicinal and synthesis communities.

ACKNOWLEDGEMENTS

TABLE OF CONTENTS

LIST OF FIGURES

LIST OF SCHEMES

LIST OF SPECTRA

LIST OF SPECTRA (CONTINUED)

LIST OF SPECTRA (CONTINUED)

LIST OF SPECTRA (CONTINUED)

LIST OF SPECTRA (CONTINUED)

CHAPTER I

INTRODUCTION

1.1 Relevance of *N*-Heterocycles

Representing 59% of all small molecule drugs, *N*-heterocycles, or azaheterocycles, are a cornerstone in medicinal chemistry with their innate adaptability against several malignancies.[1] There is a wide variety of easily accessible azaheterocycles that diverge in their molecular geometry, rigidity, aromaticity, and increased heterofunctionalization. The beauty of diversity is the emergence of unique strengths; these differences reveal an array of bioactivities and featured presences in Food and Drug Administration (FDA)-approved pharmaceuticals. Classic *5-* and *6-*membered azaheterocycles dominate in this context. As seen in **Figure 1-1**, the piperidine motif, can be found in 72% of all *N*-containing small drugs and is the most common of the azaheterocycles.[2] Inspired by nature, many azaheterocycle moieties are found in bioactive isolates from plants, fungi, and animals. Azaheterocycles can be found in several sub-classes such as antihistamines, anesthetics, antidepressants, and antibiotics. The abundance of *N*-heterocycles comes as no surprise given their resemblance to the fundamental building block: the amino acid. Thus, the diverse utilities of azaheterocycles have attracted efforts towards novel bioactivities and synthetic applications.

Please note: This image has been redacted due to copyright concerns.

Figure 0-1. Top 24 azaheterocyclic motifs found in FDA approved pharmaceuticals
Reprinted from Vitaku, E.; Smith, D. T.; and Njardarson, J. T. Copyright 2014. *J. Med. Chem.*

1.1.1. Relevance of Lactams

The main interests and challenges are the development of accessible methodology that unveils unique and highly functionalized scaffolds. In particular, lactams serve as an intermediate towards other nitrogen-containing heterocycles, such as piperidines,[3] piperazines,[4] and morpholines.[5] Lactams are used for cooling compounds,[6] nylons,[7] and even as biosensors.[8] More importantly they are also plentiful in pharmaceuticals (**Figure 1-2**). Ring-fused Neophleghenrine A (**1**) was derived from *Phlegmariurus henryi* plant found in China and Vietnam. It is used for treating Alzheimers due to its reported anti-acetylcholineesterase (AcHe)

inhibitory activity, higher levels of which exist in the brains of such patients.[9] Clausenamides derived from the southeast Asian traditional medicine plant known as "wampee" have also been found to show anti-AcHe bioactivity.[10] A marine sponge produces a lactam known as Melophlin A that was shown to have anti-mycobacterial activity, the type of bacteria responsible for tuberculosis.[11] Ubrogepant was recently approved in December 2019 for the acute treatment of migraines (with and without aura) in adults and was developed by Allergan under license from Merck & Co. It is a potent, highly-selective, competitive receptor antagonist for calcitonin gene-related peptides, a vasodilatory neuropeptide involved migraine pathophysiology. Several coixspirolactams isolated from an Indian grass crop that has long been used in traditional Chinese medicine and prevails in current health foods were shown to have significant activity against human breast cancer cell lines adlay.[12]
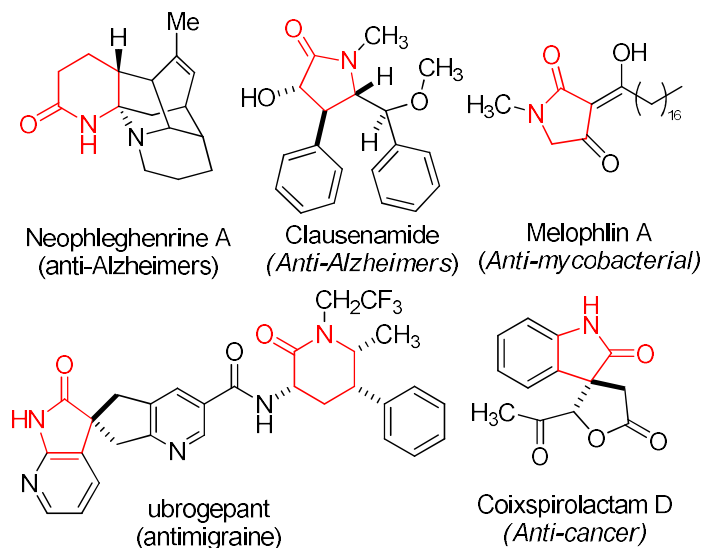
Figure 0-2. Examples of bioactive lactams

Despite the ubiquitous nature of both cyclic and acyclic amides in chemistry and biology, such moieties are lacking in **Figure 1-1**; only two lactams made it to the list. Alas, it may be attributed to the unique synthetic challenges that lactamization poses in contrast to other heterocycle syntheses. Currently, simple synthetic lactam production requires petrochemical

3

sources, very energy intensive processes, and harsh acidic reaction conditions that result in the production of large amounts of waste salts.[13] Another biological-chemical hybrid process uses microbial-produced precursors such as lysine, muconic acid, and adipic acid to form simple lactams (**Figure 1-3).**[13]

Please note: This image has been redacted due to copyright concerns.

Figure 0-3. Various biosynthetic pathways for lactams

Reprinted from Gordillo Sierra, A. R. and Alper, H. S. Copyright 2020 *Biotechnology Advances.*

Functionalized lactams can be synthetically achieved through cyclization reactions,[14] cycloaddition reactions,[15] organometallic-mediated reactions,[3] and other miscellaneous approaches such as radical processes.[16] However, given the electronic flexibility, many of these require costly transition metal catalysts, the use of many precursors, or several steps before lactamization occurs. Even *in vivo,* the lactamization step *en route* to penicillin requires a transition metal (**Figure 1-4**).[17] As more efficient syntheses are developed, there is a possibility that the lactam motif will rank higher.
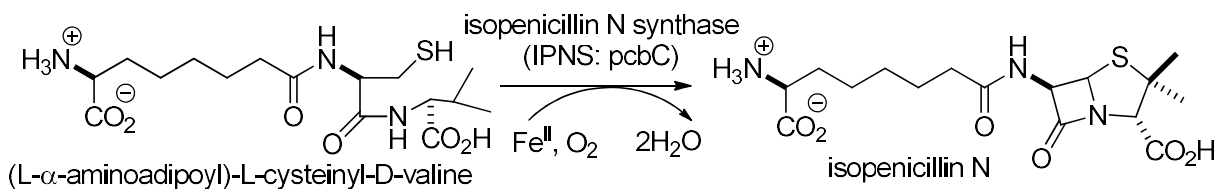
Figure 0-4. Lactamization step in natural penicillin biosynthesis

1.1.2. Relevance of Lactones

Lactones, the oxygen analogue of lactams, are similarly relevant in the medicinal and industrial world (**Figure 1-5**). As of 2018, Simvastatin, also known as Zocor™ was the 5th most prescribed drug in the U.S and it features a δ-lactone.[18] It targets HMG-CoA reductase, the rate-limiting enzyme of the cholesterol synthesis pathway.[19] Naturally derived from Feverfew, a plant found throughout the world, arises parthenolide which inhibits the IKKbeta kinase subunit involved in cytokine signaling, which is responsible for inflammation.[20] Oxandrolone, otherwise known as sold under the brand names Oxandrin or Anavar, is an androgen and anabolic steroid which is mainly used to help promote weight gain, medically as well as commercially by bodybuilders, often illegally as it is a controlled substance in many countries. It is also used to offset adverse effects caused by long-term corticosteroid therapy and to treat bone pain associated with osteoporosis. Off-label it is used to counteract wasting seen in HIV/AIDS patients and to aid recovery from severe burns[21]. Another lactone-touting drug, Warfarin competitively inhibits the vitamin K complex VKORC1, which results in the depletion of functional vitamin K reserves used in the synthesis of active clotting factors.[22] The γ-lactone known as spironolactone (or Aldalactone ™) binds to functions as an aldosterone antagonist which results in a diuretic effect in the kidneys.[23]

Figure 0-5. Examples of bioactive lactones

Given the novelty of both lactams and lactones, we seek to study the synthetic applications towards fused lactam-lactones and post diversification of the scaffold.

1.2 Frequently Encountered Challenges in Synthetic Organic Chemistry

The potential breakthrough discovery of other non-β-lactam analogues of β-lactam antibiotics as well as the under-charted territory of bicyclic *trans*-fused lactams (especially lactam-lactones) has sparked interest into the development of step-economical, cost-saving and high-yielding synthetic strategies for their construction and post-diversification in hopes of finding new bioactivities. But it is unsurprising, the lack of results in these fields, as the bane of every organic and medicinal chemist lies in selectivity. In general, three challenges are associated with the efficient construction of azaheterocycles: Chemoselectivity, regioselectivity and stereoselectivity.

1.2.1. Importance and Overcoming: Chemoselectivity

When two or more chemically active sites are present, chemoselectivity must be contended with as the reagent must be able to preferentially react with the intended functional group over the others. The other option is to protect any functional groups that may be affected, which increases cost and production time, sometimes dreadfully so. In other cases, protecting groups may not be sufficient, so synthetic routes may need to be planned to circumvent any selectivity issues. As such, chemoselective reagent systems have been developed to increase synthetic efficiency by removing the need to tiptoe around functional groups and instead directly targeting the desired site. One example of such a system is the $PPh_3 \cdot HBr$–DMSO-mediated one-step conversion of ketomethylene derivatives into flavones (**Scheme 1-1**). The work is significant because, not only is HBr or Br_2 with DMSO combined oxidative bromination known to react with olefins, but bromination of aromatics can also occur, and both are present in their starting materials (**1**). However, reaction at either of these sites is obviated by the employment of PPh_3, so instead, the alpha position of the carbonyl is oxidized (**2**). What is more impressive is that the alkene is alpha aryl, which further activates the external end of the olefin, yet it remains untouched.[24]
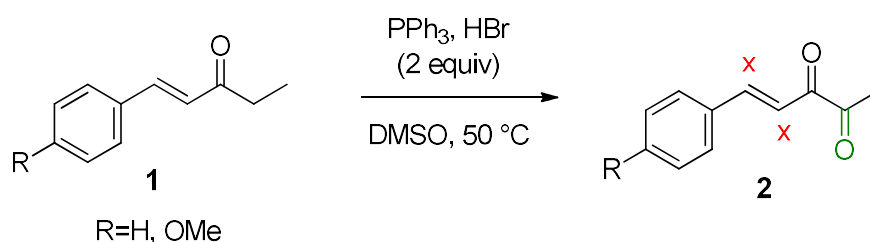
Scheme 0-1. Chemoselective conversion of ketomethylene derivatives into flavones

1.2.2. Regioselective Functionalization

Many functional groups have more than one active atom present, which poses another reactivity hurdle. Regioselectivity is defined as the site-selective addition of an unsymmetrical reagent to an unsymmetrical substrate. The most prevalent example is with unsymmetrical alkenes and alkynes, which have two sp^2 carbons that can be engaged in an Markovnikov or anti-Markovnikov. Sugars present a regioselective issue as they classically have multiple secondary alcohols, yet the one primary alcohol at C-6. One group produced a regioselective acylating reagent that astonishingly targeted the hydroxy of C-4 over the two other secondary alcohols at C-3 and C-2 (and, chemoselectively, the primary alcohol at C-6) with great regioselectivity ratios (**Scheme 1-2**).[25]
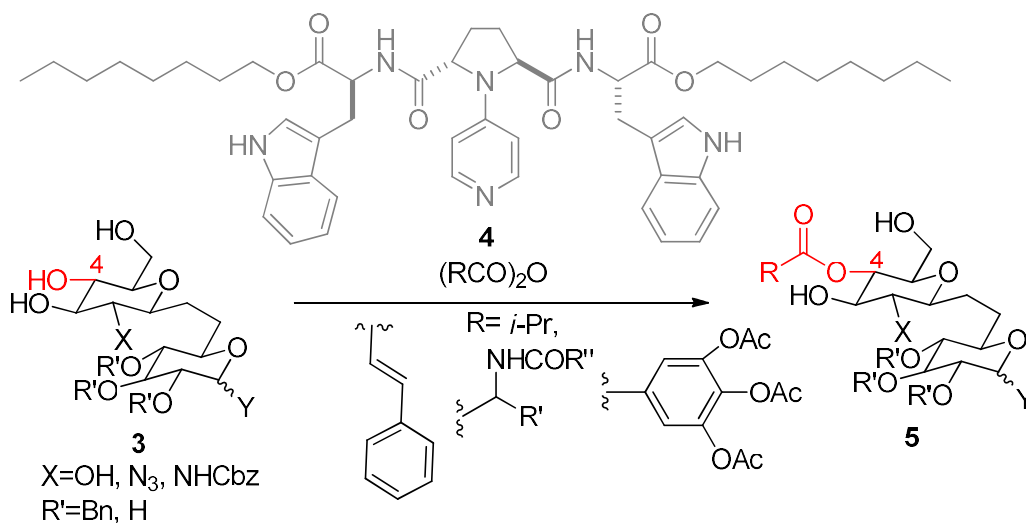
Scheme 0-2. Substrate controlled regioselective arylation of C-4 hydroxy

Another impressive transformation not only avoids arylation of the other susceptible functional groups, but also selectively difunctionalizes the alkene into an *exo* cyclized aryl-heterocycle; meaning in all examples, the internal end of the alkene was engaged for the cyclization while the external end was arylated (**Scheme 1-3**).[26] This occurred regioselectively

over the *endo* cyclization where the internal carbon would be arylated, which would have formed

six membered heterocycles.

Scheme 0-3. Regioselective dual arylation and cyclization of alkenes

1.2.3. Stereoselectivity and its Relevance in the Pharmaceutical Industry

The mantra in biochemistry that "structure equals function" becomes apparent when

considering the pharmaceutical effects of stereoselectivity. Stereo-, or enantio-selectivity refers

to the spatial-selective functionalization of molecules with same molecular formula and

connectivity. Steroselectivity is vital in pharmaceuticals because many drugs target enzymes

which have very specific electronics and physical shapes in their active sites to select for its

natural substrate over others—much like how non-keyless car ignitions not only need a

specifically shaped key but also the right coding to start the car. If an object has a similar enough

physical and electronic structure then the active site can be accessed, and much like car keys, the

spatial orientation matters along with the shape. Hence, biochemists will study the electronics

and shapes of target active sites and their substrates to build similar structures. However, unlike

car keys, a wrongly oriented drug structure can have devastating results. Currently, the FDA

requires pharmaceuticals to be at least 95:5 enantio- or diastereopure. The importance of

stereoselectivity can be seen in a variety of pharmaceuticals including ketamine,[27] thalidomide,[28]

albuterol,[29] and dobutamine[30] (**Figure 1-6**) wherein their enantiomeric counterparts are either

hazardous, inert, or of significantly different affinity to the active site.

Figure 0-6. Examples of stereocenter containing FDA approved pharmaceuticals

Ketamine features analgesic, anesthetic, and antidepressant effects and is present in two enantiomers that are both differently acting antagonists of the *N*-methyl-*D*-aspartate (NMDA) receptor. Esketamine, the (*S*) enantiomer, has up to an eight-fold higher affinity for NMDA receptors than arketamine[31] and is used as an intranasal treatment for major depressive disorder (MDD).[32] This seems odd given that arketamine showed higher and longer-lasting antidepressant effectiveness in animal models[33] while esketamine displayed more analgesic and anesthetic activity in human trials.[34] However, the interest in esketamine is in the decreased psychotomimetic and dissociative effects that were observed against the racemic mixture and pure arketamine. Subjects reported less drowsiness, lethargy, impairment of cognitive capacity, concentration capacity and primary memory loss.[35] It is clear that enantiomers must be considered as entirely separate entities in the pharmaceutical world where each one can have vastly different biological properties.

Considering that mechanisms can be influenced to proceed one way or another, but that the nature of mechanism itself cannot be altered, stereoselectivity becomes the greatest challenge in drug design. Such mechanisms may be swayed to target specific sites, but can they form the new functional group with the right spatial orientation and in good yield? Some mechanisms,

such as enolates[36], go through a planar intermediates where any preformed stereocenters risk chiral amnesia and attack at both faces can occur, leading to a mixture of products. Other mechanisms advantageously yield specific chiral relationships by virtue of the mechanism itself, as seen in halohydrin reactions of olefins,[37] which can either be advantageous or an issue. As such, the search for ideal stereoselective transformations has appealed to many organic chemists and has led to the discovery of high-yield reactions that give a single stereoisomer. A regio- and stereoselective $C(sp^3)$-$C(sp^3)$ bond forming bromolactonization was achieved using a BINOL derived catalyst. As seen in **Scheme 1-4**, Martin generates products bearing vicinal stereocenters such as **11** in highly diastereoselective arrangement from the tetra substituted alkenoic acid **9** and chiral ligand **10**.[38]
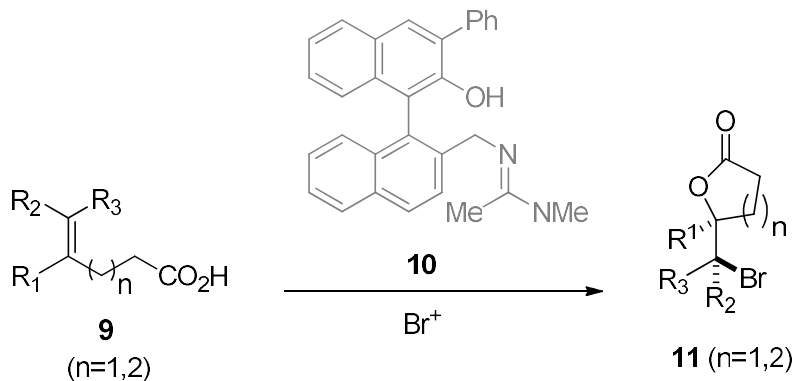
Scheme 0-4. Regio- and diastereoselective bromolactonization

1.3 Diversity-Oriented Synthesis

Diversity-Oriented Synthesis (DOS) in organic chemistry is a realm in which the various analogs of a central structural theme are investigated; this has become a popular path of research. Late-stage diversification is an appealing feat, because new medicinal effects may be found. This idea generally begins with highly affordable starting materials that act as the central building block. The goal is to produce selective methodology that alters the periphery of a molecular

skeleton in a variety of manners such that structurally similar compounds are made that subtly diverge in functionalities, size, and shape. The reverse approach is Target-Oriented-Synthesis (TOS), in which the aim is total synthesis of compounds with known merit (**Figure 1-7**). Although useful for the synthesis of natural products and drugs, as previously articulated, these structures need to be very structurally specific and enantiopure to be marketed. As such, the time commitment in the search for successfully selective transformations can be disheartening.
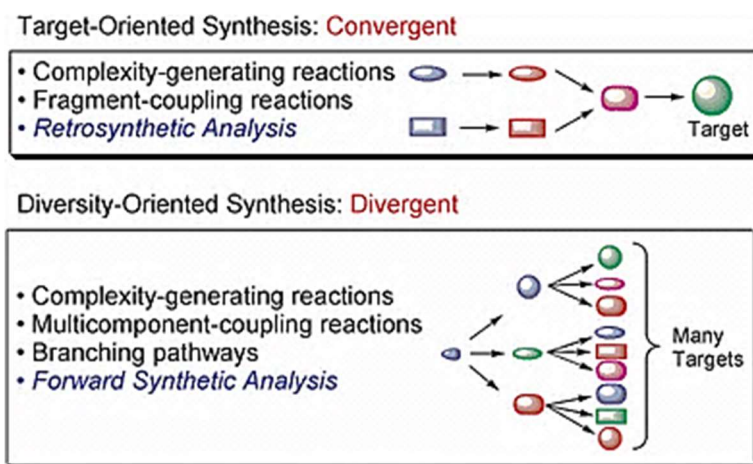
Figure 0-7. Comparison between TOS and DOS methods

One of the merits of DOS is that a variety of prevalent and highly coveted scaffolds found in pharmaceuticals are often studied as the backbones. Small molecules are an important research topic because they are versatile in synthesis, so TOS groups look to this research in search for their specific transformation of choice. Another virtue of DOS is the construction of a catalog of compounds that can be engaged in structure activity relationship (SAR) studies. Unfortunately, this is viewed as a blind, wasteful approach as it is possible no bioactivities will be discovered. The DOS method capitalizes on variety as it addresses how structure is related to activity.

1.3.1. Structure Activity Relationship (SAR) studies

One research group took a DOS approach on five different regions of a known anti-tumor

β-lactam as part of a SAR study on its tubulin colchicine targeting ability.[39] The authors were

investigating the effect of substitution phenyl ring or the presence of thiofuran in Region I, the

importance of 3,4,5-trimethoxyphenyl scaffold in Region II, the position of the -N_3 group on the

phenyl ring for Region III, the effect of a large group on the phenyl ring for Region IV, and the

importance of the H or the effect of a larger group for Region V.

In their first sets of derivatives, they varied the substitutions on phenyl groups at the C3,

C4, and C5 positions. First, they observed relatively lower antiproliferative activity in

derivatives lacking the 3,4,5-trimethoxyphenyl group at the N-1 position, indicating its

requirement for antiproliferative activity (Region II, **Figure 1-8**).
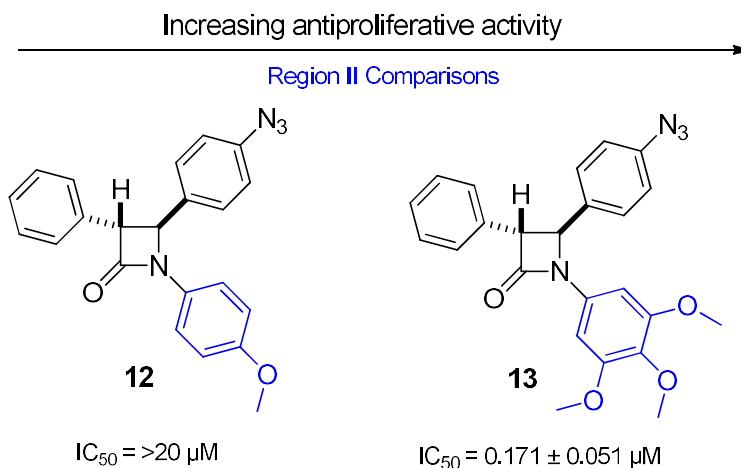
Figure 0-8. Comparison of inhibitory effects when varying Region II

Additionally, they discovered that substitution on the phenyl ring at the C3 position lost over 8-

fold activity against the growth of MGC-803 cells when the hydrogen atom was replaced with

the methoxy group (**12** vs **13**). However, this didn't matter much because when replacing the

phenyl with a thiofuran ring led to more of an increased activity (**Figure 1-9**).
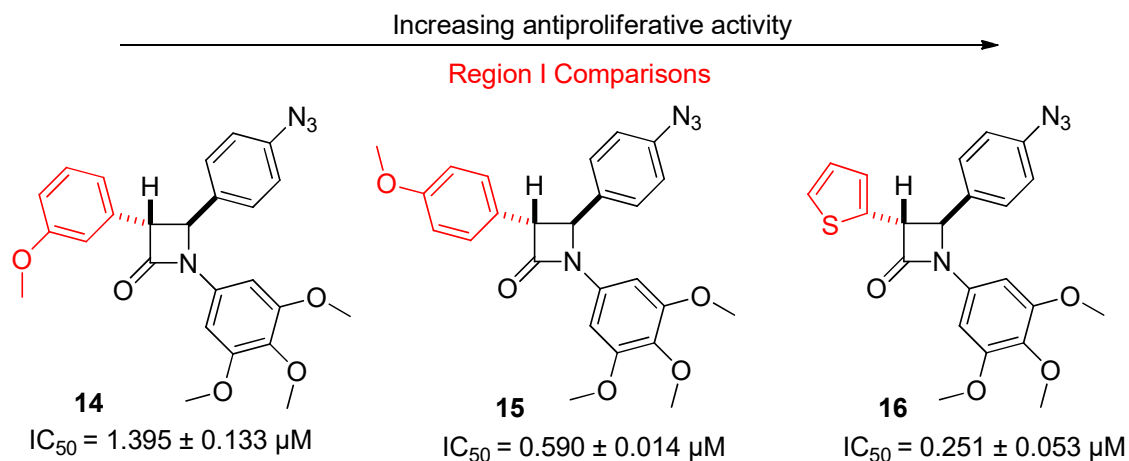
Figure 0-9. Comparison of inhibitory effects when varying Region I

When they explored the relationship between the location of azide group and its antiproliferative activity on the C-4 phenyl, they observed markedly better activity with *meta*-N_3 in **17** compared to *para*-N_3 in **18** (**Figure 1-10**).
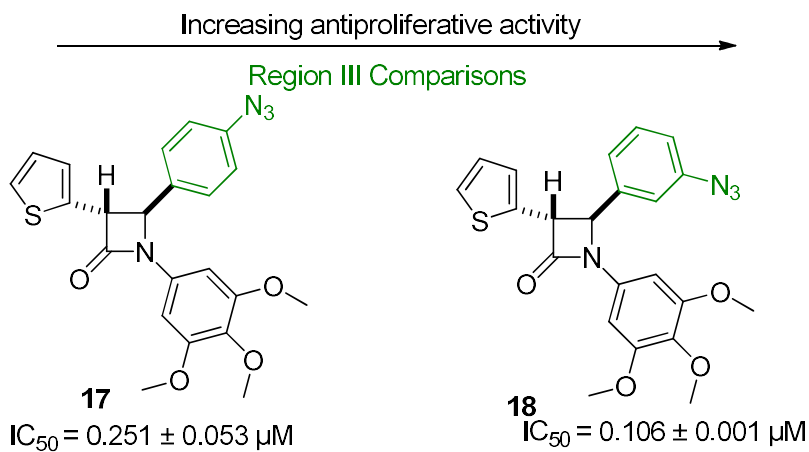
Figure 0-10. Comparison of inhibitory effects when varying Region III

Replace the azide with a large group, such as 1,2,3-triazole (**19** vs **20**), and its necessary inhibitory activity is completely lost, so the azide was proven to be required (**Figure 1-11**).
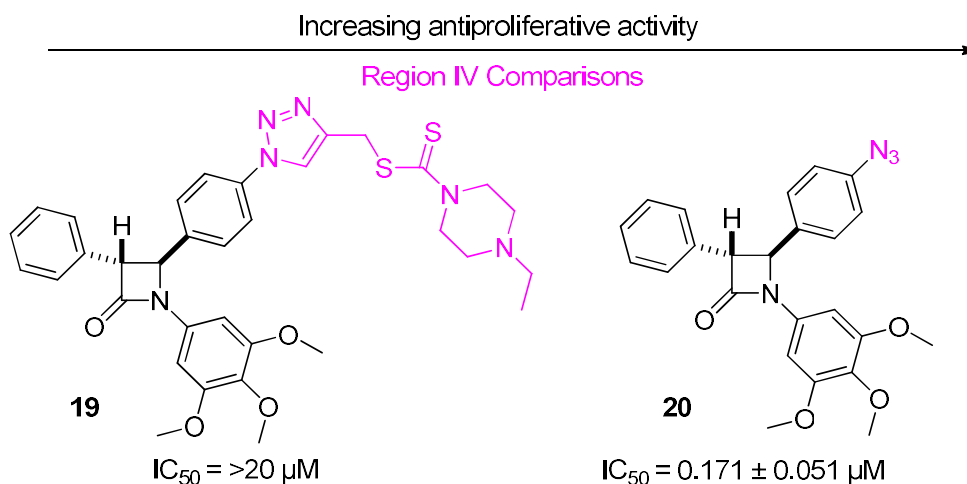
Figure 0-11. Comparison of inhibitory effects when varying Region IV

Since they recognized that a trifluoromethanesulfonyl moiety was an active group in some anticancer agents, they tried it for the *β*-lactam C-3 substituent (Region V), but unfortunately with no increase in antiproliferative activity (**Figure 1-12**).
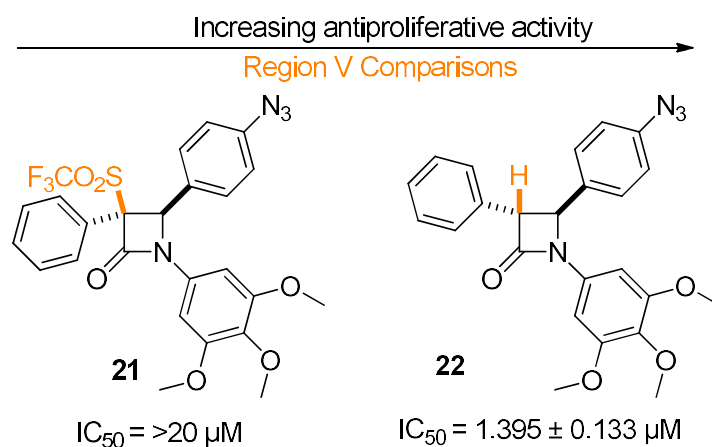
Figure 0-12. Comparison of inhibitory effects when varying Region V

Another group wrote a revealing article about the importance of SARs with respect to hepatoxicity of sympathomimetic amines.[40] It begins by reminding the community that such mimetics cannot be carelessly assumed to be interchangeable as they are often lumped together when considering their adverse effects after speculation arose on the toxicity of decongestant

1,3-dimethylpentylamine and the alkaloid ephedrine given their visual likeness amphetamines (**Figure 1-13**).
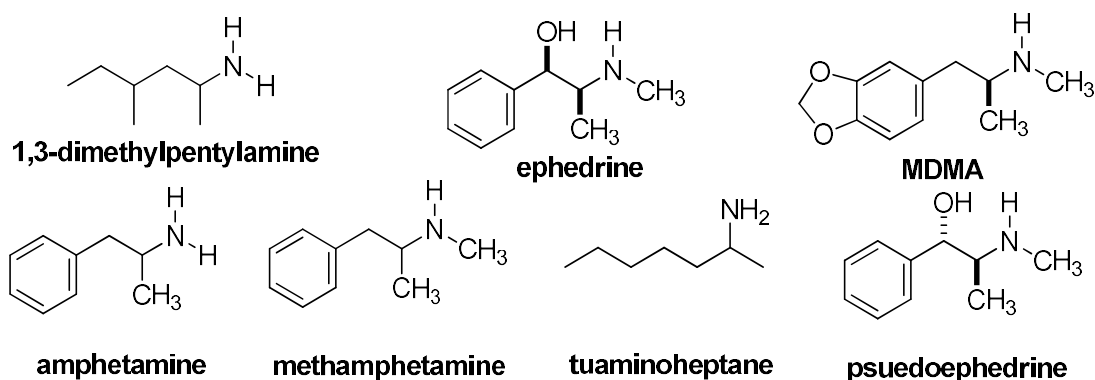
Figure 0-13. Comparison of illicit and pharmaceutical sympathomimetic amines.

MDMA, amphetamine and methamphetamine can cause liver injury via the production of reactive metabolites or neurotransmitter efflux. Amphetamine and MDMA hepatoxicity is proposed to be caused from the formation of a glutathione conjugate via aromatic hydroxylation, leading to glutathione depletion and oxidative stress. Lacking the necessary aromatic ring, compounds such as tuaminoheptane and 1,3-dimethylamylamine obviate this adversity. While pseudoephedrine and ephedrine have the aromatic ring, they apparently are not privy to aromatic hydroxylation in humans. Amphetamines work to increase efflux of neurotransmitters such as dopamine, serotonin and norepinephrine. 1,3-dimethylamylamine was inactive for dopamine and serotonin transporters but showed modest activity with norepinephrine transporters (K_i of 649 nmol). On the other hand, amphetamine and MDMA, possessed far more appreciable K_i values of 109 and 897 nmol; 5728 and 948 nmol; and 101 and 398 nmol, for the dopamine, serotonin, and norepinephrine transmitters, respectively. Hence, 1,3-dimethylamylamine is selective towards norepinephrine, unlike the other two amphetamines. These studies reflect how pharmacologically distinct each of these superficially similar sympathomimetic structures are.

1.4 Available Ring-forming Vicinal Difunctionalizations

Many transformations exploit the unsymmetrical nature of alkenes so two new functions are installed on both active carbons. More so, olefins are advantageous moieties that act as functional handles for intramolecular cyclization. These ideas have been combined, and the complexity of such a transformation usually requires catalysts to be selective.

1.4.1.Haloamination

Haloaminations resulting in piperidines have long been achieved for simple terminal alkenyl chloroamines[41]. The mechanism actually proceeds through a *5-exo* pathway, but the resulting 2-chloromethylpyrrolidine rearranges through an aziridinium ion to give the six membered product (**Scheme 1-5**). While copper chloride produced the highest yields, the highest *ee* was obtained using $CuPF_6$ with a TMEDA ligand.
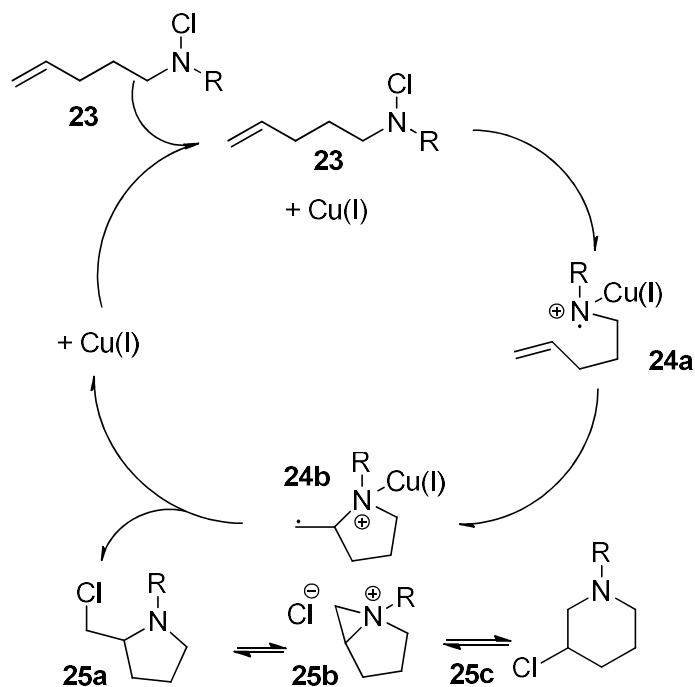
Scheme 0-5. Catalytic copper-mediated halocycloamination

1.4.2.Selenium-Mediated Halolactonization

Selenium has also been used to mediate halolactonizations with NBS (**Scheme 1-6**).[42] Simple δ-alkenoic acids with aromatic substitution on the internal carbon yielded *6-exo* lactones. The *7-endo* product was obviated due to the aromatic substituent on the internal end of the alkene stabilizing the brominium transition state in favor of the *6-endo* pathway.
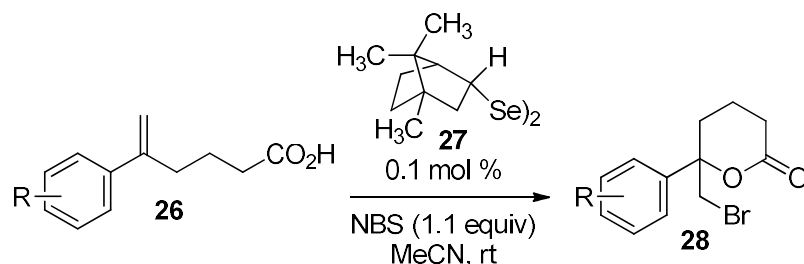
Scheme 0-6. Selenium mediated halolactonizations of δ-alkenoic acids

1.4.3. Thiotrifluoromethyl-lactonization/lactamization

One approach to vicinal functionalization that leads to lactamization/lactonization is mediated by trifluoromethylthiosaccharin which engages the alkene for the nucleophilic attack of the acid or amide, leaving behind a pendant thiotrifluoromethyl group. The transformation proceeds through a *5-exo* mechanism yielding γ-lactams (**Scheme 1-7**). However, the process struggles with enantioselectivity, with the highest *ee* reached at 23% when BINOL was used as a catalyst.[43]
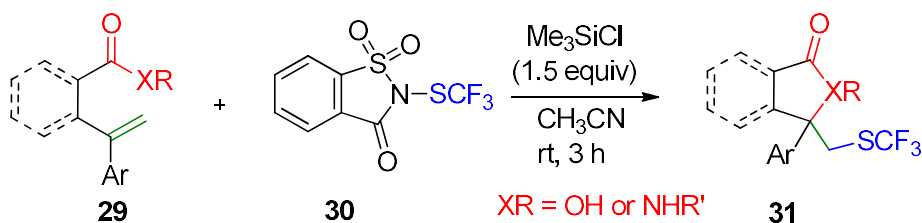
Scheme 0-7. Lewis Acid Mediated Difunctionalization

1.4.4. Aminolactonization

An elegant vicinal difunctionalization of alkenes resulting in *5-exo* intramolecular cyclization comes from Hemric et al. who achieved aminolactonization (**Scheme 1-8**).[44] The approach hinges on the use of an electrophilic amine source, which is unfortunately commercially unavailable and requires a multi-step synthesis.

Scheme 0-8. Aminolactonization with in-house produced *o*-benzoylhydroxylamine

1.4.5. Photoredox Catalyzed Alkylation/Lactonization

Another group achieved simultaneous alkylation and lactonization under blue light using Ir(ppy)$_2$(dtbbpy)PF$_6$ as a catalyst (**Scheme 1-9**).[45] Interestingly, the mechanism proceeds first by alkylation. Then, the resulting carbocation is hydroxylated and lactonization occurs via dehydration to yield the *6-exo* lactones of type **36**.
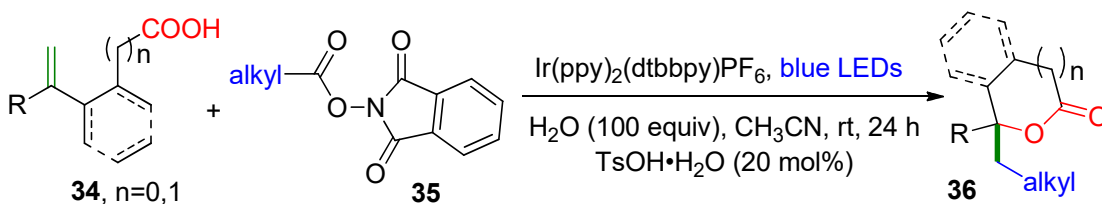
Scheme 0-9. Blue light and iridium catalyzed dual lactonization and alkylation.

1.4.6. Chlorolactonization with iodobenzene dichloride

Selective *6-endo* cyclizations have been achieved for methyl *o*-alkenylbenzoates (**Scheme 1-10**)[46] and is impressive because, usually, the *6-endo* pathway is only preferred when the electronics of the sixth carbon are stabilized by a pendant aryl group during the transition phase. This was achieved by employment of dichloroiodobenzene, a very expensive oxidative chlorine

source. Only the *6-endo* cyclized products were observed, but the authors are unsure if the reaction proceeds via a radical or ionic pathway, so no comment was provided as to why attack by the oxygen of the external end of the alkene occurs exclusively.
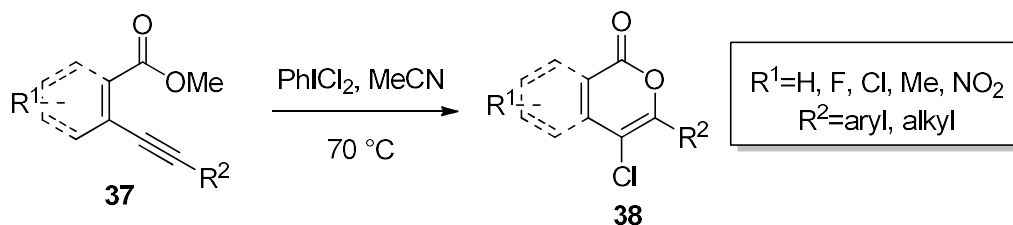
Scheme 0-10. Chlorolactonization of alkynoates

1.4.7. Enantioselective Bromolactonization with Phthalazine Catalysts

An enantioselective catalyzed bromolactonization of an alkene yields a spirolactone of type **42a** and could very well have cyclized into fused lactone **42b** with a different catalyst (**Scheme 1-11**).[47] Like the aforementioned Denmark method, NBS is used as the halogen source, yet this catalyst instead coordinates with the bromonium ion which drives the oxygen anion to engage the β-aryl position over the expected α-aryl.
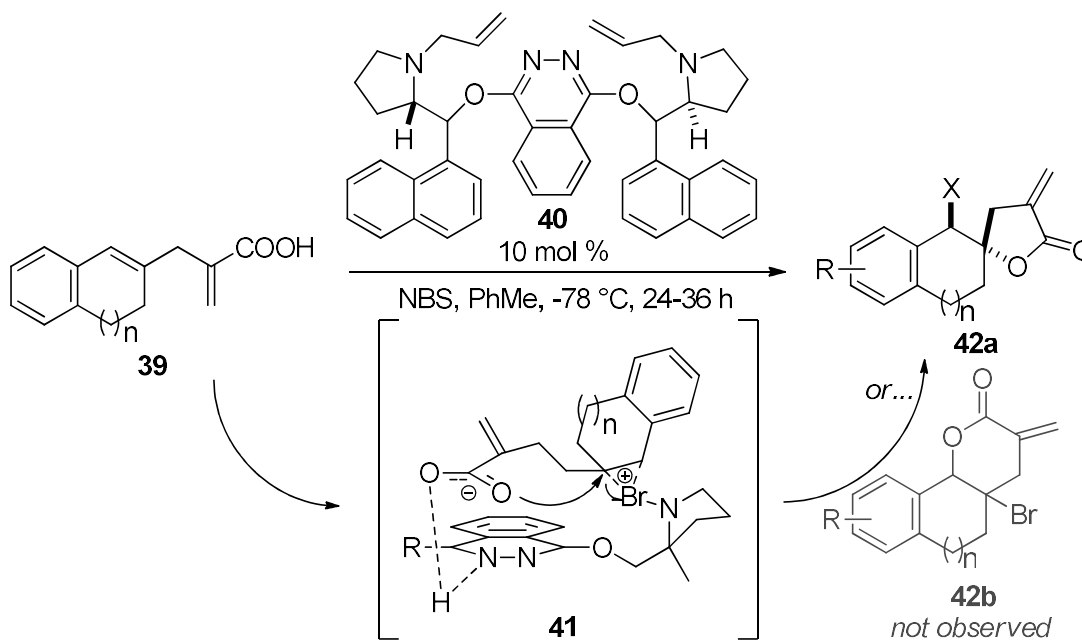
Scheme 0-11. Enantioselective halolactonization resulting in spirolactone

20

1.5 Current Approaches Towards Fused Lactam-Lactones

Aside from being overshadowed by the infamy of β-lactams, a search for *trans*-fused δ,δ-lactam-lactones yields no results, perhaps owed to the difficulty and uniqueness in their construction. Nevertheless, there are examples of lactams and lactones that have been *trans*-fused to other carbo- and heterocycles, as well as some reports of *cis*-fused lactam-lactones

1.5.1. Oxidative radical cyclization of α-amidomalonates

Oxidative radical reactions have been popular in the construction of carbon–carbon and carbon–heteroatom bonds as control over multiple stereocenters can be realized. Manganese (III) acetate has been employed to form an electron-deficient C-centered radical from both the malonate and its acidic α-hydrogen (**Scheme 1-12**).[48] The two radicals engage both carbons of the alkene, forming the classic lactam-lactone scaffold. However, chemo- and regioselectivity were issues; cyclization at the terminal end varied from 20-70% but was improved by protecting the amido nitrogen with *p*-methoxybenzyl group. Copper(II) triflate was also used to ameliorate this.
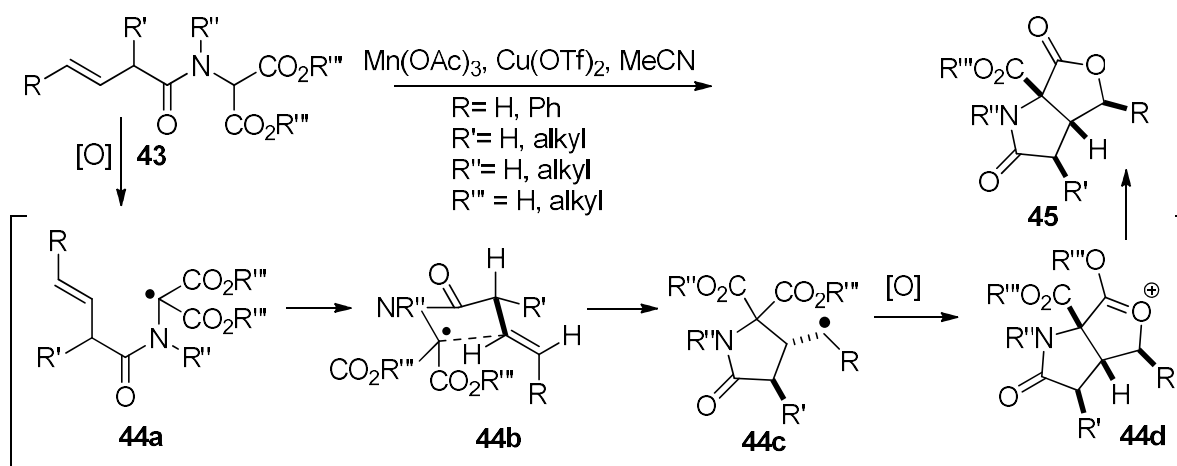
Scheme 0-12. Oxidative Radical Cyclization of α-amidomalonates

21

1.5.2. Expansion of β-lactams to form trans-*fused Lactam Bicycles*

Another method capitalizes on ring opening of a *β*-lactam to form *trans*-fused γ-lactams via intramolecular nucleophilic trapping of *N*-acyliminium intermediates (**Scheme 1-13**).[49] The driving cationic intermediate is generated via Lewis acid catalysis with AgBF$_4$ which mediates the dissociation of the chloro atom. This leads to the formation of tertiary carbenium ions that engage in an intramolecular rearrangement where the C3−C4 bond is opened and forms *N*-acyliminium ions that are trapped by the free hydroxyl to yield bicyclic γ-lactams. The diastereoselectivity is influenced by the sterics of the phenoxy or alkoxy substituent of the *N*-acyliminium moiety in their intermediates, giving *trans* isomers. They also propose that the ether group at the top face may have a conformational effect on the pentacycle, which could reduce the directing effect of the top face ether.
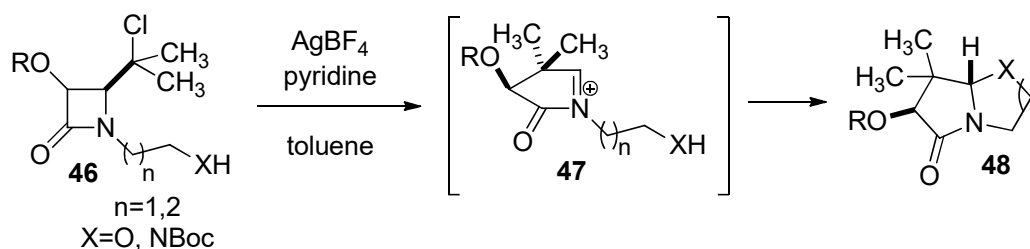
Scheme 0-13. Ring expansion of β-lactams yielding fused γ-lactones

1.5.3. Ugi Reaction with concommitant β-Lactamization

One group employed an Ugi reaction[50] with isocyanide **50** on γ-keto acid **49** to obtain their *trans*-fused γ-lactam which was subsequently methanolized to yield the 1,3-diol for lactonization (**Scheme 1-14**). The nitro group of the isocyanide was reduced and the formed aniline underwent diazotization and subsequent benzotriazole formation via a *5-endo-dig* cyclization of the amide. Finally, a catalytic amount of triethylamine engaged the amide with the *syn*-faced alcohol to form lactam-lactone **54**. Though spirolactonization was possible, the *cis*-

fused lactone may have been achieved because of that hydroxyl group being on the same side as the amide. However, the limitation of this methodology is that synthesis of γ-keto acid **49** requires 6 steps.[51]
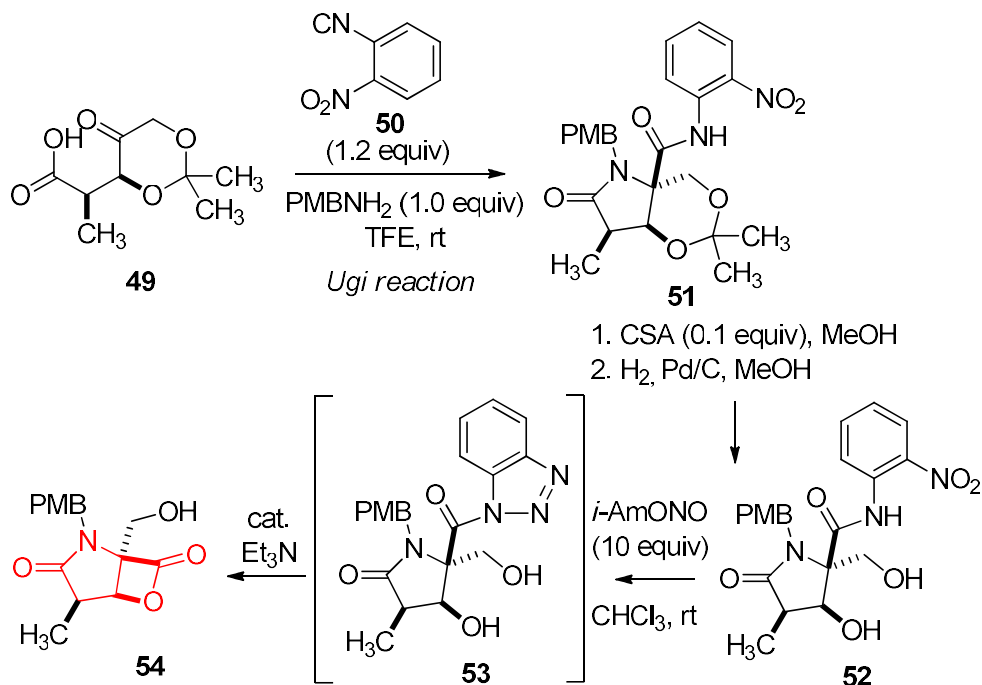
Scheme 0-14. Multistep synthesis of fused lactam-lactone

1.5.4. Rhodium Catalyzed Intramolecular Lactonization of Lactamoyl α-

Diazoacetates

Rather than utilizing a carboxylic acid or hydroxyl oxygen for annulation, one group instead opted for C-H insertion using 4- or 5-α-diazoacetoxylactams as their means for constructing fused lactam-lactones (**Scheme 1-15**).[52] The transformation occurred with a rhodium catalyst which was able to coordinate with the α-diazo group for regio- and stereoselective C-H insertion. The reaction struggles with competing dimer formation, however, and the diazoacetoxylactams of type **55** require a 6-step synthesis themselves.
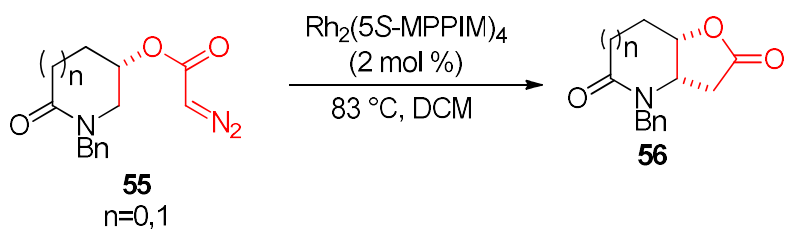
Scheme 0-15. Intramolecular Rh-catalyzed Lactonization of Lactamoyl Ester

1.6 Significance of Lactam and Lactone Chemistry

Throughout the paper, the varying applications of lactams and lactones have been briefly mentioned. Both scaffolds are prevalent in pharmaceuticals.

1.6.1. Relevance of Lactams

As seen in **Figure 1-14**, there are currently numerous examples of non-β-lactams featured in medicinal chemistry. In addition to the aforementioned commercially available pharmaceuticals, screening studies have produced lactams with a range of bioactivities, including antimigraine seen in **61** and antinausea effects in **62**.[54] Structure **63** was shown to be markedly stable in plasma as well as sporting anticoagulant effects *in vitro*.[55]
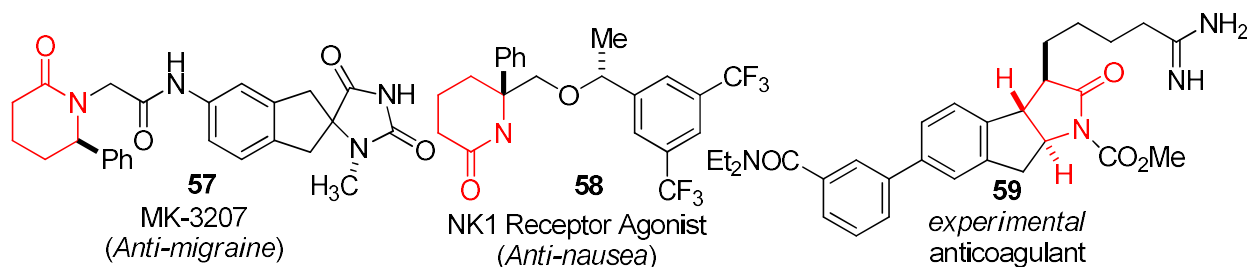
Figure 0-14. Bioactivities of several lactams

As common as infections are, the discovery of penicillin, the original β-lactam antibiotic derived naturally from *penicillium* fungi, rocked the world with its supreme antibacterial properties. Its discovery ushered in the most proliferative class of antibiotics that dominate the field: β-lactam antibiotics. This is for two reasons. First, considering the basic building blocks

that are amino acids, it becomes apparent that β-lactams are simply more readily available. One natural synthetic route involves lactamization via ATP-dependent adenylation of an *L*-Arginine substrate followed by intramolecular acyl substitution that is mediated by a β-lactam synthetase or, in other cases, a carbapenam synthetase (**Figure 1-15**). [56]
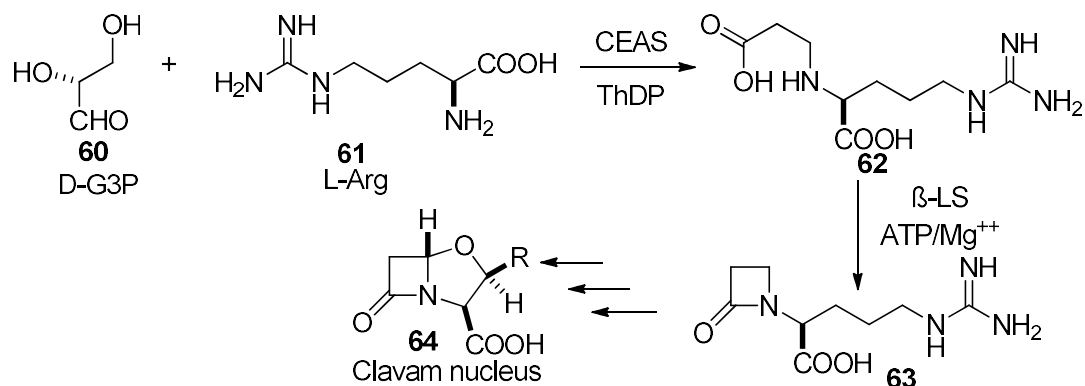
Figure 0-15. Natural production of β-lactams

In fact, the core structure of all penicillins and cephalosporins used clinically is manufactured naturally by fermentation.[57] The moiety is also synthetically achieved in the lab by electronically similar means.[58] Second, however peculiar the utility of these highly strained, 4-membered rings, it is, of course, this very peculiarity that brings its antibacterial advantage. In addition to physically accessing the active site of D,D-transpeptidase domains of Penicillin Binding Proteins (PBPs), the lactam must be able to acylate the nucleophilic serine hydroxy reside of the active site to form inert ester-linked complexes (**Figure 1-16**). PBP is, thus, detrimentally blocked so its natural substrates, the cell wall building blocks in which the antibiotics mimic, can no longer bind and cell death is initiated. This new ester-linked, acyl-enzyme complex then must resist both catalytic hydrolysis into an acid as well as reversibility back to the lactam, which would allow the PBP enzyme to continue building cell walls. Of course, lactam ring size is related to its reactivity, and apparently, β-lactams are not only excellent substrates for the acylation of serine, but also form stable acyl-enzyme complexes.[57]

Please note: This image has been redacted due to copyright concerns.

Figure 0-16. Mechanism of β-lactam antibiotics.
Reprinted from Wang, D. Y. et al. Copyright 2016 *Future Medicinal Chemistry*.[57]

1.6.2. Relevance of Fused Lactam-Lactones

Notably, the *trans*-lactam template has been found to be widely applicable to a number of serine proteases, such as human neutrophil elastase and human cytomegalovirus inhibitors, and are reported to be active intracellularly, stable in plasma, and orally active *in vivo*.[53] There are a handful of fused lactam-lactones in pharmaceuticals (**Figure 1-17**). Neooxazolomycin, a *cis*-fused lactam-lactone antibiotic drug, was discovered from a strain of *Streptomyces* by Uemura and co-workers in 1985, along with seven other structurally unique lactam-lactones. Remarkably, the structures presented diverse and robust antibacterial and antiviral activities in addition to *in vivo* antitumor activity.[59] Omuralide was first identified as a lactonized metabolite of a lactamyl structure found in a culture broth of a *Streptomyces* species. Cell permeable unlike its lactone-lacking predecessor, it targets proteasome 20S and inhibits its proteolytic activity. The proteasome has become a target for cancer therapy as it is responsible for the normal turnover of cellular proteins. Structurally related salinosporamide A, was actually isolated from a marine actinomycete bacteria, *Salinispora tropica*, is a more effective proteasome inhibitor and a promising anticancer drug.[60] Awajanomycin was found in marine fungus from Japanese sea mud and showed potent anticytotoxic activity against human adenocarcinoma cancer lines.[61]
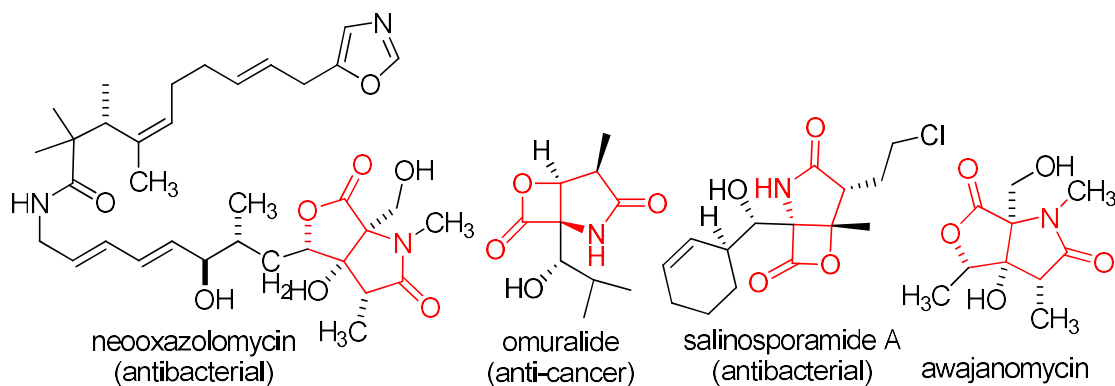
Figure 0-17. Examples of bioactive fused lactam-lactones.

Since fused lactam-lactones seem to be a rare moiety, they may be disregarded for commercial consideration. However, as drug targets become more complex and the emergence of alleged "undruggable targets" continues, i.e. protein− protein interactions and protein−DNA interactions, so too must drugs become more complex and contain a number of rigidifying (such as macrocycles, polycycles, olefins, etc.) and protein-binding elements. The lack of reported endogenous fused lactam-lactones in addition to synthetic SAR studies may very well be an oversight of the community. Considering the infancy of the technology and methodologies which have led to revolutionary medicine such as penicillin and its subsequent SAR studies that have helped to increase the life expectancy in the U.S. from 47 in 1900 to 77 today,[62] there is still so much to explore. We have only just begun, almost literally, dipping our toes into the sea of medicinal natural products. Thus, the lactam-lactone moiety becomes a perfect candidate for DOS combined SAR studies.

1.7 STATEMENT OF PURPOSE:

The specific aims of this thesis are as follows:

- Develop a modular and regio, chemo, and stereoselective protocol for the construction and post-diversification of *trans*-fused lactam-lactones.

- Explore the efficacy of various substrates in performing intramolecular cyclizations on acid bearing allylic lactams by vicinal functionalization of the alkene.

- Empirically and semi-empirically investigate the fate of cyclization with respect to regioselectivity.

DIRECT ACCESS TO *TRANS*-FUSED LACTAM-LACTONES BY
STEREOSELECTIVE AND REGIODIVERGENT HALOLACTONIZATION OF ALLYLIC
LACTAM ACIDS

2.1 Introduction

When the large-scale resistance to the β-lactam core structure developed with the
bacterial evolution of β-lactamases in the 1980s, γ-lactams became the focus of antibiotic
research. The outlook was promising since γ-lactams show similar pyramidal distortions around
the amide bond to those of β-lactams, which has been associated with antibacterial activity.[63] Of
course, the challenge was that lactam ring size is related to the reactivity of the amide, and both
features are crucial in their mechanism of action. However, multiple Structure-Activity-
Relationship (SAR) studies revealed that the larger, five-membered structures screened struggled
either with mainly hydrolysis at the active site[64] or the inability to acylate the target.[65] Currently,
there are only a handful of non-β-lactam antibiotics acting with the same mechanism (**Figure 2-
1**).
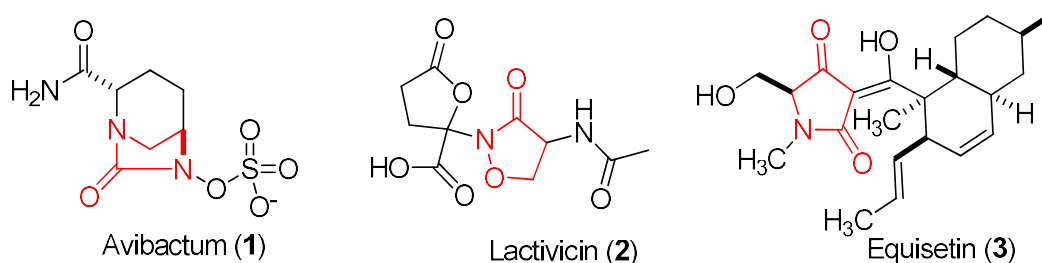
Figure 2-1. Examples of non β-lactam antibiotics acting with the same mechanism

Intriguingly, a more recent comparison of lactam ring size with respect to hydrolytic
stability concluded that the six-membered lactam is a superior approach towards the
development of novel lactam anti-infectives given its comparable hydrolysis rate to the β-

lactam.[64] Presumably, the δ-lactam is favorable due to the formation of a tetrahedral intermediate that causes the ring to adopt a notably stable, chair conformation during the rate limiting step of acylation; hence it becomes more likely to remain intact and inhibiting the penicillin binding protein (PBP). Fittingly, there has been renewed interest in finding viable non-β-lactam antibiotics to combat β-lactamase resistance, especially as new synthetic routes to the lactam core structure are discovered alongside mechanistic, and energetic insights into their formations and lability.

More exclusive than individual lactams are polycyclic lactams which can be found in many natural products and pharmaceuticals exhibiting novel biological properties. For one, nearly all the famed β-lactam antibiotics are fused lactam bicycles, including those seen in the cephem and penam moieties, the 4th and 8th most common drug moieties previously featured in **Figure 1-2**. Fused *trans*-5,5-bicyclic lactams have been shown to have antiviral activity against human cytomegalovirus[65] and hepatitis C.[53] The fused lactam-lactone motif consequently unveils more bioactivities, wielding anti-cancer activity as seen in Omuralide (**4**), Salinosporamide A (**5**), Awajamycin (**6**), and Neoxazolomycin (**7**). Although literature searches reveal these seem to be the extent of relevant bioactive of fused lactam lactones, likely owing to their synthetic difficulty and unique scaffold, bicyclic lactam-lactones are useful as chiral building blocks in alkaloid synthesis.[52]
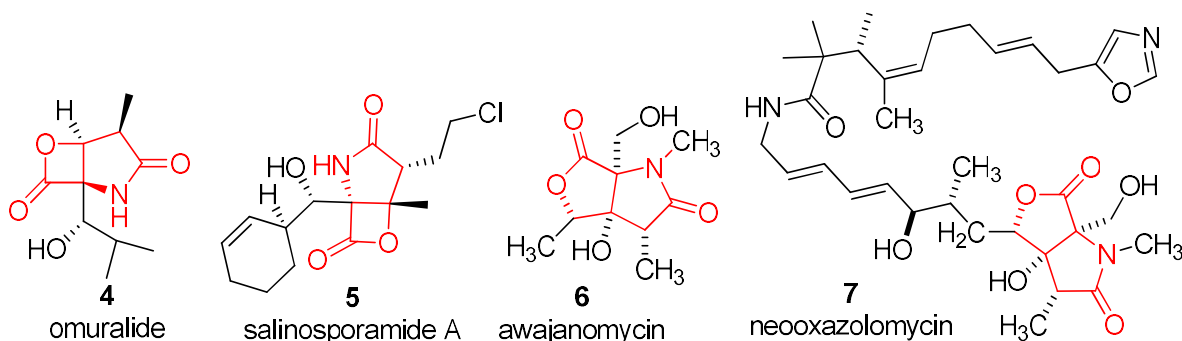
Figure 2-2 Examples of bioactive fused lactam-lactones

There are several ways in which fused lactam-lactones can be constructed; of the most straightforward, one can begin with a lactam and install the lactone functionality or vice versa. As outlined previously, methods of constructing fused lactam-lactones include an impressive one-step lactonization-lactamization of an alkenyl α-amidomalonate using manganese (III) acetate in an oxidative radical process,[48] an Ugi reaction between an isocyanide and a γ-keto acid followed by methanolization preceding lactonization,[50] and the employment of rhodium catalysts to achieve a C-H insertion from lactamoyl α-diazo esters.[52] However, these syntheses both require several steps just to create the starting materials, and thus present time and cost issues.

The present study seeks to achieve halolactonizations of γ-alkenoic lactamoyl acids by utilizing the pendant alkene in vicinal difunctionalization. Among the many methods for the construction of common-ring lactones,[66] halogen-initiated cyclization of unsaturated carboxylic acids is a valuable and direct approach for the stereoselective synthesis of halogenated lactones.[67,68,69] Another advantage is the increased versatility that comes with the generated halogen and lactone motifs that can be engaged in late-stage diversification. A variety of intramolecular additions across π-bonds that yield fused lactones have been reported: trifluoromethylthiosaccharin mediated trifluoromethyl-lactonization,[43] blue light and Ir(ppy)$_2$(dtbbpy)PF$_6$ catalyzed alkyl-lactonization,[45] and halolactonizations with diiodobenzene.[46] However, the transformations required fanciful and uneconomical design to side-step regioselectivity or diastereoselectivity issues largely with the goal of attaining a specific conformation, otherwise such selectivity issues were limitations of the design. The present study seeks to achieve CCR-derived lactone-fused lactams bearing four stereocenters with great selectivity in less than 3 steps.

A modular and cost-economic transformation, the Castagnoli-Cushman reaction (CCR) of imines to cyclic anhydrides presents well-designed access to vicinally functionalized azaheterocycles. The transformation is attractive in that it utilizes feedstock chemicals such as aldehydes, amines and anhydrides, it is very diastereoselective, and builds a highly functional scaffold begging for SAR studies. This reaction was initially applied to reactive cyclic anhydrides such as homophthalic anhydride.[70] However, several anhydrides are now amenable to CCR methodology, including succinic anhydride,[71] sulfone- and cyano-substituted succinic anhydrides,[72,73] glutaric anhydride,[74] diglycolic and thiodiglycolic anhydrides,[75] as well as benzannulated adipic anhydride.[76]

The successful reaction of various anhydrides with 1,3-azadienes to yield vicinally functionalized allylic lactam acids of type **8**, (**Figure 2-3A**) is the major focus of our group.[77,78] We previously reported the synthetic utility of the lactam unit resident in **8**, in Vilsmeier-Haack reactions.[79] Importantly, successful bicyclizations through the construction of pentannulated lactams such as **8a1**[80] and dihydropyran-fused lactams of type **8a2**[81] from CCR-derived allylic lactam acids (**Figure 2-3A**) served as motivation for us to explore halolactonization. Given our prior success with CCR methodology,[77–81] the emergence of β-lactam-antibiotic resistant bacteria, and the true novelty of 6-membered fused lactam-lactone chemistry, we became interested in questioning the fate of **8** in halolactonization (**Figure 2-3B**). Halolactonization was selected as the mode of reactivity for the lure to stereospecifically install the two new chiral centers across the π-bond to yield sp^3-rich fused lactam-lactones bearing a halogen functional handle and bearing four contiguous stereocenters. Starting from simple commodity chemicals such as amines, enals, and anhydrides, the regioselective and scalable construction of these modular lactam-fused lactones is achievable in only two synthetic manipulations. We anticipate

33

that such a cost-effective strategy would undeniably expand the 3D-structural realm for the unearthing of new small molecules with medicinal value. We are not oblivious to the fact that stereoselective halolactonization of γ-alkenoic acids have been well-studied. However, the prior reports suggest that electrophilic halogenating reagents preferentially produce γ-butyrolactone products with exocyclic halomethyl substituents in moderate-to-high diastereoselectivities.[82–88] Particularly, extensive studies by Denmark and coworkers on simple γ-alkenoic acids found that 5-*exo* halolactones were predominantly observed (**Figure 2-3C**).[89]

Figure 2-3. (A) Previous work on CCR-derived adducts, (B) Proposed halolactonization of CCR adducts with NXS, (C) Existing halolactonization report

2.2 Results & Discussion

The study was initiated by subjecting lactam acid **8a** to the reaction conditions described in **Scheme 2-1**, using *N*-iodosuccinimide (NIS). Although previous reports suggest that *trans*

alkenes with external aryl substitutions would encourage *6-endo* regioselectivity,[82–89] the

uncertainty of whether the system would react *5-exo* or *6-endo* and to what ratios was still

intriguing given the constraint of being fused to the lactam. Another advantage is for

diastereoselectivity, since the carboxylic acid is forced by its parent ring to attack only from one

side and halohydrin reactions proceed through a planar transition state, leaving one available

configuration for the two new stereocenters. However, it was unsure whether the epimerization

would occur during the course of the reaction. Intriguingly, after 2 h, lactam-lactone **9a** was

obtained in good yield. To great delight, the *5-exo* product **16** was entirely evaded. Given the

method's striking success, various structural iterations of the lactamoyl acid were interrogated to

determine substrate scope (**Scheme 2-1**). The regio-/diasteroselectivity and yields were

challenged by modulating three different features; the class of heterocycle, the alkene's aryl

substituent, and various *N* substituents. In select cases, the variations did cause minor effects on

diastereomer ratios, but the overall transformation proved to be exceptionally modular and

economical in yield and selectivity. *Gem*-dimethylated piperidines are ubiquitous in the

pharmacopoeia. As of 2017, 3.7% FDA-approved drugs in the US contained the *gem*-dimethyl

group.[90] Medicinal chemists have widely explored the *gem*-dimethyl group in developing

bioactive molecules because of the possibility to (1) decrease toxicity, (2) obtain improved drug

metabolism and pharmacokinetic profiles, (3) moderate the pKa of vicinal functionalities, (4)

bring symmetry into a monomethyl substituted chiral center, (5) increase target engagement,

potency, and selectivity, and (6) apply the Thorpe−Ingold conformational effect to achieve

difficult ring-forming transformations.[91] Given all these advantages, it was another thrilling

discovery to find that *gem*-dimethylated lactam-lactones **9k/l** are obtainable in synthetically

attractive yields. Vicinally functionalized chiral pyrrolidinones are present in many alkaloid

natural products and pharmaceuticals, including pramanicin (antifungi), salinosporamide A (anticancer), omuralide (proteasome inhibitor), clausenamide (antidementia), and lactacystin (proteasome inhibitor). Gratifyingly, several pyrrolidinones were demonstrated to be amenable to selective halolactonization, giving rise to 5,6-bicycles such as **9m-r**. As more medicinal chemists become privy to exploring 3D-structural space, bicyclic morpholines are being viewed as valued targets for pharmaceutical companies. Fittingly, our halolactonization method is applicable to potentially fragile morpholinone acids, affording bicyclic morpholines such as **9s-w**. This level of modularity and generality is impressive seeing as expanding reactivity trends across various *N*-heterocycles is usually not a straightforward task.

Activation of the pendant aryl group was predicted to likely be the most influential variable, since it directly affects the electronics of the targeted *sp²* carbon, yet regio- and diastereoselectivity were virtually unphased and yield slightly increased. More basic *N*-alkyl substituted lactams are also competent substrates in this mode of reactivity (*e.g.,* **9h–j** and **9o–r**).

Finally, we have found that less reactive *N*-bromosuccinimide (NBS) reacts similarly to NIS. However significantly less reactive *N*-chlorosuccinimide (NCS) failed to react under the identified conditions.
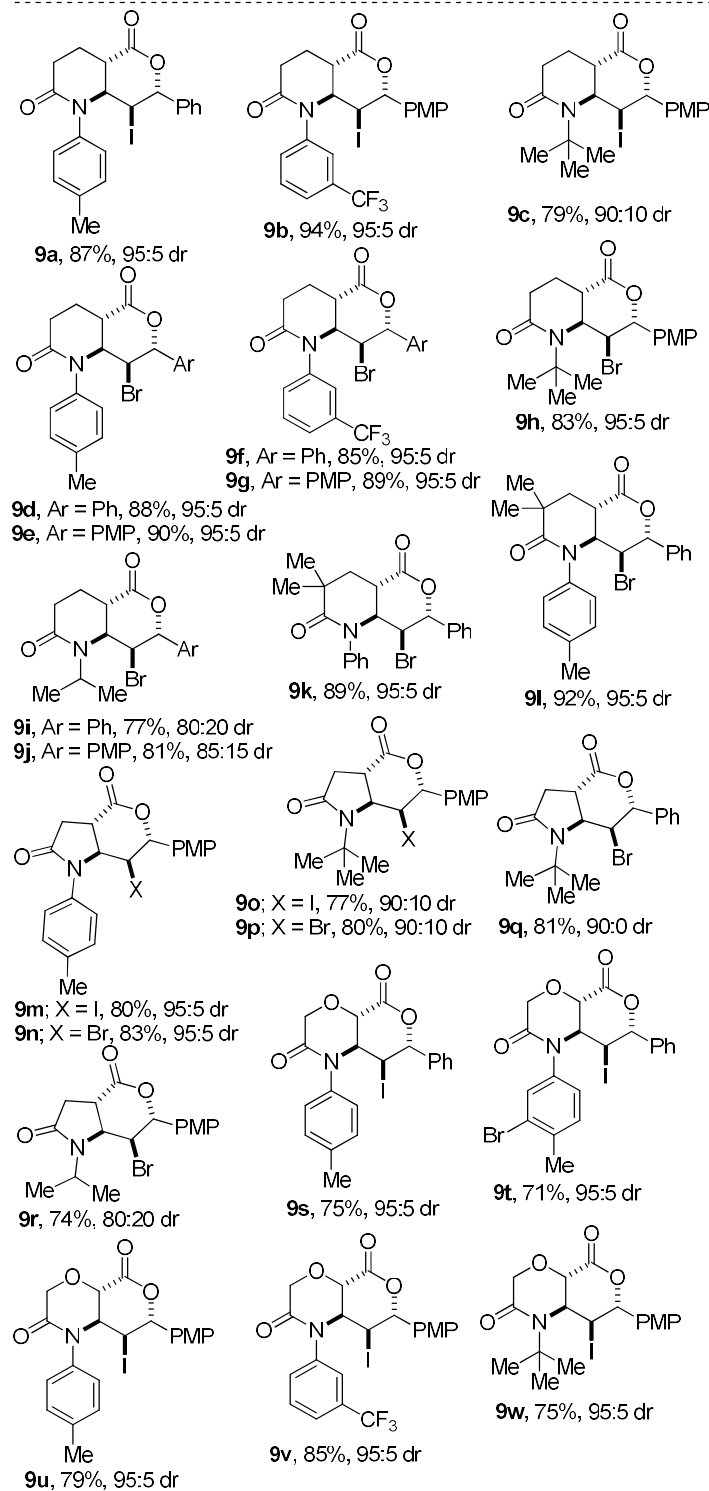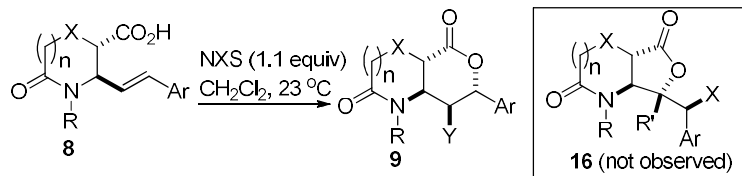
Scheme 2-1. Scope of halolactonization of various allylic lactam acids

After successfully constructing a library of lactam-fused lactones from disubstituted alkenoic acids, we next sought to explore the amenability of trisubstituted alkenoic acids in the same mode of reactivity. We reasoned that such substrates would allow for unambiguous assignment/confirmation of the *6-endo* regioisomers through NMR analysis. Perhaps more enticing was the prospect of installing a medicinally attractive tetrasubstituted halogen-bearing stereocenter, which could in turn be converted to an all-carbon quaternary center following a C–C cross-coupling event. As depicted in **Figure 2-4**, the use of a trisubstituted alkene was expected to directly illuminate the difference between the 5-*exo* and 6-*endo* cyclization products (*i.e.,* **16c** and **17c**). We know that the most downfield sp^3-hybridized carbon is the oxygen-bearing stereogenic carbon (see red arrow in **16c** and blue arrow in **17c**). The DEPT-135 NMR spectrum (which only shows hydrogen-bearing carbons) of **16c** is not expected to have a resonance between 80 and 100 ppm. On the other hand, the DEPT-135 spectrum of **17c** is expected to show the presence of a hydrogen-bearing sp^3 carbon centered between 80 and 100 ppm. The DEPT-135 spectra depicted in **Figure 2-4** clearly show the presence of a methine around 90 ppm in the case of **17c**. Importantly, as expected, 5-*exo* product **16c** (which was prepared through an independent route) does not show any DEPT-135 signals between 80 and 100 ppm. This result clearly indicates that the 6-*endo* cyclization product is the major regioisomer in these studies.
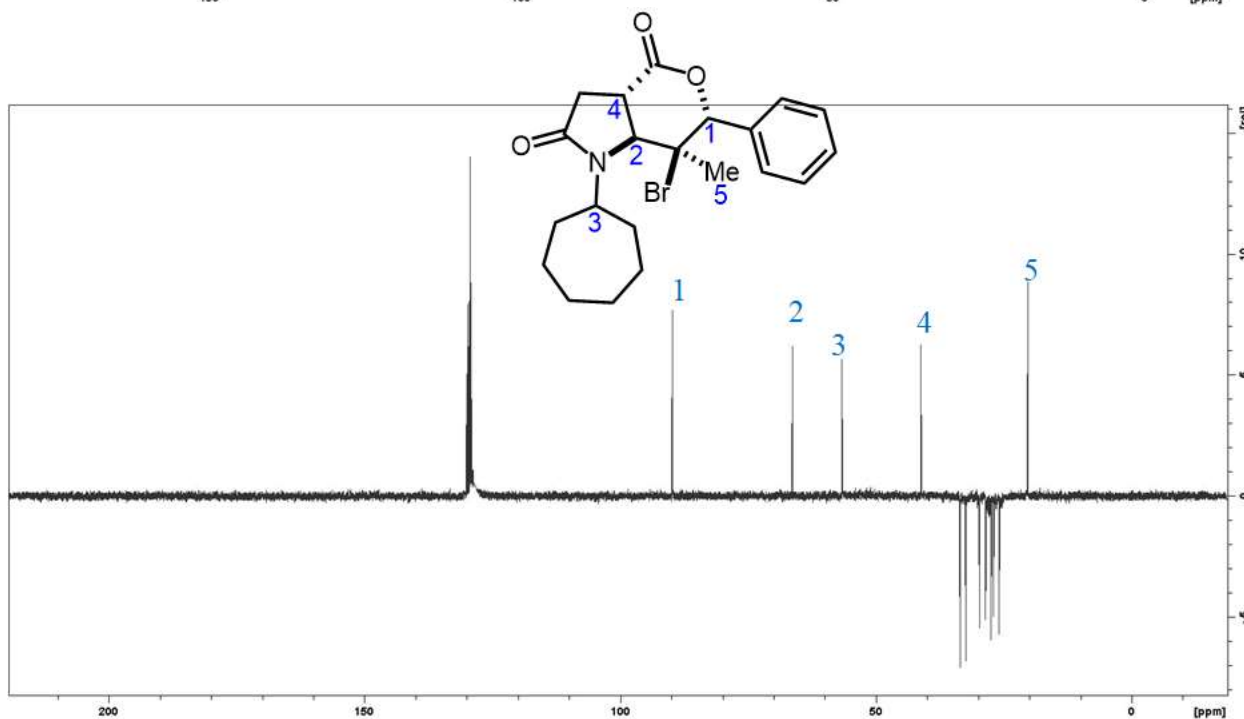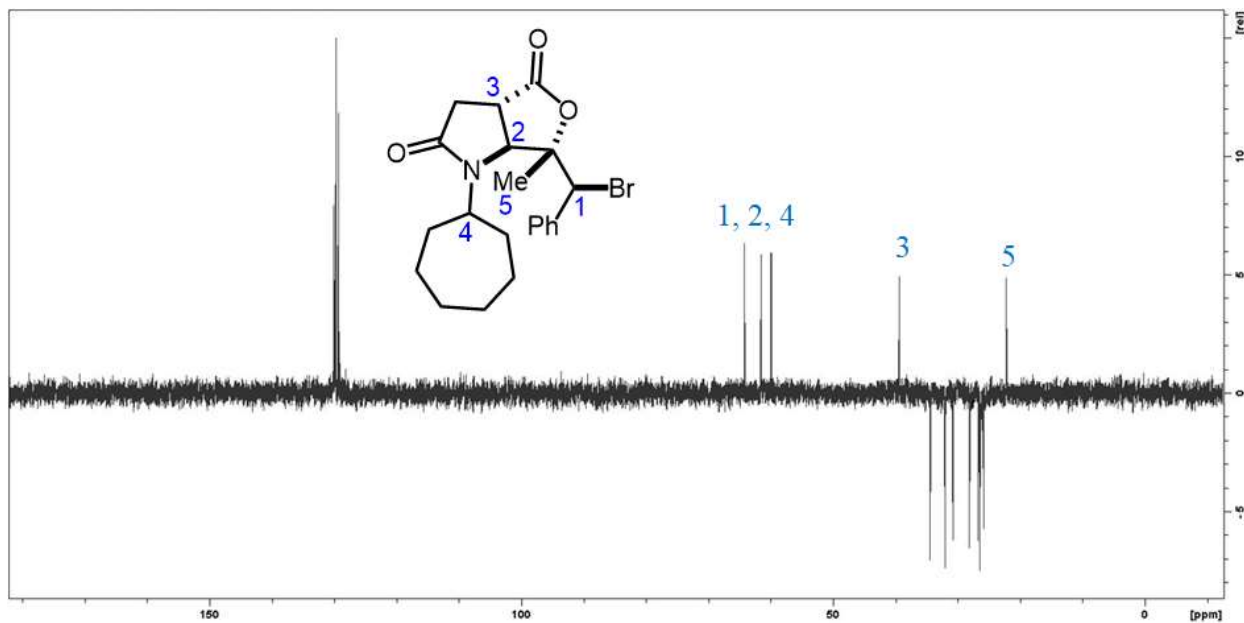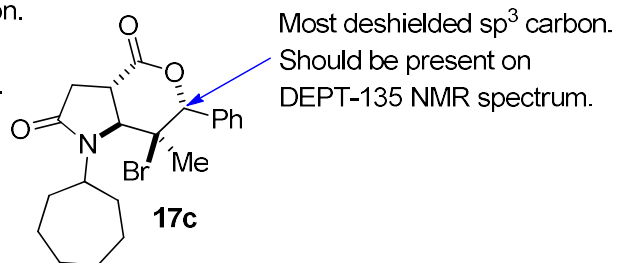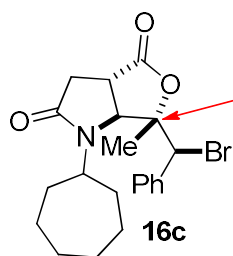
Figure 2-4. Differentiation of 5-*exo* and 6-*endo* cyclization products by DEPT-135.

As shown in **Scheme 2-2**, the chemoselectivity of the bromolactonization was challenged by a competing allylic *N* substituent with an added temptation of closer proximity of the second alkene with the butyrolactam. With great satisfaction, the conversion of the second alkene was obviated and the *6-endo* product (**17d**) still triumphed and with high diastereoselectivity. Comparable yields and diastereomer ratios were attained with the methyl substituted structures. Impressively, a lactam-lactone bearing two tetrasubstituted stereocenters has been constructed in high diastereoselectivity (**17e**).
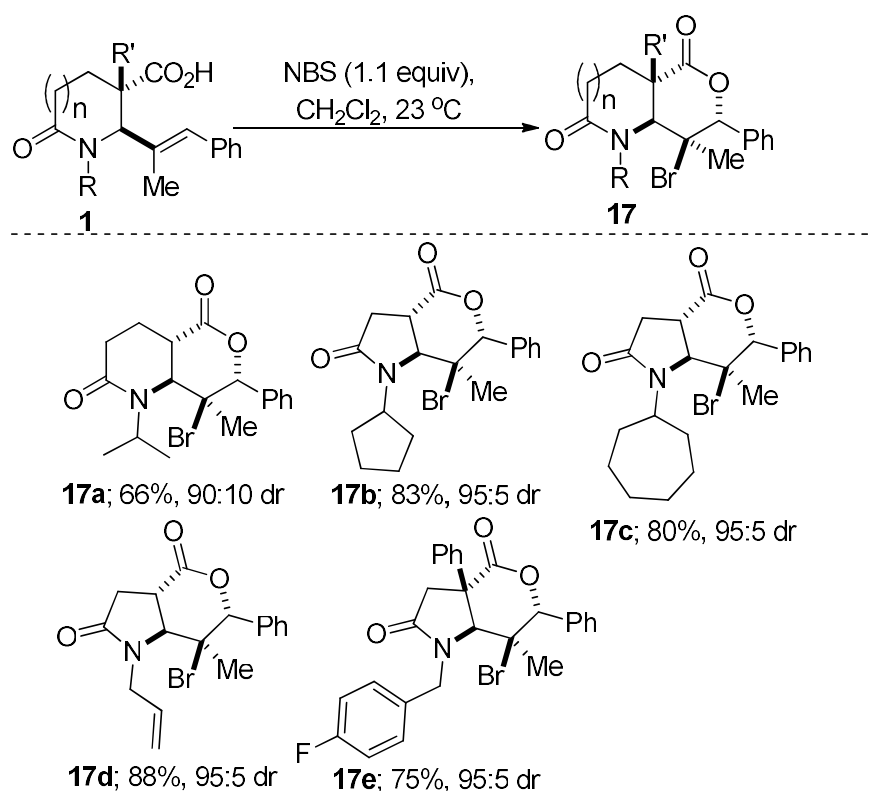
Scheme 2-2. Halolactonization of trisubstitued γ-alkenoic acids.

The success of the halolactonizations sets the stage for post-diversification studies. For example, the bromine may be used as a functional handle. It was demonstrated that bromides **9d/f** undergo SN2-style amination to yield **18a/b** (**Figure 2-4**). Of note, these amination products could serve as precursors to coveted β-amino alcohols such as **19**. Such β-amino

alcohols are abundant in natural products and are well-known building blocks for the preparation of complex molecules and are useful ligands and auxiliaries for asymmetric synthesis.[92] The scaffold is also resident in bioactive molecules such as ephedrine and pseudoephedrine (**Figure 1-13**). We have found that chemoselective addition of methylmagnesium bromide to the lactone motif present in **9h** furnishes bromohydrin **20**.
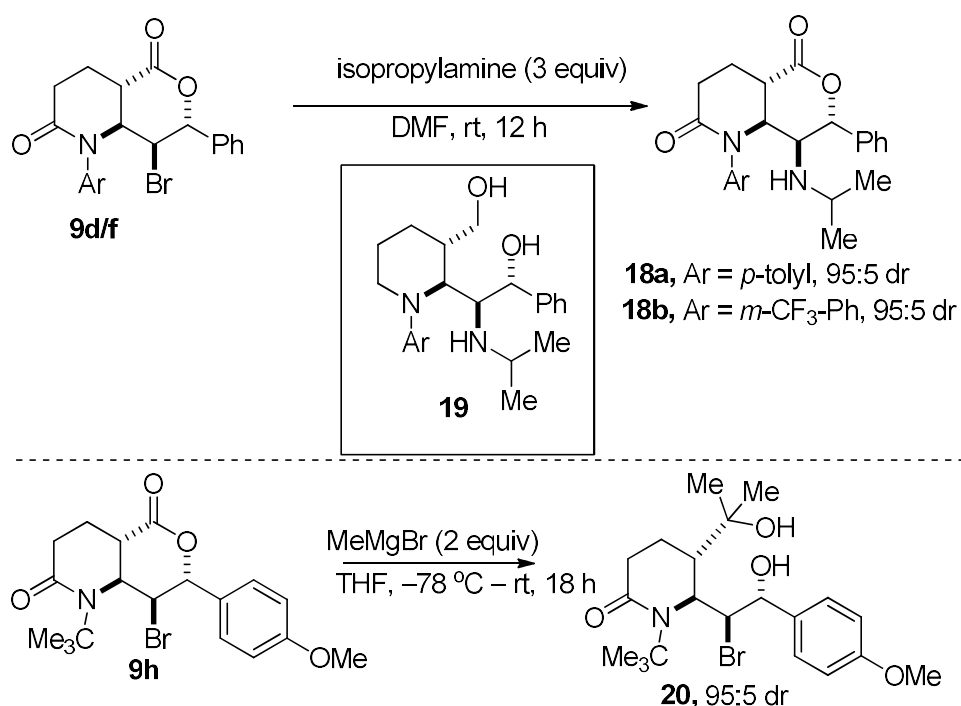
Figure 2-5. Post-diversification of fused-lactam-halolactone products

One of the inherent limitations of this methodology is the incompatibility of certain anhydrides with 1,3-azadienes. Highly reactive anhydrides such as homophthalic anhydride have the propensity to form the Tamura product over the Castagnoli-Cushman product, when treated with 1,3-azadienes. In these cases, the alkene instead of the imine undergoes formal cycloaddition.[93] As such, the scope is limited to certain enolizable anhydrides. The current observations suggest that the halolactonization step is heavily biased towards *6-endo* cyclization due to the stability provided by the pendant aryl group in the transition state of the external

carbon (**Scheme 2-2**). More studies are required to see if the regioselectivity can be influenced by alternative systems, especially those where the styrenyl motif is replaced by an unactivated alkene.
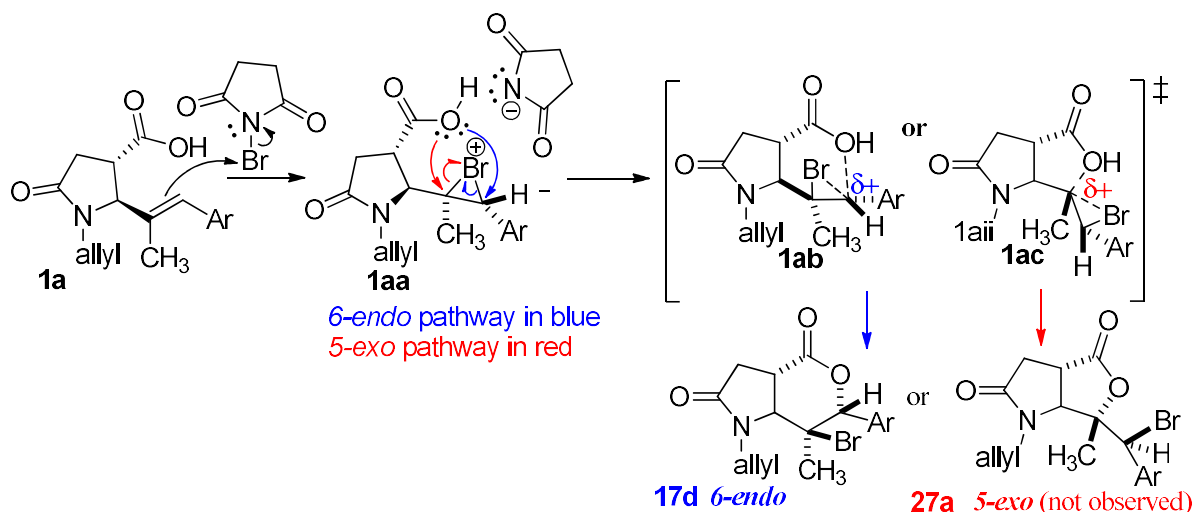
Scheme 2-2. Suggested mechanism of halolactonization

2.3 Conclusion:

The results successfully demonstrate that halolactonizations of CCR-derived, γ-alkenoic lactam acids represent a highly chemo-, regio-, and diastereoselective, and economical route towards *trans*-fused lactam-halolactones. Aside from the magnificent selectivity that was demonstrated, the other merits of this transformation are that it obviates the need for costly starting materials and hazardous catalysts. Rather, the impressively modular scaffold is achieved with readily affordable starting materials in less than three steps under straightforward methods. The wide applicability and efficiency of the transformation presents an opportunity for SAR studies on such a system, especially as medicinal chemists begin exploring 3D space and deviating from the saturated β-lactam chemistry. Post-diversification of the lactam-lactones suggests that β-amino alcohols are within appreciable reach. Lastly, the fate of cyclization in the

context of *6-endo vs 5-exo* is currently being explored with using computational methods to better illuminate the tunability of the reaction. These results will be disclosed in due course.

2.4 Methods: General Procedure

An inert atmosphere of nitrogen and freshly distilled solvents were employed for air and moisture sensitive reagents. Silica gel (230-400 mesh) column chromatography was performed. Thin-layer chromatography (TLC) was performed using Silicycle SiliaplateTM glass backed plates (250 μm thickness, 60 Å porosity, F-254 indicator) and visualized using UV (254 nm) or KMnO$_4$ stain. CDCl$_3$ was used as a solvent at room temperature for ^{1}H, ^{13}C, and DEPT-135 NMR spectra. Chemical shifts are quoted in parts per million (ppm).

2.4.1.General Procedure A: Synthesis of 1,3-azadienes

A mixture of *trans*-cinnamaldehyde (10 mmol) and the desired primary amine (1-2 equiv) was prepared in benzene (50 mL). Magnesium sulfate (2 g) was added and stirred at room temperature. The suspension was monitored daily for aldehyde consumption using ^{1}H-NMR. The mixture was filtered and concentrated under reduced pressure to afford 1,3-azadienes such as **10**.

2.4.2.   General Procedure B: Synthesis of γ-Alkenoic Lactamoyl Acids

A 5 mL screw-cap vial was flame-dried and molecular sieves (5 Å) were added. In the vial, solution of the 1,3-azadiene (1.0 mL, 0.10 M in freshly distilled toluene) was added followed by the anhydride (1 equiv) at room temperature and then warmed in a pre-heated oil bath measured at 100 °C. After total conversion of the 1,3-azadiene (as indicated by TLC and NMR), the mixture was cooled to room temperature, washed several times with petroleum ether, and then concentrated under reduced pressure to yield crude lactamoyl acids.

2.4.3.General Procedure C: Halolactonization of γ-Alkenoic Lactamoyl Acids

A 5 mL screw-cap vial was flame-dried, evacuated, and flushed with nitrogen. The *N*-halosuccinimide (1.1 equiv) was added to the vial, sealed with a rubber septum, and placed under nitrogen atmosphere. A solution of the γ-alkenoic lactamoyl acid (1.0 mL, 0.10 M in anhydrous dichloromethane) was added to the vial at room temperature. After complete consumption of the lactam acid (as judged by TLC and NMR), the mixture was quenched with sodium sulfate, then washed with ethyl acetate and brine. The product was concentrated under reduced pressure and purified under silica flash chromatography to afford the fused lactam-lactones.

2.5 Peak Assignments

2.5.1. Valerolactams

i. *Peak Assignment for **9a***

Prepared from acid **8a** (335.4 mg, 1.0 mmol) and NIS (247.5 mg, 1.1 equiv) using General Procedure C. Time = 2 h. Purification: Flash chromatography on silica eluting with hexane/EtOAc (75:25). Yield = 401.1 mg, 87%. ^{1}H NMR (400 MHz, Chloroform-*d*) δ 7.51 – 7.34 (m, 3H), 7.25 – 7.08 (m, 4H), 6.96 – 6.88 (m, 2H), 5.92 (d, *J* = 1.9 Hz, 1H), 4.34 (t, *J* = 2.3 Hz, 1H), 3.32 (td, *J* = 12.2, 2.7 Hz, 1H), 3.11 (dd, *J* = 11.8, 2.7 Hz, 1H), 2.9 – 2.61 (m, 3H), 2.37 (s, 3H), 2.15 – 1.94 (m, 1H). ^{13}C NMR (101 MHz, CDCl₃) δ 169.7, 169.1, 146.2, 138.9, 138.0, 134.5, 129.9, 129.5, 129.3, 129.0, 128.7, 128.3, 127.7, 124.8, 119.2, 86.2, 55.6, 43.3, 34.2, 32.5, 29.8, 29.6, 21.2, 20.8. Chemical Formula: $C_{21}H_{20}INO_3$ Exact Mass: 461.0488 g/mol

ii. *Peak Assignment for **9b***

Prepared from acid **8b** (419.4 mg, 1.0 mmol) and NIS (247.5 mg, 1.1 equiv) using General Procedure C. T = 20 °C, time = 2 h. Purification: Flash chromatography on silica eluting with hexane/EtOAc (75:25). Yield = 470.1 mg, 94%. ^{1}H NMR (400 MHz, Chloroform-*d*) δ 7.57 – 7.54 (m, 1H), 7.48 (t, *J* = 7.9 Hz, 1H), 7.38 (dt, *J* = 8.0, 1.6 Hz, 1H), 7.15 (s, 1H), 7.03 (d, 2H), 6.88 (d, 2H), 5.8 (d, *J* = 2.1 Hz, 1H), 4.18 (t, *J* = 2.1 Hz, 1H), 3.79 (s, 3H), 3.32 – 3.18 (m, 2H), 2.72 – 2.58 (m, 3H), 2.08 – 1.87 (m, 1H). ^{13}C NMR (101 MHz, CDCl₃) δ 169.5, 168.9, 160.0, 137.9, 133.0, 130.7, 129.7, 126.0, 124.8, 124.7, 114.9, 85.0, 55.5, 55.3, 43.1, 33.9, 32.5, 20.6. Chemical Formula: $C_{22}H_{19}F_3INO_4$ Exact Mass: 545.0311 g/mol

iii. *Peak Assignment for **9c***

Prepared from **8c** (331.4 mg, 1.0 mmol) and treated with NIS (247.5 mg, 1.1 equiv) using General Procedure C. T = 20 °C, time = 2 h. Purification: Flash chromatography on silica eluting with hexane/EtOAc (75:25). Yield = 325.5 mg, 79%. ^{1}H NMR (400 MHz, Chloroform-*d*) δ 7.32 (d, *J* = 7.5 Hz, 2H), 6.92 (d, *J* = 7.5 Hz, 2H), 5.83 (d, *J* = 5.5 Hz, 1H), 4.85 (t, *J* = 4.9 Hz, 1H), 3.89 – 3.66 (m, 4H), 3.21 (dd, *J* = 11.5, 4.3 Hz, 1H), 2.84 (td, *J* = 12.0, 3.0 Hz, 1H), 2.57 (ddd, *J* = 18.0, 4.5, 1.9 Hz, 1H), 2.43 (ddd, *J* = 18.0, 13.2, 5.1 Hz, 1H), 2.22 (ddd, *J* = 13.1, 5.3, 2.6 Hz, 1H), 1.40 (s, 9H). ^{13}C NMR (101 MHz, CDCl₃) δ 172.7, 172.1, 160.2, 129.3, 127.7, 114.6, 86.5,

58.9, 55.4, 55.1, 47.3, 43.5, 35.0, 29.6, 18.6. Chemical Formula: $C_{19}H_{24}INO_4$ Exact Mass: 457.0750 g/mol

Prepared from **8d** (335.4 mg, 1.0 mmol) and treated with NBS (195.8 mg, 1.1 equiv) using General Procedure C. T = 20 °C, time = 2 h. Purification: Flash chromatography on silica eluting with hexane/EtOAc (75:25). Yield = 364.6 mg, 88%. ^{1}H NMR (400 MHz, Chloroform-*d*) δ 7.51 – 7.34 (m, 3H), 7.25 – 7.08 (m, 4H), 6.96 – 6.88 (m, 2H), 5.92 (d, *J* = 1.9 Hz, 1H), 4.34 (t, *J* = 2.3 Hz, 1H), 3.32 (td, *J* = 12.2, 2.7 Hz, 1H), 3.11 (dd, *J* = 11.8, 2.7 Hz, 1H), 2.80 – 2.61 (m, 3H), 2.37 (s, 3H), 2.15 – 1.94 (m, 1H). ^{13}C NMR (101 MHz, CDCl₃) δ 175.7, 169.4, 138.0, 136.5, 134.8, 130.5, 129.4, 129.0, 129.0 128.3, 127.8, 120.0, 86.0, 61.3, 52.8, 38.5, 30.0, 21.2, 20.2. Chemical Formula: $C_{21}H_{20}BrNO_3$ Exact Mass: 413.0627 g/mol

Prepared from **8e** (335.4 mg, 1.0 mmol) and treated with NBS (195.8 mg, 1.1 equiv) using General Procedure C. T = 20 °C, time = 2 h. Purification: Flash chromatography on silica eluting with hexane/EtOAc (75:25). Yield = 399.9 mg, 90%. ^{1}H NMR (400 MHz, Chloroform-*d*) δ 7.20 (d, 2H), 7.16 (d, 2H), 6.90 – 6.82 (m, 4H), 5.77 (dt, *J* = 1.9, 0.8 Hz, 1H), 4.20 (t, *J* = 2.3 Hz, 1H), 3.95 (dd, *J* = 12.0, 2.6 Hz, 1H), 3.81 (s, 3H), 3.36 (td, *J* = 12.3, 2.6 Hz, 1H), 2.73 – 2.58 (m, 3H), 2.33 (s, 3H), 1.94 – 1.86 (m, 1H), 1.18 – 1.07 (m, 1H). ^{13}C NMR (101 MHz, CDCl₃) δ 170.2, 169.2, 159.9, 138.1, 134.7, 130.0, 129.9, 127.6, 126.2, 114.6, 84.6, 56.0, 55.5, 52.6, 39.8, 32.4, 21.3, 20.9. Chemical Formula: $C_{22}H_{22}BrNO_4$ Exact Mass: 443.0732 g/mol

Prepared from **8f** (389.4 mg, 1.0 mmol) and treated with NBS (195.8 mg, 1.1 equiv) using General Procedure C. T = 20 °C, time = 2 h. Purification: Flash chromatography on silica eluting with hexane/EtOAc (75:25). Yield = 398.0 mg, 85%. ^{1}H NMR (400 MHz, Chloroform-*d*) δ 7.58 (d, *J* = 7.9 Hz, 1H), 7.53 (t, *J* = 7.8 Hz, 1H), 7.40 – 7.29 (m, 4H), 7.13 – 7.06 (m, 3H), 5.82 (d, *J* = 1.9 Hz, 1H), 4.16 – 4.02 (m, 2H), 3.37 (td, *J* = 12.4, 2.0 Hz, 1H), 2.63 – 2.57 (m, 3H), 1.99 – 1.88 (m, 1H). ^{13}C NMR (101 MHz, CDCl₃) δ 169.9, 168.7, 138.0, 137.8, 132.6, 129.9, 129.6, 129.3, 125.0, 124.9, 124.5, 84.3, 55.7, 51.4, 39.8, 32.4, 20.7. Chemical Formula: $C_{21}H_{17}BrF_3NO_3$ Exact Mass: 467.0344 g/mol

Prepared from **8g** (4119.4 mg, 1.0 mmol) and treated with NBS (195.8 mg, 1.1 equiv) using General Procedure C. T = 20 °C, time = 2 h. Purification: Flash chromatography on silica eluting with hexane/EtOAc (75:25). Yield = 320.4 mg, 89%. ^{1}H NMR (400 MHz, Chloroform-d_3) δ 7.61 – 7.53 (m, 2H), 7.41 (d, J = 7.8 Hz, 1H), 7.16 (s, 1H), 7.08 (d, 2H), 6.90 (d, 2H), 5.70 (d, J = 2.3 Hz, 1H), 4.17 (t, J = 2.3 Hz, 1H), 4.02 (dd, J = 11.9, 2.5 Hz, 1H), 3.84 – 3.77 (m, 4H), 3.38 (td, J = 12.3, 2.6 Hz, 1H), 2.62 – 2.50 (m, 2H), 2.09 – 1.93 (m, 1H). ^{13}C NMR (101 MHz, CDCl$_3$) δ 169.6, 168.8, 160.1, 138.1, 132.6, 129.9, 129.7, 125.9, 124.9, 124.9, 114.9, 84.2, 55.8, 55.5, 51.90, 39.8, 32.5, 20.9. Chemical Formula: C$_{22}$H$_{19}$BrF$_3$NO$_4$ Exact Mass: 497.0450 g/mol

viii. *Peak Assignment for* **9h**

Prepared from **8h** (331.4 mg, 1.0 mmol) and treated with NBS (195.8 mg, 1.1 equiv) using General Procedure C. T = 20 °C, time = 2 h. Purification: Flash chromatography on silica eluting with hexane/EtOAc (75:25). Yield = 340.6 mg, 83%. ^{1}H NMR (400 MHz, Chloroform-d) δ 7.26 (d, J = 8.2 Hz, 2H), 6.87 (d, J = 8.2 Hz, 2H), 5.58 (d, J = 5.2 Hz, 1H), 4.68 (t, J = 4.4 Hz, 1H), 3.92 (dd, J = 11.5, 3.8 Hz, 1H), 3.69 (s, 3H), 2.95 (qd, J = 13.8, 12.1, 4.3 Hz, 1H), 2.67 – 2.50 (m, 1H), 2.54 – 2.41 (m, 1H), 2.33 (ddd, J = 18.4, 13.2, 5.5 Hz, 1H), 1.34 (s, 9H). ^{13}C NMR (101 MHz, CDCl$_3$) δ 173.0, 171.8, 160.2, 129.2, 127.7, 127.4, 114.5, 85.0, 61.5, 58.5, 55.4, 55.4, 54.7, 41.0, 34.9, 30.6, 29.1, 18.5. Chemical Formula: C$_{19}$H$_{24}$BrNO$_4$ Exact Mass: 409.0889 g/mol

ix. *Peak Assignment for* **9i**

Prepared from **8i** (287.3 mg, 1.0 mmol) and treated with NBS (195.8 mg, 1.1 equiv) using General Procedure C. T = 20 °C, time = 2 h. Purification: Flash chromatography on silica eluting with hexane/EtOAc (75:25). Yield = 282.0 mg, 77%. ^{1}H NMR (400 MHz, Chloroform-d) δ 7.44 – 7.27 (m, 5H), 5.31 + 5.17 (d, J = 9.8 Hz, 1H), 4.32 – 4.23 (m, 2H), 3.73 (p, J = 6.7 Hz, 1H), 3.32 – 3.17 (m, 1H), 2.77 – 2.62 (m, 1H), 2.42 – 2.26 (m, 2H), 2.16 – 1.96 (m, 1H), 1.50 (d, J = 6.8 Hz, 3H), 1.30 (d, J = 6.8 Hz, 3H). ^{13}C NMR (101 MHz, CDCl$_3$) δ 170.4, 170.0, 136.0, 129.8, 129.4, 129.4, 129.3, 128.8, 128.6, 127.7, 125.6, 84.7, 82.7, 62.6, 55.7, 55.1, 54.3, 51.5, 40.0, 39.4, 33.0, 30.3, 21.5, 21.4, 20.6, 19.0. Chemical Formula: C$_{17}$H$_{20}$BrNO$_3$ Exact Mass: 365.0627 g/mol

Prepared from **8j** (317.4 mg, 1.0 mmol) and treated with NBS (195.8 mg, 1.1 equiv) using General Procedure C. T = 20 °C, time = 2 h. Purification: Flash chromatography on silica eluting with hexane/EtOAc (75:25). Yield = 320.9, 81%. ^{1}H NMR (400 MHz, Chloroform-*d*) δ 7.25 (d, *J* = 7.9 Hz, 2H), 6.80 (d, *J* = 7.9 Hz, 2H), 5.72 (d, *J* = 3.9 Hz, 1H), 4.69 (t, *J* = 3.8 Hz, 1H), 3.77 (s, 3H), 3.68 – 3.57 (m, 2H), 3.12 (td, *J* = 12.3, 3.1 Hz, 1H), 2.40 – 2.32 (m, 3H), 1.66 – 1.56 (m, 1H), 1.25 (d, *J* = 6.6 Hz, 3H), 1.21 (d, *J* = 6.6 Hz, 3H). ^{13}C NMR (101 MHz, CDCl$_3$) δ 170.6, 170.6, 160.2, 129.4, 127.5, 127.1, 114.6, 84.5, 56.04 55.5, 55.3, 49.7, 39.9, 33.0, 20.2, 19.9. Chemical Formula: C$_{18}$H$_{22}$BrNO$_4$ Exact Mass: 395.0732 g/mol

Prepared from **8k** (349.4 mg, 1.0 mmol) and treated with NBS (195.8 mg, 1.1 equiv) using General Procedure C. T = 20 °C, time = 2 h. Purification: Flash chromatography on silica eluting with hexane/EtOAc (75:25). Yield = 381.2 mg, 89%. ^{1}H NMR (400 MHz, Chloroform-*d*) δ 7.21 – 7.07 (m, 6H), 7.07 – 6.96 (m, 2H), 6.87 – 6.80 (m, 2H), 5.69 (d, *J* = 2.0 Hz, 1H), 4.02 (d, *J* = 2.3 Hz, 1H), 3.83 (dd, *J* = 12.1, 2.5 Hz, 1H), 3.47 (td, *J* = 12.6, 3.0 Hz, 1H), 2.30 (dd, *J* = 13.8, 3.0 Hz, 1H), 1.90 – 1.77 (m, 1H), 1.30 (s, 3H), 1.13 (s, 3H). ^{13}C NMR (101 MHz, CDCl$_3$) δ 176.0, 169.7, 138.1, 137.9, 129.4, 129.2, 129.1, 128.0, 127.9, 124.8, 84.7, 56.4, 52.9, 39.4, 36.5, 35.0, 27.9, 27.7. Chemical Formula: C$_{22}$H$_{22}$BrNO$_3$ Exact Mass: 427.0783 g/mol

Prepared from **8l** (363.4 mg, 1.0 mmol) and treated with NBS (195.8 mg, 1.1 equiv) using General Procedure C. T = 20 °C, time = 2 h. Purification: Flash chromatography on silica eluting with hexane/EtOAc (75:25). Yield = 406.9 mg, 92%. ^{1}H NMR (400 MHz, Chloroform-*d*) δ 7.41 – 7.38 (m, 3H), 7.19 – 7.11 (m, 4H), 6.88 (d, 2H), 5.86 (d, *J* = 2.3 Hz, 1H), 4.23 (t, *J* = 2.3 Hz, 1H), 3.97 (dd, *J* = 12.2, 2.6 Hz, 1H), 3.62 (td, *J* = 12.6, 3.0 Hz, 1H), 2.46 (dd, *J* = 13.7, 3.0 Hz, 1H), 2.35 (s, 3H), 1.99 (t, *J* = 13.4 Hz, 1H), 1.46 (s, 3H), 1.29 (s, 3H). ^{13}C NMR (101 MHz, CDCl$_3$) δ 176.0, 169.7, 138.0, 137.7, 135.1, 129.8, 129.3, 129.1, 127.6, 124.8, 84.8, 56.5, 53.0, 39.4, 36.6, 35.0, 27.8, 27.7, 21.2. Chemical Formula: C23H24BrNO3 Exact Mass: 441.0940

2.5.2. Pyrrolidinones

i.   Peak Assignment for **9m**

Prepared from **8m** (351.4 mg, 1.0 mmol) and treated with NIS (247.5 mg, 1.1 equiv) using General Procedure C. T = 20 °C, time = 2 h. Purification: Flash chromatography on silica eluting with hexane/EtOAc (75:25). Yield = 381.8 mg, 80%. ^{1}H NMR (400 MHz, Chloroform-d) δ 7.39 (d, J = 7.5 Hz, 2H), 7.22 (d, J = 8.1 Hz, 2H), 7.16 (d, J = 8.1 Hz, 2H), 6.84 (d, J = 7.5 Hz, 2H), 5.86 (d, J = 6.6 Hz, 1H), 4.68 (dd, J = 6.6, 5.8 Hz, 1H), 3.81 (s, 3H), 3.80 – 3.69 (m, 1H), 3.37 (td, J = 11.0, 9.2 Hz, 1H), 2.98 (dd, J = 11.6, 2.4 Hz, 2H), 2.30 (s, 3H). ^{13}C NMR (101 MHz, CDCl$_3$) δ 172.5, 170.5, 160.5, 136.3, 133.8, 123.0, 129.9, 128.2, 128.1, 126.4, 123.1, 114.5, 87.7, 58.4, 55.5, 4.7, 34.1, 31.1, 28.1, 21.1. Chemical Formula: C$_{21}$H$_{20}$INO$_4$ Exact Mass: 477.0437 g/mol

ii.   Peak Assignment for **9n**

Prepared from **8n** (351.4 mg, 1.0 mmol) and treated with NBS (195.8 mg, 1.1 equiv) using General Procedure C. T = 20 °C, time = 2 h. Purification: Flash chromatography on silica eluting with hexane/EtOAc (75:25). Yield = 357.1 mg, 87%. ^{1}H NMR (400 MHz, Chloroform-d) δ 7.36 (d, J = 7.2 Hz, 2H), 7.22 (d, J = 8.5 Hz, 2H), 7.16 (d, J = 8.5 Hz, 2H), 6.89 (d, J = 7.2 Hz, 2H), 5.69 (d, J = 5.6 Hz, 1H), 4.57 (t, J = 5.4 Hz, 1H), 4.44 – 4.38 (m, 1H), 3.76 (s, 3H), 3.58 – 3.46 (m, 1H), 2.83 – 2.72 (m, 2H), 2.31 (s, 3H). ^{13}C NMR (101 MHz, CDCl$_3$) δ 172.5, 170.2, 160.4, 136.5, 133.7, 123.0, 129.9, 128.4, 127.7, 126.4, 123.1, 114.5, 86.3, 58.6, 55.5, 51.9, 37.3, 31.2, 21.1. Chemical Formula: C$_{21}$H$_{20}$BrNO$_4$ Exact Mass: 429.0576 g/mol

iii.   Peak Assignment for **9o**

Prepared from **8o** (317.4 mg, 1.0 mmol) and treated with NIS (247.5 mg, 1.1 equiv) using General Procedure C. T = 20 °C, time = 2 h. Purification: Flash chromatography on silica eluting with hexane/EtOAc (75:25). Yield = 341.3 mg, 77%. ^{1}H NMR (400 MHz, Chloroform-d) δ 7.39 (d, J = 9.0 Hz 2H), 6.95 (d, J = 9.0 Hz, 2H), 5.84 (d, J = 6.7 Hz, 1H), 4.65 (dd, J = 6.7, 5.2 Hz, 1H), 3.85 (s, 3H), 3.17 (dd, J = 11.0, 5.2 Hz, 1H), 3.06 (td, J = 10.8, 9.2 Hz, 1H), 2.66 – 2.56 (m, 2H), 1.44 (s, 9H). ^{13}C NMR (101 MHz, CDCl$_3$) δ 176.4, 171.6, 160.4, 130.5, 128.3, 114.5, 87.4, 60.6, 57.5, 55.5, 44.7, 38.2, 31.7, 28.0. Chemical Formula: C$_{18}$H$_{22}$INO$_4$ Exact Mass: 443.0594 g/mol

Prepared from **8p** (317.4 mg, 1.0 mmol) and treated with NBS (195.8 mg, 1.1 equiv) using General Procedure C. T = 20 °C, time = 2 h. Purification: Flash chromatography on silica eluting with hexane/EtOAc (75:25). Yield = 317.0 mg, 87%. ^{1}H NMR (400 MHz, Chloroform-*d*) δ 7.39 (d, *J* = 9.0 Hz 2H), 6.97 (d, *J* = 9.0 Hz, 2H), 5.63 (d, *J* = 6.1 Hz, 1H), 4.59 (dd, *J* = 6.0, 5.0 Hz, 1H), 3.94 – 3.78 (m, 4H), 3.24 (td, *J* = 11.3, 9.2 Hz, 1H), 2.73 – 2.57 (m, 2H), 1.45 (s, 9H). ^{13}C NMR (101 MHz, CDCl$_3$) δ 171.2, 160.4, 127.9, 126.4, 114.5, 85.8, 60.3, 58.8, 57.3, 55.5, 36.9, 31.7, 27.7. Chemical Formula: C$_{18}$H$_{22}$BrNO$_4$ Exact Mass: 395.0732 g/mol

v. *Peak Assignment for* **9q**

Prepared from **8q** (287.3 mg, 1.0 mmol) and treated with NBS (195.8 mg, 1.1 equiv) using General Procedure C. T = 20 °C, time = 2 h. Purification: Flash chromatography on silica eluting with hexane/EtOAc (75:25). Yield = 296.7 mg, 81%. ^{1}H NMR (400 MHz, Chloroform-*d*) δ 7.47 – 7.37 (m, 5H), 5.63 (d, *J* = 6.0 Hz, 1H), 4.54 (dd, *J* = 6.0, 5.0 Hz, 2H), 3.74 (dd, *J* = 11.1, 5.0 Hz, 1H), 2.71 – 2.64 (m, 1H), 2.61 – 2.56 (m, 1H), 1.50 (s, 9H). ^{13}C NMR (101 MHz, CDCl$_3$) δ 175.8, 171.1, 136.5, 129.6, 129.3, 128.9, 126.4, 86.0, 60.3, 58.6, 57.4, 37.0, 31.7, 27.8. Chemical Formula: C$_{17}$H$_{20}$BrNO$_3$ Exact Mass: 365.0627 g/mol

vi. *Peak Assignment for* **9r**

Prepared from **8r** (303.3 mg, 1.0 mmol) and treated with NBS (195.8 mg, 1.1 equiv) using General Procedure C. T = 20 °C, time = 2 h. Purification: Flash chromatography on silica eluting with hexane/EtOAc (75:25). Yield = 282.9 mg, 87%. ^{1}H NMR (400 MHz, CD$_3$CN) δ 7.33 (d, 2H), 6.98 (d, 2H), 5.66 (d, *J* = 7.1 Hz, 1H), 4.67 (dd, 1H), 3.95 (dd, *J* = 11.7, 5.4 Hz, 1H), 3.79 (s, 3H), 3.47 (hept, *J* = 6.8 Hz, 1H), 3.38 – 3.22 (m, 1H), 2.56 – 2.42 (m, 2H), 1.41 (d, *J* = 6.7 Hz, 3H), 1.28 (d, *J* = 6.7 Hz, 3H). ^{13}C NMR (101 MHz, CDCl$_3$) δ 174.8, 171.2, 160.5, 129.7, 128.9, 117.5, 114.3, 86.8, 85.9, 60.9, 58.8, 55.2, 55.2, 53.6, 52.89, 47.5, 46.4, 37.6, 36.9, 31.6, 31.2, 20.1, 19.5, 17.5, 17.1. Chemical Formula: C$_{17}$H$_{20}$BrNO$_4$ Exact Mass: 381.0576 g/mol

2.5.3.Morpholinones

i. Peak Assignment for **9s**

Prepared from **8s** (337.4 mg, 1.0 mmol) and treated with NIS (247.5 mg, 1.1 equiv) using General Procedure C. T = 20 °C, time = 2 h. Purification: Flash chromatography on silica eluting with hexane/EtOAc (75:25). Yield = 347.4 mg, 75%. ^{1}H NMR (400 MHz, Chloroform-*d*) δ 7.43 – 7.41 (m, 3H), 7.26 – 7.16 (m, 4H), 7.00 (d, *J* = 8.3 Hz, 2H), 5.95 (s, 1H), 4.89 (d, *J* = 10.8 Hz, 1H), 4.55 (d, *J* = 12.0 Hz, 2H), 4.38 (s, 1H), 3.44 (d, *J* = 3.0 Hz, 1H), 2.38 (s, 3H). ^{13}C NMR (101 MHz, CDCl$_3$) δ 166.1, 165.7, 138.6, 138.2, 132.4, 130.1, 129.5, 129.3, 127.3, 124.8, 86.8, 75.5, 69.4, 53.2, 29.4, 21.3. Chemical Formula: C$_{20}$H$_{18}$INO$_4$ Exact Mass: 463.0281 g/mol

ii. Peak Assignment for **9t**

Prepared from **8t** (335.4 mg, 1.0 mmol) and treated with NIS (247.5 mg, 1.1 equiv) using General Procedure C. T = 20 °C, time = 2 h. Purification: Flash chromatography on silica eluting with hexane/EtOAc (75:25). Yield = 394.2 mg, 87%. ^{1}H NMR (400 MHz, Chloroform-*d*) δ 7.53 (d, *J* = 8.2 Hz, 1H), 7.41 – 7.22 (m, 3H), 7.25 – 7.14 (m, 2H), 7.09 – 7.01 (m, 1H), 6.70 (s, 1H), 5.19 (s, 1H), 4.85 (d, *J* = 17.4 Hz, 1H), 4.65 (d, *J* = 8.2 Hz, 1H), 4.59 – 4.46 (m, 1H), 4.50 – 4.39 (m, 1H), 4.37 – 4.26 (m, 1H), 2.19 (s, 3H). ^{13}C NMR (101 MHz, CDCl$_3$) δ 171.7, 165.6, 142.7, 136.8, 134.4, 131.9, 130.1, 129.0, 128.9, 128.8, 127.8, 127.6, 125.3, 72.4, 64.7, 60.7, 56.1, 55.8, 21.1. Chemical Formula: C$_{20}$H$_{17}$BrINO$_4$ Exact Mass: 540.9386 g/mol

iii. Peak Assignment for **9u**

Prepared from **8u** (367.4 mg, 1.0 mmol) and treated with NIS (247.5 mg, 1.1 equiv) using General Procedure C. T = 20 °C, time = 2 h. Purification: Flash chromatography on silica eluting with hexane/EtOAc (75:25). Yield = 350.2 mg, 79%. ^{1}H NMR (400 MHz, Chloroform-*d*) δ 7.18 (d, *J* = 7.2 Hz, 2H), 7.13 (d, *J* = 8.3 Hz, 2H), 7.01 (d, *J* = 8.3 Hz, 2H), 6.92 (d, *J* = 7.2 Hz, 2H), 5.90 (s, 1H), 4.85 (d, *J* = 10.9 Hz, 1H), 4.54 (s, 2H), 4.35 (d, *J* = 3.1 Hz, 1H), 3.84 (s, 3H), 3.44 (dd, *J* = 10.8, 3.1 Hz, 1H), 2.36 (s, 6H). ^{13}C NMR (101 MHz, CDCl$_3$) δ 166.1, 165.9, 160.0, 138.5, 132.5, 130.1, 130.1, 127.3, 126.2, 114.7, 86.7, 75.4, 69.4, 55.5, 53.2, 29.9, 21.3. Chemical Formula: C$_{21}$H$_{20}$INO$_5$ Exact Mass: 493.0386 g/mol

Prepared from **8v** (421.4 mg, 1.0 mmol) and treated with NIS (247.5 mg, 1.1 equiv) using General Procedure C. T = 20 °C, time = 2 h. Purification: Flash chromatography on silica eluting with hexane/EtOAc (75:25). Yield = 465.2 mg, 87%. ^{1}H NMR (400 MHz, Chloroform-*d*) δ 7.73 – 7.71 (m, 2H), 7.63 (t, *J* = 1.9 Hz, 1H), 7.49 (d, *J* = 2.0 Hz, 1H), 7.16 (d, *J* = 6.9 Hz, 2H), 6.94 (d, *J* = 6.9 Hz, 2H), 5.91 (d, *J* = 2.9 Hz, 1H), 5.31 (s, 1H), 4.88 (d, *J* = 10.8 Hz, 1H), 4.57 – 4.54 (m, 1H), 4.34 – 4.23 (m, 1H), 3.80 (s, 3H), 3.56 (dd, *J* = 10.8, 3.1 Hz, 1H). ^{13}C NMR (101 MHz, CDCl$_3$) δ 168.9, 165.8, 165.5, 160.2, 135.7, 132.0, 130.1, 123.0, 129.9, 126.1, 126.1, 125.9, 125.7, 125.7, 125.1, 125.1, 115.0, 86.3, 75.3, 69.3, 68.1, 55.5, 53.0, 28.9. Chemical Formula: C$_{21}$H$_{17}$F$_3$INO$_5$ Exact Mass: 547.0104 g/mol

v. *Peak Assignment for* **9w**

Prepared from **8w** (333.4 mg, 1.0 mmol) and treated with NIS (247.5 mg, 1.1 equiv) using General Procedure C. T = 20 °C, time = 2 h. Purification: Flash chromatography on silica eluting with hexane/EtOAc (75:25). Yield = 344.4 mg, 75%. ^{1}H NMR (400 MHz, Chloroform-*d*) δ 7.36 (d, *J* = 7.1 Hz, 1H), 6.98 (d, *J* = 7.1 Hz, 2H), 5.86 (d, *J* = 5.7 Hz, 1H), 4.88 (dd, *J* = 5.7, 4.7 Hz, 1H), 4.50 (d, *J* = 11.4 Hz, 1H), 4.34 (d, *J* = 15.4 Hz, 1H), 4.32 – 4.21 (m, 1H), 3.84 (s, 3H), 3.40 (dd, *J* = 11.4, 4.6 Hz, 1H), 1.45 (s, 9H). ^{13}C NMR (101 MHz, CDCl$_3$) δ 169.4, 167.9, 160.5, 127.7, 114.7, 85.8, 74.4, 70.4, 55.5, 53.5, 42.1, 29.4, 28.5. Chemical Formula: C$_{18}$H$_{22}$INO$_5$ Exact Mass: 459.0543 g/mol

2.5.4. α-methyl Substituted Isomers

i. *Peak Assignment for* **17a**

Prepared from **1a** (301.4 mg, 1.0 mmol) and treated with NBS (195.8 mg, 1.1 equiv) using General Procedure C. T = 20 °C, time = 2 h. Purification: Flash chromatography on silica eluting with hexane/EtOAc (75:25). Yield = 250.9 mg, 66%. ^{1}H NMR (400 MHz, Chloroform-*d*) δ 7.55 – 7.28 (m, 5H), 5.11 (s, 1H), 4.39 (d, *J* = 12.2 Hz, 1H), 3.66 – 3.54 (m, 1H), 2.64 (dd, *J* = 16.2, 7.4 Hz, 1H), 2.39 – 2.27 (m, 2H), 1.87 – 1.72 (m, 2H), 1.66 (s, 3H), 1.32 – 1.26 (m, 6H). ^{13}C NMR (101 MHz, CDCl$_3$) δ 176.9, 173.9, 137.0, 129.4, 129.0, 128.1, 89.6, 61.1, 59.2, 53.4, 46.8, 42.3, 32.3, 22.7, 22.3, 21.1, 19.9. Chemical Formula: C$_{18}$H$_{22}$BrNO$_3$ Exact Mass: 379.0783 g/mol

Prepared from **1b** (414.3 mg, 1.0 mmol) and treated with NBS (195.8 mg, 1.1 equiv) using General Procedure C. T = 20 °C, time = 2 h. Purification: Flash chromatography on silica eluting with hexane/EtOAc (75:25). Yield = 325.6 mg, 83%. ^{1}H NMR (400 MHz, Chloroform-*d*) δ 7.62 – 7.42 (m, 5H), 5.88 (s, 1H), 4.71 – 4.52 (m, 1H), 4.39 (d, *J* = 12.2 Hz, 1H), 3.02 (td, *J* = 12.2, 7.5 Hz, 1H), 2.64 (dd, *J* = 16.2, 7.4 Hz, 1H), 2.59 – 2.39 (m, 2H), 1.97 – 1.85 (m, 4H), 1.69 (s, 3H), 1.62 – 1.49 (m, 2H). ^{13}C NMR (101 MHz, CDCl$_3$) δ 173.9, 167.8, 133.0, 129.4, 129.0, 128.1, 89.6, 67.1, 64.2, 55.4, 40.8, 32.3, 28.9, 27.7, 25.5, 25.0, 19.9. Chemical Formula: C$_{19}$H$_{22}$BrNO$_3$ Exact Mass: 391.0783 g/mol

iii.   *Peak Assignment for* **17c**

Prepared from **1c** (341.4 mg, 1.0 mmol) and treated with NBS (195.8 mg, 1.1 equiv) using General Procedure C. T = 20 °C, time = 2 h. Purification: Flash chromatography on silica eluting with hexane/EtOAc (75:25). Yield = 336.3 mg, 80%. ^{1}H NMR (400 MHz, Chloroform-*d*) δ 7.54 – 7.38 (m, 5H), 5.87 (s, 1H), 4.40 (d, *J* = 12.3 Hz, 1H), 4.21 (tt, *J* = 10.6, 3.7 Hz, 1H), 3.03 (td, *J* = 12.3, 7.6 Hz, 1H), 2.62 – 2.43 (m, 2H), 1.87 – 1.26 (m, 15H). ^{13}C NMR (101 MHz, CDCl$_3$) δ 174.3, 168.0, 130.1, 129.0, 128.0, 89.5, 65.9, 64.4, 56.3, 40.8, 33.2, 32.1, 29.3, 28.2, 27.1, 26.7, 25.6, 19.9. Chemical Formula: C$_{21}$H$_{26}$BrNO$_3$ Exact Mass: 419.1096 g/mol

iv.   *Peak Assignment for* **17d**

Prepared from **1d** (285.3 mg, 1.0 mmol) and treated with NBS (195.8 mg, 1.1 equiv) using General Procedure C. T = 20 °C, time = 2 h. Purification: Flash chromatography on silica eluting with hexane/EtOAc (75:25). Yield = 320.5 mg, 88%. ^{1}H NMR (400 MHz, Chloroform-*d*) δ 7.59 – 7.32 (m, 5H), 6.36 (s, 1H), 5.79 (dddd, *J* = 17.4, 10.3, 7.4, 4.3 Hz, 1H), 5.30 – 5.10 (m, 2H), 4.84 (dd, *J* = 5.0, 1.3 Hz, 1H), 4.79 (ddt, *J* = 15.5, 4.0, 1.8 Hz, 1H),, 4.21 (s, 1H), 3.75 – 3.69 (m, 1H), 3.22 (dd, *J* = 15.5, 7.4 Hz, 1H), 2.51 (dt, *J* = 12.7, 5.2 Hz, 1H), 1.94 (s, 3H). ^{13}C NMR (101 MHz, CDCl$_3$) δ 175.8, 166.6, 136.0, 132.0, 131.2, 129.0, 128.5, 127.5, 118.5, 77.9, 62.5, 46.4, 41.3, 28.2, 16.6. Chemical Formula: C$_{17}$H$_{18}$BrNO$_3$ Exact Mass: 363.0470 g/mol

v.   Peak Assignment for 17f

Prepared from **1e** (429.4 mg, 1.0 mmol) and treated with NBS (195.8 mg, 1.1 equiv) using General Procedure C. T = 20 °C, time = 2 h. Purification: Flash chromatography on silica eluting with hexane/EtOAc (75:25). Yield = 381.3 mg, 75%. ^{1}H NMR (400 MHz, Chloroform-*d*) δ 7.34 – 7.07 (m, 14H), 5.34 (s, 1H), 5.21 (d, *J* = 14.8 Hz, 1H), 4.21 (s, 1H), 3.84 (d, *J* = 14.8 Hz, 1H), 2.74 – 2.56 (m, 2H), 1.60 (s, 3H). ^{13}C NMR (101 MHz, CDCl$_3$) δ 177.5, 175.8, 163.8, 163.7, 161.4, 161.3, 142.3, 130.9, 130.9, 129.7, 129.6, 129.3, 128.1, 127.9, 127.4, 124.7, 115.8, 115.6, 83.1, 74.7, 64.3, 42.1, 37.2, 18.0. Chemical Formula: C$_{27}$H$_{23}$BrFNO$_3$ Exact Mass: 507.0845 g/mol

2.5.5. Applications of Lactam-Lactones

i.   Peak Assignment for 18a

Prepared from **9d** (414.3 mg, 1.0 mmol) and treated with isopropylamine (177.3 mg, 3 equiv) using General Procedure E. T = 20 °C, time = 12 h. Purification: Flash chromatography on silica eluting with hexane/EtOAc (75:25). Yield = 381.3 mg, 75%. ^{1}H NMR (400 MHz, Chloroform-*d*) δ 7.14 – 6.93 (m, 9H), 5.62 – 5.60 (d, *J*=7.60 Hz, 1H), 4.10 – 4.06 (t, *J*=7.25, 7.25 Hz, 1H), 3.97–3.88 (m, 1H), 3.48 (d, *J*=2.20 Hz, 1H), 2.48 – 2.33 (m, 3H), 2.22 – 2.14 (s, 3H), 2.02 – 1.97 (s, 1H), 1.09 (s, 1H), 0.99 – 0.89 (dd, *J*=7.26, 7.26 Hz, 9H). ^{13}C NMR (101 MHz, CDCl$_3$) δ 170.7, 169.8, 138.5, 137.4, 136.1, 130.1, 129.5, 128.5, 127.9, 125.7, 119.9, 77.5, 77.1, 76.8, 64.2, 63.0, 55.6, 44.4, 42.0, 31.45, 29.4, 24.3, 22.8, 22.5, 21.3. Chemical Formula: C$_{24}$H$_{28}$N$_2$O$_3$ Exact Mass: 392.2100 g/mol

ii.   Peak Assignment for 18b

Prepared from **9f** (468.3 mg, 1.0 mmol) and treated with isopropylamine (177.3 mg, 3 equiv) using General Procedure E. T = 20 °C, time = 12 h. Purification: Flash chromatography on silica eluting with hexane/EtOAc (75:25). ^{1}H NMR (400 MHz, Chloroform-*d*) δ 7.29– 7.21 (dd, *J*=8.35, 8.44 Hz, 2H) , 6.97–6.85 (m, 4H), 6.74 – 6.67 (m, 2H), 6.51 (s, 1H) 6.3 8– 4.33 (m, 1H), 4.01 – 3.96(dd, *J*=8.47, 2.65, 8.47 Hz), 3.68 – 3.61 (m, 3H), 2.62 – 2.49 (m, 2H) 2.38 – 2.28 (m, 4H), 2.20 – 2.11 (m, 3H), 1.95 – 1.89 (m, 1H).^{13}C NMR (101 MHz, CDCl$_3$) δ 168.8, 158.9, 135.1, 129.9, 129.6, 127.6, 125.7, 120.1, 114.2, 77.4, 77.1, 76.8, 61.6, 59.4, 55.6, 55.3, 42.2, 32.9, 30.5, 29.6, 21.0, 20.6, 20.0. Chemical Formula: C$_{24}$H$_{25}$F$_3$N$_2$O$_3$ Exact Mass: 446.1817 g/mol

Prepared from **9h** (410.3 mg, 1.0 mmol) and treated with methyl magnesium bromide (238.5 mg, 2.0 equiv) using General Procedure F. T = –78 °C to rt, time = 18 h. Purification: Flash chromatography on silica eluting with hexane/EtOAc (75:25). ^{1}H NMR (400 MHz, Chloroform-*d*) 7.84—7.79 (d*, J*=20.0 Hz, 2H), 6.91—6.87 (d, *J*=16.0 Hz, 2H), 5.23—5.13 (d, *J*=9.29 Hz, 1H), 4.54—4.46(dd, *J*=2.61, 6.52, 2.68 Hz, 1H), 4.23—4.18(s, 1H), 3.84—3.81(s, 3H), 3.77—3.71(m, 4H), 3.34—3.28(m, 1H), 2.62—2.40(m, 3H), 2.16—2.02(m, 2H), 1.44—1.36(m, 3H), 1.29—1.24(s, 9H). ^{13}C NMR (101 MHz, Chloroform-*d*) δ 192.0, 173.3, 164.7, 131.2, 127.8, 127.3, 125.8, 114.9, 114.6, 114.0, 103.7, 84.5, 77.5, 77.1, 76.8, 58.9, 58.7, 55.8, 48.8, 38.1, 32.5, 29.2, 28.8, 28.7, 28.5, 28.4, 17.3. Chemical Formula: $C_{21}H_{32}BrNO_4$ Exact Mass: 441.1515 g/mol

REFERENCES

(1)   Vitaku, E.; Smith, D. T.; Njardarson, J. T. Analysis of the Structural Diversity, Substitution Patterns, and Frequency of Nitrogen Heterocycles among U.S. FDA Approved Pharmaceuticals. *J. Med. Chem.* **2014**, *57* (24), 10257–10274. https://doi.org/10.1021/jm501100b (accessed Jul 21, 2020).

(2)   Vitaku, E.; Smith, D. T.; Njardarson, J. T. Analysis of the Structural Diversity, Substitution Patterns, and Frequency of Nitrogen Heterocycles among U.S. FDA Approved Pharmaceuticals. *J. Med. Chem.* **2014**, *57* (24), 10257–10274. https://doi.org/10.1021/jm501100b (accessed Jul 21, 2020).

(3)   Fang, B.; Zheng, H.; Zhao, C.; Jing, P.; Li, H.; Xie, X.; She, X. Synthesis of the Tetracyclic Core (ABCE Rings) of Daphenylline. *J. Org. Chem.* **2012**, *77* (18), 8367–8373. https://doi.org/10.1021/jo301533f (accessed Jul 21, 2020).

(4)   Zhang, Y.; Rothman, R. B.; Dersch, C. M.; de Costa, B. R.; Jacobson, A. E.; Rice, K. C. Synthesis and Transporter Binding Properties of Bridged Piperazine Analogues of 1-{2-[Bis(4-Fluorophenyl)Methoxy]Ethyl}-4-(3-Phenylpropyl)Piperazine (GBR 12909). *J. Med. Chem.* **2000**, *43* (25), 4840–4849. https://doi.org/10.1021/jm000300r (accessed Jul 21, 2020).

(5)   Brands, K. M. J.; Payack, J. F.; Rosen, J. D.; Nelson, T. D.; Candelario, A.; Huffman, M. A.; Zhao, M. M.; Li, J.; Craig, B.; Song, Z. J.; Tschaen, D. M.; Hansen, K.; Devine, P. N.; Pye, P. J.; Rossen, K.; Dormer, P. G.; Reamer, R. A.; Welch, C. J.; Mathre, D. J.; Tsou, N. N.; McNamara, J. M.; Reider, P. J. Efficient Synthesis of NK1 Receptor Antagonist Aprepitant Using a Crystallization-Induced Diastereoselective Transformation. *J. Am. Chem. Soc.* **2003**, *125* (8), 2129–2135. https://doi.org/10.1021/ja027458g (accessed Jul 21, 2020).

(6)   Bharate, S. S.; Bharate, S. B. Modulation of Thermoreceptor TRPM8 by Cooling Compounds. *ACS Chem. Neurosci.* **2012**, *3* (4), 248–267. https://doi.org/10.1021/cn300006u (accessed Jul 21, 2020).

(7)   MacDonald, M. J.; Cornejo, N. R.; Gellman, S. H. Inhibition of Ice Recrystallization by Nylon-3 Polymers. *ACS Macro Lett.* **2017**, *6* (7), 695–699. https://doi.org/10.1021/acsmacrolett.7b00396 (accessed Jul 21, 2020).

(8)   Zhang, J.; Barajas, J. F.; Burdu, M.; Ruegg, T. L.; Dias, B.; Keasling, J. D. Development of a Transcription Factor-Based Lactam Biosensor. *ACS Synth. Biol.* **2017**, *6* (3), 439–445. https://doi.org/10.1021/acssynbio.6b00136 (accessed Jul 21, 2020).

(9)   Dong, L.-B.; Wu, X.-D.; Shi, X.; Zhang, Z.-J.; Yang, J.; Zhao, Q.-S. Phleghenrines A–D and Neophleghenrine A, Bioactive and Structurally Rigid Lycopodium Alkaloids from Phlegmariurus Henryi. *Org. Lett.* **2016**, *18* (18), 4498–4501. https://doi.org/10.1021/acs.orglett.6b02065 (accessed Jul 21, 2020).

(10)   Shen, D.-Y.; Nguyen, T. N.; Wu, S.-J.; Shiao, Y.-J.; Hung, H.-Y.; Kuo, P.-C.; Kuo, D.-H.; Thang, T. D.; Wu, T.-S. γ- and δ-Lactams from the Leaves of Clausena Lansium. *J. Nat. Prod.* **2015**, *78* (11), 2521–2530. https://doi.org/10.1021/acs.jnatprod.5b00148 (accessed Jul 21, 2020).

(11)   Arai, M.; Yamano, Y.; Kamiya, K.; Setiawan, A.; Kobayashi, M. Anti-Dormant Mycobacterial Activity and Target Molecule of Melophlins, Tetramic Acid Derivatives Isolated from a Marine Sponge of Melophlus Sp. *J. Nat. Med.* **2016**, *70* (3), 467–475. https://doi.org/10.1007/s11418-016-1005-1 (accessed Jul 21, 2020).

(12) Chung, C.-P.; Hsu, C.-Y.; Lin, J.-H.; Kuo, Y.-H.; Chiang, W.; Lin, Y.-L. Antiproliferative Lactams and Spiroenone from Adlay Bran in Human Breast Cancer Cell Lines. *J. Agric. Food Chem.* **2011**, *59* (4), 1185–1194. https://doi.org/10.1021/jf104088x (accessed Jul 21, 2020).

(13) Gordillo Sierra, A. R.; Alper, H. S. Progress in the Metabolic Engineering of Bio-Based Lactams and Their ω-Amino Acids Precursors. *Biotechnol. Adv.* **2020**, *43*, 107587. https://doi.org/10.1016/j.biotechadv.2020.107587 (accessed Jul 21, 2020).

(14) Hu, T.; Li, C. Synthesis of Lactams via Copper-Catalyzed Intramolecular Vinylation of Amides. *Org. Lett.* **2005**, *7* (10), 2035–2038. https://doi.org/10.1021/ol0505555 (accessed Jul 21, 2020).

(15) Kim, I.; Roh, S. W.; Lee, D. G.; Lee, C. Rhodium-Catalyzed Oxygenative [2 + 2] Cycloaddition of Terminal Alkynes and Imines for the Synthesis of β-Lactams. *Org. Lett.* **2014**, *16* (9), 2482–2485. https://doi.org/10.1021/ol500856z (accessed Jul 21, 2020).

(16) Lorenc, C.; Vibbert, H. B.; Yao, C.; Norton, J. R.; Rauch, M. H· Transfer-Initiated Synthesis of γ-Lactams: Interpretation of Cycloisomerization and Hydrogenation Ratios. *ACS Catal.* **2019**, 10294–10298. https://doi.org/10.1021/acscatal.9b03678 (accessed Jul 21, 2020).

(17) B. Hamed, R.; Ruben Gomez-Castellanos, J.; Henry, L.; Ducho, C.; A. McDonough, M.; J. Schofield, C. The Enzymes of β-Lactam Biosynthesis. *Nat. Prod. Rep.* **2013**, *30* (1), 21–107. https://doi.org/10.1039/C2NP20065A (accessed Jul 21, 2020).

(18) Fuentes, V. A.; Pineda, D. M.; Venkata, C. K. Comprehension of Top 200 Prescribed Drugs in the US as a Resource for Pharmacy Teaching, Training and Practice. *Pharmacy* **2018**, *6* (2). https://doi.org/10.3390/pharmacy6020043 (accessed Jul 21, 2020).

(19) Talreja, O.; Kerndt, C.C.; Cassagnol, M. Simvastatin. In *StatPearls;* StatPearls Publishing: Treasure Island (FL); November 4, 2020. https://www.ncbi.nlm.nih.gov/books/NBK532919/. (accessed Dec 6, 2020).

(20) Kwok, B. H.; Koh, B.; Ndubuisi, M. I.; Elofsson, M.; Crews, C. M. The Anti-Inflammatory Natural Product Parthenolide from the Medicinal Herb Feverfew Directly Binds to and Inhibits IkappaB Kinase. *Chem. Biol.* **2001**, *8* (8), 759–766. https://doi.org/10.1016/s1074-5521(01)00049-7. (accessed Jul 21, 2020)..

(21) Kicman, A. T. Pharmacology of Anabolic Steroids. *Br. J. Pharmacol.* **2008**, *154* (3), 502–521. https://doi.org/10.1038/bjp.2008.165.

(22) Patel, S.; Singh, R.; Preuss, C.V.; Patel, N. In *StatPearls;* StatPearls Publishing: Treasure Island (FL); September 28, 2020. https://www.ncbi.nlm.nih.gov/books/NBK470313/ (accessed Dec 6, 2020).

(23) Carone, L.; Oxberry, S. G.; Twycross, R.; Charlesworth, S.; Mihalyo, M.; Wilcock, A. Spironolactone. *J. Pain Symptom Manage.* **2017**, *53* (2), 288–292. https://doi.org/10.1016/j.jpainsymman.2016.12.320 (accessed Jul 21, 2020).

(24) Mal, K.; Kaur, A., Haque, F.; Das, I. PPh3·HBr–DMSO: A Reagent System for Diverse Chemoselective Transformations. *J. Org. Chem.***2015**, *80* (12), 6400-6410https://pubs-acs-org.ezp.lib.cwu.edu/doi/10.1021/acs.joc.5b00846 (accessed Jul 21, 2020).

(25) Ueda, Y.; Muramatsu, W.; Mishiro, K.; Furuta, T.; Kawabata, T. Functional Group Tolerance in Organocatalytic Regioselective Acylation of Carbohydrates. *J. Org. Chem.* **2009**, *74* (22), 8802–8805. https://doi.org/10.1021/jo901569v (accessed Jul 21, 2020). (26) Rosen, B. R.; Ney, J. E.; Wolfe, J. P. Use of Aryl Chlorides as Electrophiles in Pd-

Catalyzed Alkene Difunctionalization Reactions. *J. Org. Chem.* **2010**, *75* (8), 2756–2759. https://doi.org/10.1021/jo100344k (accessed Jul 21, 2020).

(27) Andrade, C. Ketamine for Depression, 3: Does Chirality Matter? *J. Clin. Psychiatry* **2017**, *78* (6), e674–e677. https://doi.org/10.4088/JCP.17f11681 (accessed Jul 21, 2020).

(28) Kim, J. H.; Scialli, A. R. Thalidomide: The Tragedy of Birth Defects and the Effective Treatment of Disease. *Toxicol. Sci.* **2011**, *122* (1), 1–6. https://doi.org/10.1093/toxsci/kfr088 (accessed Jul 21, 2020).

(29) Henderson, W. R.; Banerjee, E. R.; Chi, E. Y. Differential Effects of (S)- and (R)-Enantiomers of Albuterol in a Mouse Asthma Model. *J. Allergy Clin. Immunol.* **2005**, *116* (2), 332–340. https://doi.org/10.1016/j.jaci.2005.04.013 (accessed Jul 21, 2020).

(30) Dubin, A.; Lattanzio, B.; Gatti, L. The Spectrum of Cardiovascular Effects of Dobutamine - from Healthy Subjects to Septic Shock Patients. *Rev. Bras. Ter. Intensiva* **2017**, *29* (4), 490–498. https://doi.org/10.5935/0103-507X.20170068 (accessed Jul 21, 2020).

(31) Tyler, M. W.; Yourish, H. B.; Ionescu, D. F.; Haggarty, S. J. Classics in Chemical Neuroscience: Ketamine. *ACS Chem. Neurosci.* **2017**, *8* (6), 1122–1134. https://doi.org/10.1021/acschemneuro.7b00074 (accessed Jul 21, 2020).

(32) FDA Approves New Nasal Spray Medication for Treatment-Resistant Depression; Available Only at a Certified Doctor's Office or Clinic, 2019. https://www.fda.gov/news-events/press-announcements/fda-approves-new-nasal-spray-medication-treatment-resistant-depression-available-only-certified (accessed Dec 6, 2020).

(33) Zhang, J. C.; Li, S. X.; Hashimoto, K. R (-)-Ketamine Shows Greater Potency and Longer Lasting Antidepressant Effects than S (+)-Ketamine. *Pharmacol. Biochem. Behav.* **2014**, *116*, 137–141. https://doi.org/10.1016/j.pbb.2013.11.033 (accessed Jul 21, 2020).

(34) Molero, P.; Ramos-Quiroga, J. A.; Martin-Santos, R.; Calvo-Sánchez, E.; Gutiérrez-Rojas, L.; Meana, J. J. Antidepressant Efficacy and Tolerability of Ketamine and Esketamine: A Critical Review. *CNS Drugs* **2018**, *32* (5), 411–420. https://doi.org/10.1007/s40263-018-0519-3 (accessed Jul 21, 2020).

(35) Muller, J.; Pentyala, S.; Dilger, J.; Pentyala, S. Ketamine Enantiomers in the Rapid and Sustained Antidepressant Effects. *Ther. Adv. Psychopharmacol.* **2016**, *6* (3), 185–192. https://doi.org/10.1177/2045125316631267 (accessed Jul 21, 2020).

(36) Truong, T. P.; Bailey, S. J.; Golliher, A. E.; Monroy, E. Y.; Shrestha, U. K.; Maio, W. A. Exploiting Carvone To Demonstrate Both Stereocontrol and Regiocontrol: 1,2- vs 1,4-Addition of Grignard Reagents and Organocuprates. *J. Chem. Educ.* 2018, 95 (3), 438–444. https://doi.org/10.1021/acs.jchemed.7b00892 (accessed Jul 26, 2020).

(37) Andersh, B.; Bosma, W. B.; Hammar, M. K.; Graves, J. A.; Moon, K. N.; Newborn, C. R. Addition of "HOBr" to Trans-Anethole: Investigation of the Regioselectivity and the Stereoselectivity of an Addition Reaction. *J. Chem. Educ.* **2013**, *90* (11), 1504–1508. https://doi.org/10.1021/ed3003435 (accessed Jul 26, 2020).

(38) Paull, D. H.; Fang, C.; Donald, J. R.; Pansick, A. D.; Martin, S. F. Bifunctional Catalyst Promotes Highly Enantioselective Bromolactonizations To Generate Stereogenic C–Br Bonds. *J. Am. Chem. Soc.* **2012**, *134* (27), 11128–11131. https://doi.org/10.1021/ja305117m (accessed Jul 26, 2020).

(39) Fu, D.-J.; Fu, L.; Liu, Y.-C.; Wang, J.-W.; Wang, Y.-Q.; Han, B.-K.; Li, X.-R.; Zhang, C.; Li, F.; Song, J.; Zhao, B.; Mao, R.-W.; Zhao, R.-H.; Zhang, S.-Y.; Zhang, L.; Zhang, Y.-B.; Liu, H.-M. Structure-Activity Relationship Studies of β -Lactam-Azide Analogues as

Orally Active Antitumor Agents Targeting the Tubulin Colchicine Site. *Sci. Rep.* **2017**, *7* (1), 12788. https://doi.org/10.1038/s41598-017-12912-4 (accessed Jul 26, 2020).

(40)   Willson, C. Sympathomimetic Amine Compounds and Hepatotoxicity: Not All Are Alike—Key Distinctions Noted in a Short Review. *Toxicol. Rep.* **2019**, *6*, 26–33. https://doi.org/10.1016/j.toxrep.2018.11.013 (accessed Jul 26, 2020).

(41)   Heuger, G.; Kalsow, S.; Göttlich, R. Copper(I) Catalysts for the Stereoselective Addition of N-Chloroamines to Double Bonds: A Diastereoselective Radical Cyclisation. *Eur. J. Org. Chem.* **2002**, *2002* (11), 1848–1854. https://doi.org/10.1002/1099-0690(200206)2002:11<1848::AID-EJOC1848>3.0.CO;2-V (accessed Jul 26, 2020).

(42)   Denmark, S. E.; Edwards, M. G. On the Mechanism of the Selenolactonization Reaction with Selenenyl Halides. *J. Org. Chem.* **2006**, *71* (19), 7293–7306. https://doi.org/10.1021/jo0610457 (accessed Jul 26, 2020).

(43)   Xu, C.; Shen, Q. Lewis Acid Mediated Trifluoromethylthio Lactonization/Lactamization. *Org. Lett.* **2015**, *17* (18), 4561–4563. https://doi.org/10.1021/acs.orglett.5b02315 (accessed Jul 26, 2020).

(44)   Hemric, B. N.; Shen, K.; Wang, Q. Copper-Catalyzed Amino Lactonization and Amino Oxygenation of Alkenes Using O-Benzoylhydroxylamines. *J. Am. Chem. Soc.* **2016**, *138* (18), 5813–5816. https://doi.org/10.1021/jacs.6b02840 (accessed Jul 26, 2020).

(45)   Sha, W.; Shengyang, N.; Han, J.; and Pan, Y. Access to Alkyl-Substituted Lactone via Photoredox-Catalyzed Alkylation/Lactonization of Unsaturated Carboxylic Acids. *Org. Let.* **2017**, *19* (21), 5900-5903. https://pubs-acs-org.ezp.lib.cwu.edu/doi/10.1021/acs.orglett.7b02899 (accessed Jul 27, 2020).

(46)   Xing, L.; Zhang, Y.; Li, B.; Du, Y. Synthesis of 4-Chloroisocoumarins via Intramolecular Halolactonization of o-Alkynylbenzoates: PhICl2-Mediated C–O/C–Cl Bond Formation. *Org. Lett.* **2019**, *21* (7), 1989–1993. https://doi.org/10.1021/acs.orglett.9b00047 (accessed Jul 27, 2020).

(47)   Gan, M.; Wang, W.; Wang, H.; Wang, Y.; Jiang, X. Enantioselective Halolactonizations Using Amino-Acid-Derived Phthalazine Catalysts. *Org. Lett.* **2019**, *21* (20), 8275–8279. https://doi.org/10.1021/acs.orglett.9b03028 (accessed Jul 27, 2020).

(48)   Logan, A. W. J.; Sprague, S. J.; Foster, R. W.; Marx, L. B.; Garzya, V.; Hallside, M. S.; Thompson, A. L.; Burton, J. W. Diastereoselective Synthesis of Fused Lactone-Pyrrolidinones; Application to a Formal Synthesis of (−)-Salinosporamide A. *Org. Lett.* **2014**, *16* (16), 4078–4081. https://doi.org/10.1021/ol501662t (accessed Jul 27, 2020).

(49)   Dekeukeleire, S.; D'hooghe, M.; De Kimpe, N. Diastereoselective Synthesis of Bicyclic γ-Lactams via Ring Expansion of Monocyclic β-Lactams. *J. Org. Chem.* **2009**, *74* (4), 1644–1649. https://doi.org/10.1021/jo802459j (accessed Jul 27, 2020).

(50)   Gilley, C. B.; Kobayashi, Y. 2-Nitrophenyl Isocyanide as a Versatile Convertible Isocyanide: Rapid Access to a Fused γ-Lactam β-Lactone Bicycle. *J. Org. Chem.* **2008**, *73* (11), 4198–4204. https://doi.org/10.1021/jo800486k (accessed Jul 27, 2020).

(51)   Gilley, C. B.; Buller, M. J.; Kobayashi, Y. New Entry to Convertible Isocyanides for the Ugi Reaction and Its Application to the Stereocontrolled Formal Total Synthesis of the Proteasome Inhibitor Omuralide. *Org. Lett.* **2007**, *9* (18), 3631–3634. https://doi.org/10.1021/ol701446y (accessed Jul 27, 2020).

(52)   Wee, A. G. H.; Fan, G.-J.; Bayirinoba, H. M. Nonracemic Bicyclic Lactam Lactones via Regio- and Cis-Diastereocontrolled C−H Insertion. Asymmetric Synthesis of (8S,8aS)-

Octahydroindolizidin-8-Ol and (1S,8aS)-Octahydroindolizidin-1-Ol. *J. Org. Chem.* **2009**, *74* (21), 8261–8271. https://doi.org/10.1021/jo901790g (accessed Jul 27, 2020).

(53)   Andrews, D. M.; Carey, S. J.; Chaignot, H.; Coomber, B. A.; Gray, N. M.; Hind, S. L.; Jones, P. S.; Mills, G.; Robinson, J. E.; Slater, M. J. Pyrrolidine-5,5-Trans-Lactams. 1. Synthesis and Incorporation into Inhibitors of Hepatitis C Virus NS3/4A Protease. *Org. Lett.* **2002**, *4* (25), 4475–4478. https://doi.org/10.1021/ol027013x (accessed Jul 27, 2020).

(54)   Yuan, Q.; Sigman, M. S. Palladium-Catalyzed Enantioselective Relay Heck Arylation of Enelactams: Accessing α,β-Unsaturated δ-Lactams. *J. Am. Chem. Soc.* **2018**, *140* (21), 6527–6530. https://doi.org/10.1021/jacs.8b02752 (accessed Jul 27, 2020).

(55)   Pass, M.; Abu-Rabie, S.; Baxter, A.; Conroy, R.; Coote, S. J.; Craven, A. P.; Finch, H.; Hindley, S.; Kelly, H. A.; Lowdon, A. W.; et al. Thrombin Inhibitors Based on [5,5] Trans-Fused Indane Lactams. *Bioorg. Med. Chem. Lett.* **1999**, *9* (12), 1657–1662. https://doi.org/10.1016/S0960-894X(99)00244-9 (accessed Jul 27, 2020).

(56)   Townsend, C. A. Convergent Biosynthetic Pathways to β-Lactam Antibiotics. *Curr. Opin. Chem. Biol.* **2016**, *35*, 97–108. https://doi.org/10.1016/j.cbpa.2016.09.013 (accessed Jul 27, 2020).

(57)   Wang, D. Y.; Abboud, M. I.; Markoulides, M. S.; Brem, J.; Schofield, C. J. The Road to Avibactam: The First Clinically Useful Non-β-Lactam Working Somewhat like a β-Lactam. *Future Med. Chem.* **2016**, *8* (10), 1063–1084. https://doi.org/10.4155/fmc-2016-0078 (accessed Jul 27, 2020).

(58)   Fantinati, A.; Zanirato, V.; Marchetti, P.; Trapella, C. The Fascinating Chemistry of α-Haloamides. *ChemistryOpen* **2020**, *9* (2), 100–170. https://doi.org/10.1002/open.201900220 (accessed Jul 27, 2020).

(59)   Onyango, E. O.; Tsurumoto, J.; Imai, N.; Takahashi, K.; Ishihara, J.; Hatakeyama, S. Total Synthesis of Neooxazolomycin. *Angew. Chem. Int. Ed.* **2007**, *46* (35), 6703–6705. https://doi.org/10.1002/anie.200702229 (accessed Jul 27, 2020).

(60)   Legeay, J.-C.; Langlois, N. Nitrone [2+3]-Cycloadditions in Stereocontrolled Synthesis of a Potent Proteasome Inhibitor: (−)-Omuralide. *J. Org. Chem.* **2007**, *72* (26), 10108–10113. https://doi.org/10.1021/jo701968d (accessed Jul 27, 2020).

(61)   Jang, J.-H.; Kanoh, K.; Adachi, K.; Shizuri, Y. Awajanomycin, a Cytotoxic γ-Lactone-δ-Lactam Metabolite from Marine-Derived Acremonium Sp. AWA16-1. *J. Nat. Prod.* **2006**, *69* (9), 1358–1360. https://doi.org/10.1021/np060170a (accessed Jul 27, 2020).

(62)   Center for Disease Control. Life Expectancy at Birth, at Age 65, and at Age 75, by Sex, Race, and Hispanic Origin: United States, Selected Years 1900–2017. https://www.cdc.gov/nchs/data/hus/2017/015.pdf (accessed Jul 27, 2020).

(63)   Baldwin, J. E.; Lynch, G. P.; Pitlik, J. γ-Lactam Analogues of β-Lactam Antibiotics. *J. Antibiot.* **1991**, *44* (1), 1-24. https://doi.org/10.7164/antibiotics.44.1 (accessed Jul 27, 2020).

(64)   Imming, P.; Klar, B.; Dix, D. Hydrolytic Stability versus Ring Size in Lactams: Implications for the Development of Lactam Antibiotics and Other Serine Protease Inhibitors. *J. Med. Chem.* **2000**, *43* (22), 4328–4331. https://doi.org/10.1021/jm000921k (accessed Jul 27, 2020).

(65)   Aszodi, J.; Rowlands, D. A.; Mauvais, P.; Collette, P.; Bonnefoy, A.; Lampilas, M. Design and Synthesis of Bridged γ-Lactams as Analogues of β-Lactam Antibiotics. *Bioorg. Med. Chem. Lett.* **2004**, *14* (10), 2489–2492. https://doi.org/10.1016/j.bmcl.2004.03.004 (accessed Jul 27, 2020).

(66) Maier, M.; Carreira, E. M.; Panek, J. S. Three Carbon—Heteroatom Bonds: Acid Halides; Carboxylic Acids and Acid Salts / Esters and Lactones; Peroxy Acids and R(CO)OX Compounds; R(CO)X, X = S, Se, Te. *Science of Synthesis*; Thieme: Stuttgart, 2010; Vol. 20, pp 1421–1551 (accessed Jul 27, 2020).

(67) French, A. N.; Bissmire, S.; Wirth, T. Iodine Electrophiles in Stereoselective Reactions: Recent Developments and Synthetic Applications. *Chem. Soc. Rev.* **2004**, *33* (6), 354–362. https://doi.org/10.1039/B310389G (accessed Jul 27, 2020).

(68) Murai, K.; Fujioka, H. Recent Progress in Organocatalytic Asymmetric Halocyclization. *Heterocycles* **2013**, *87* (4), 763–805. https://doi.org/10.3987/REV-12-762.

(69) Cheng, Y. A.; Yu, W. Z.; Yeung, Y.-Y. Recent Advances in Asymmetric Intra- and Intermolecular Halofunctionalizations of Alkenes. *Org. Biomol. Chem.* **2014**, *12* (15), 2333–2343. https://doi.org/10.1039/C3OB42335B (accessed Jul 27, 2020).

(70) Cushman, M.; Gentry, J.; Dekow, F. W. Condensation of Imines with Homophthalic Anhydrides. A Convergent Synthesis of Cis-and Trans-13-Methyltetrahydroprotoberberines. *J. Org. Chem.* **1977**, *42* (7), 1111–1116. https://doi.org/10.1021/jo00427a001 (accessed Jul 27, 2020).

(71) Castagnoli, N. The Condensation of Succinic Anhydride with Benzylidinemethylamine. A Stereoselective Synthesis of Trans- and Cis-1-Methyl-4-Carboxy-5-Phenyl-2-Pyrrolidinone. *J. Org. Chem.* **1969**, *34* (10), 3187–3189. https://doi.org/10.1021/jo01262a081 (accessed Jul 27, 2020).

(72) Sorto, N. A.; Di Maso, M. J.; Muñoz, M. A.; Dougherty, R. J.; Fettinger, J. C.; Shaw, J. T. Diastereoselective Synthesis of γ- And δ-Lactams from Imines and Sulfone-Substituted Anhydrides. *J. Org. Chem.* **2014**, *79* (6), 2601–2610. https://doi.org/10.1021/jo500050n (accessed Jul 27, 2020).

(73) Tan, D. Q.; Younai, A.; Pattawong, O.; Fettinger, J. C.; Cheong, P. H. Y.; Shaw, J. T. Stereoselective Synthesis of γ-Lactams from Imines and Cyanosuccinic Anhydrides. *Org. Lett.* **2013**, *15* (19), 5126–5129. https://doi.org/10.1021/ol402554n (accessed Jul 27, 2020).

(74) Cushman, M.; Castagnoli, N. Synthesis of Pharmacologically Active Nitrogen Analogs of the Tetrahydrocannabinols. *J. Org. Chem.* **1974**, *39* (11), 1546–1550. https://doi.org/10.1021/jo00924a021 (accessed Jul 27, 2020).

(75) Dar'In, D.; Bakulina, O.; Chizhova, M.; Krasavin, M. New Heterocyclic Product Space for the Castagnoli-Cushman Three-Component Reaction. *Org. Lett.* **2015**, *17* (15), 3930–3933. https://doi.org/10.1021/acs.orglett.5b02014 (accessed Sep 25, 2020).

(76) Adamovskyi, M. I.; Ryabukhin, S. V.; Sibgatulin, D. A.; Rusanov, E.; Grygorenko, O. O. Beyond the Five and Six: Evaluation of Seven-Membered Cyclic Anhydrides in the Castagnoli-Cushman Reaction. *Org. Lett.* **2017**, *19* (1), 130–133. https://doi.org/10.1021/acs.orglett.6b03426 (accessed Sep 25, 2020).

(77) Braunstein, H.; Langevin, S.; Khim, M.; Adamson, J.; Hovenkotter, K.; Kotlarz, L.; Mansker, B.; Beng, T. K. Modular Access to Vicinally Functionalized Allylic (Thio)Morpholinonates and Piperidinonates by Substrate-Controlled Annulation of 1,3-Azadienes with Hexacyclic Anhydrides. *Org. Biomol. Chem.* **2016**, *14* (37), 8864–8872. https://doi.org/10.1039/C6OB01526C (accessed Sep 25, 2020).

(78) Beng, T. K.; Moreno, A. Copper-Catalyzed Alkenylation of Novel N-Iodoarylated Allylic Ketopiperazinonates with Unactivated Alkenes. *New J. Chem.* **2020**, *44* (11), 4257–4261. https://doi.org/10.1039/C9NJ06178A (accessed Sep 25, 2020).

(79) Omar Farah, A.; Archibald, R.; J. Rodriguez, M.J.; Moreno, A.; Dondji, B.; Beng, T. Flexible Access to 2,3,5,6-Tetrasubstituted Dehydropiperidines by Ni- or Co-Catalyzed Site-Selective Cross-Coupling Using Vilsmeier-Haack-Derived α-Chloro-β-Formyltetrahydropyridines. *Tetrahedron Lett.* **2018**, *59* (38), 3495-3498. https://doi.org/10.1016/j.tetlet.2018.08.023 (accessed Sep 25, 2020).

(80) Hovenkotter, K.; Braunstein, H.; Langevin, S.; Beng, T. K. Expedient and Modular Access to 2-Azabicyclic Architectures by Iron-Catalyzed Dehydrative Coupling of Alcohol-Bearing Allylic Lactams. *Org. Biomol. Chem.* **2017**, *15* (5), 1217–1221. https://doi.org/10.1039/C6OB02652D (accessed Sep 25, 2020).

(81) Beng, T. K.; Bauder, M.; Rodriguez, M. J.; Moreno, A. Copper-Catalyzed Regioselective Dehydrogenative Alkoxylation of Morpholinonyl Alkenols: Application to the Synthesis of Spirotricyclic Dihydropyrans and of Trans-Fused Bicyclic Morpholines. *New J. Chem.* **2018**, *42* (20), 16451–16455. https://doi.org/10.1039/C8NJ03890B (accessed Sep 25, 2020).

(82) Fang, C.; Paull, D. H.; Hethcox, J. C.; Shugrue, C. R.; Martin, S. F. Enantioselective Iodolactonization of Disubstituted Olefinic Acids Using a Bifunctional Catalyst. *Org. Lett.* **2012**, *14* (24), 6290–6293. https://doi.org/10.1021/ol3030555 (accessed Sep 25, 2020).

(83) Klosowski, D. W.; Hethcox, J. C.; Paull, D. H.; Fang, C.; Donald, J. R.; Shugrue, C. R.; Pansick, A. D.; Martin, S. F. Enantioselective Halolactonization Reactions Using BINOL-Derived Bifunctional Catalysts: Methodology, Diversification, and Applications. *J. Org. Chem.* **2018**, *83* (11), 5954-5968. https://doi.org/10.1021/acs.joc.8b00490 (accessed Sep 25, 2020).

(84) Klosowski, D. W.; Martin, S. F. Synthesis of (+)-Disparlure via Enantioselective Iodolactonization. *Org. Lett.* **2018**, *20* (5), 1269–1271. https://doi.org/10.1021/acs.orglett.7b03911 (accessed Sep 25, 2020).

(85) Yousefi, R.; Ashtekar, K. D.; Whitehead, D. C.; Jackson, J. E.; Borhan, B. Dissecting the Stereocontrol Elements of a Catalytic Asymmetric Chlorolactonization: Syn Addition Obviates Bridging Chloronium. *J. Am. Chem. Soc.* **2013**, *135* (39), 14524–14527. https://doi.org/10.1021/ja4072145 (accessed Sep 25, 2020).

(86) Veitch, G. E.; Jacobsen, E. N. Tertiary Aminourea-Catalyzed Enantioselective Iodolactonization. *Angew. Chem. Int. Ed.* **2010**, *49* (40), 7332–7335. https://doi.org/10.1002/anie.201003681 (accessed Sep 25, 2020).

(87) Nishikawa, Y.; Hamamoto, Y.; Satoh, R.; Akada, N.; Kajita, S.; Nomoto, M.; Miyata, M.; Nakamura, M.; Matsubara, C.; Hara, O. Enantioselective Bromolactonization of Trisubstituted Olefinic Acids Catalyzed by Chiral Pyridyl Phosphoramides. *Chem. – Eur. J.* **2018**, *24* (71), 18880–18885. https://doi.org/10.1002/chem.201804630 (accessed Sep 25, 2020).

(88) Denmark, S. E.; Ryabchuk, P.; Burk, M. T.; Gilbert, B. B. Toward Catalytic, Enantioselective Chlorolactonization of 1,2-Disubstituted Styrenyl Carboxylic Acids. *J. Org. Chem.* **2016**, *81* (21), 10411–10423. https://doi.org/10.1021/acs.joc.6b01455. (accessed Sep 25, 2020) (accessed Sep 25, 2020).

(89) Denmark, S. E.; Burk, M. T. Lewis Base Catalysis of Bromo- and Iodolactonization, and Cycloetherification. *Proc. Natl. Acad. Sci. U. S. A.* **2010**, *107* (48), 20655–20660. https://doi.org/10.1073/pnas.1005296107. (accessed Sep 25, 2020).

(90) Wishart, D. S.; Knox, C.; Guo, A. C.; Shrivastava, S.; Hassanali, M.; Stothard, P.; Chang, Z.; Woolsey, J. DrugBank: A Comprehensive Resource for in Silico Drug Discovery and

Exploration. *Nucleic Acids Res.* **2006**, *34* (Database issue), D668–D672. https://doi.org/10.1093/nar/gkj067 (accessed Sep 25, 2020).

(91) Beesley, R. M.; Ingold, C. K.; Thorpe, J. F. CXIX.—The Formation and Stability of Spiro-Compounds. Part I. Spiro-Compounds from Cyclohexane. *J. Chem. Soc. Trans.* **1915**, *107* (0), 1080–1106. https://doi.org/10.1039/CT9150701080. (accessed Sep 25, 2020).

(92) Fache, F.; Schulz, E.; Tommasino, M. L.; Lemaire, M. Nitrogen-Containing Ligands for Asymmetric Homogeneous and Heterogeneous Catalysis. *Chem. Rev.* **2000**, *100* (6), 2159–2232. https://doi.org/10.1021/cr9902897. (accessed Sep 25, 2020).

(93) González-López, M.; Shaw, J. T. Cyclic Anhydrides in Formal Cycloadditions and Multicomponent Reactions. *Chem. Rev.* **2009**, *109* (1), 164–189. https://doi.org/10.1021/cr8002714. (accessed Sep 25, 2020).

(94) Smith, F. T.; Atigadda, R. V. Condensation of Homophthalic Anhydrides with Heterocyclic Imines and DMAD under Mild Conditions. *J. Heterocycl. Chem.* **1991**, *28* (7), 1813–1815. https://doi.org/10.1002/jhet.5570280728. (accessed Sep 25, 2020).

(95) Sawama, Y.; Shibata, K.; Sawama, Y.; Takubo, M.; Monguchi, Y.; Krause, N.; Sajiki, H. Iron-Catalyzed Ring-Opening Azidation and Allylation of O-Heterocycles. *Org. Lett.* **2013**, *15* (20), 5282–5285. https://doi.org/10.1021/ol402511r. (accessed Sep 25, 2020).

SPECTROGRAPHIC DATA

3.1 Valerolactams
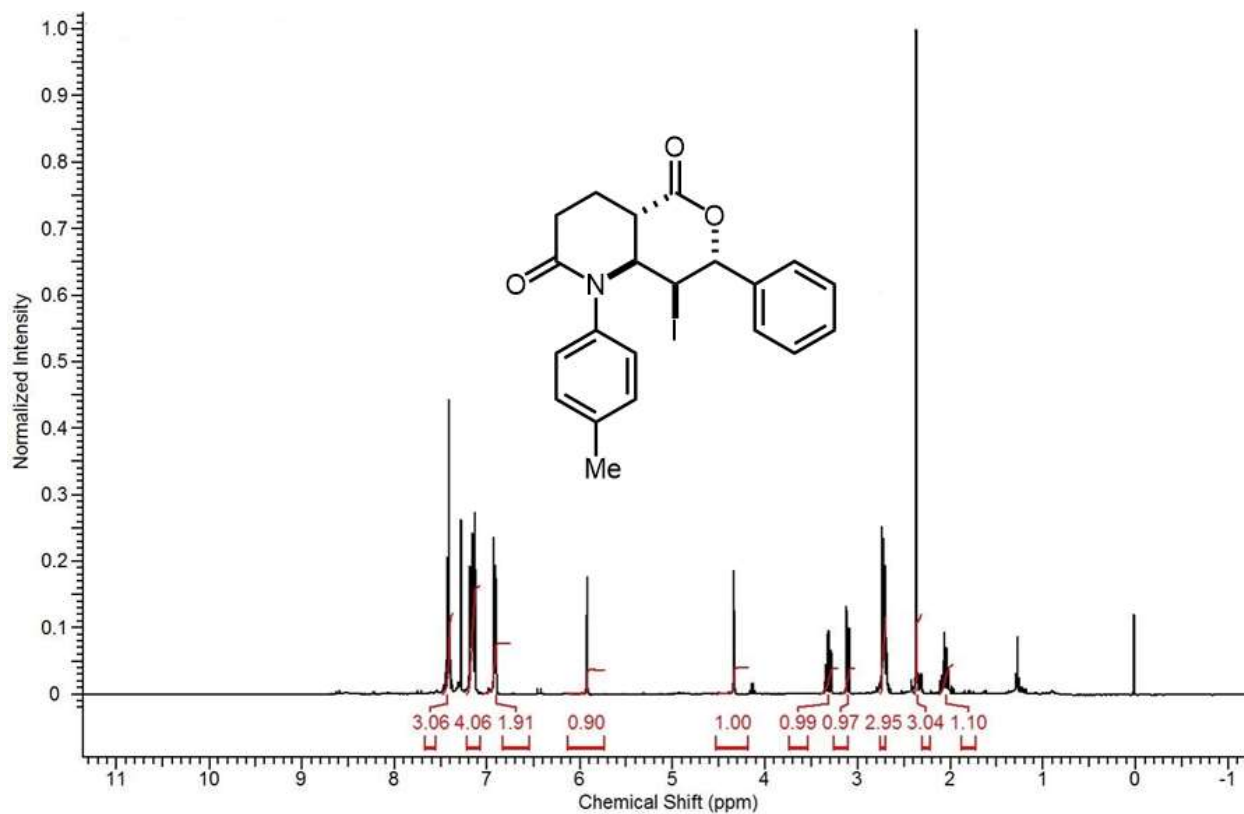
Spectra 3-1. ^{1}H-NMR spectrum for structure **9a**
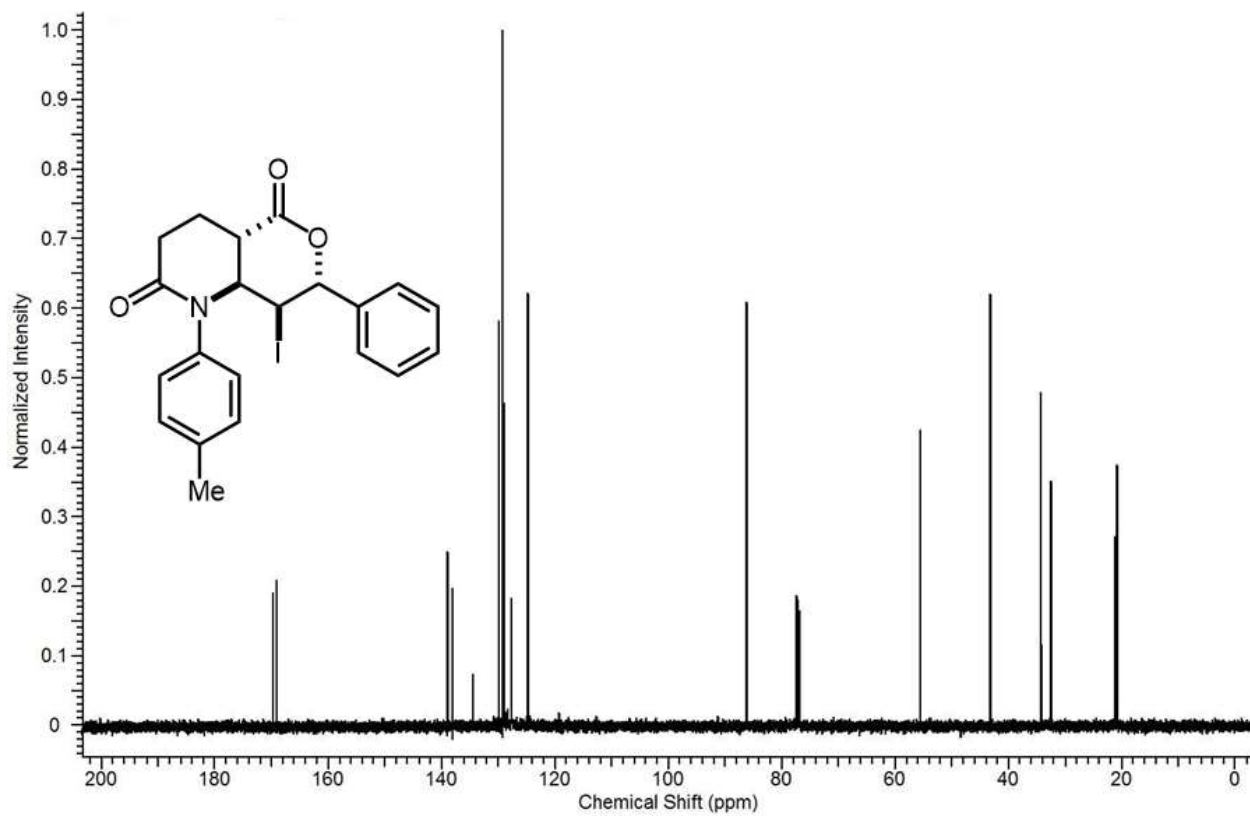
Spectra 3-2. ^{13}C-NMR spectrum of structure **9a**
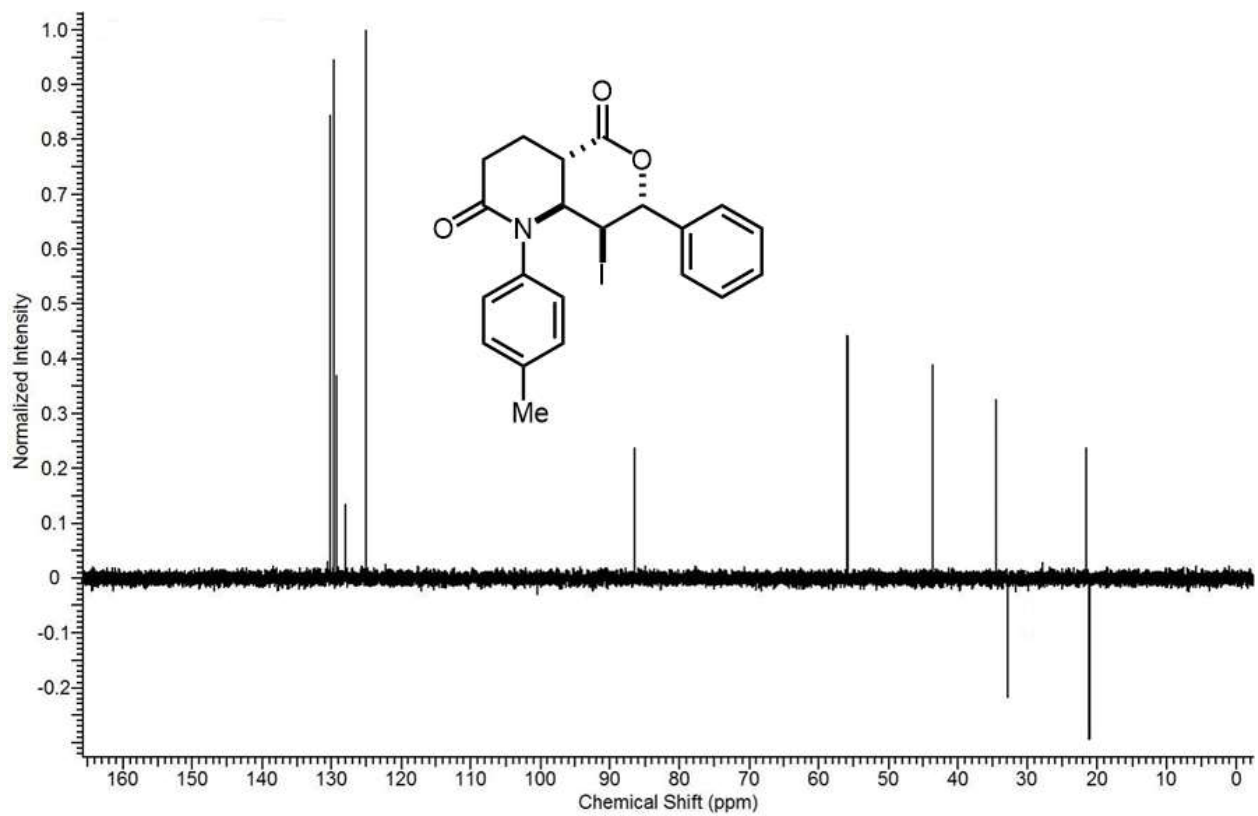
Spectra 3-3. DEPT-NMR spectrum of structure **9a**
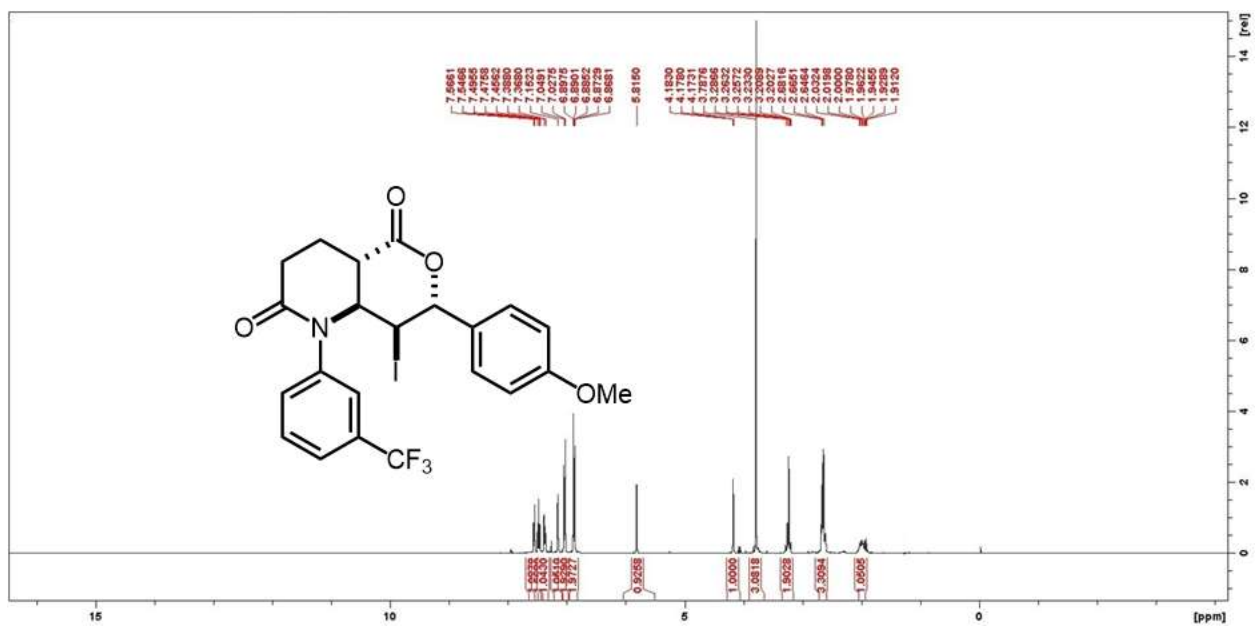
Spectra 3-4. ^{1}H-NMR spectrum for structure **9b**

Spectra 3-5. ^{13}C-NMR spectrum of structure **9b**

Spectra 3-6. DEPT-NMR spectrum of structure **9b**
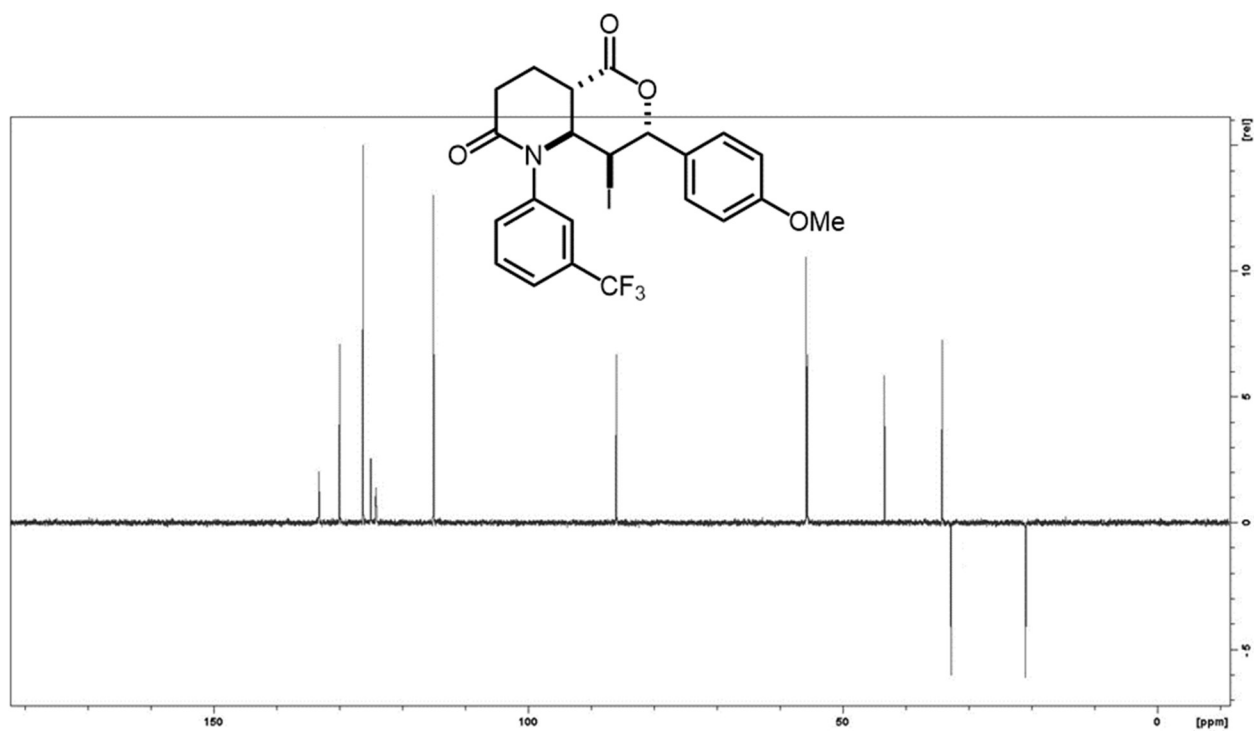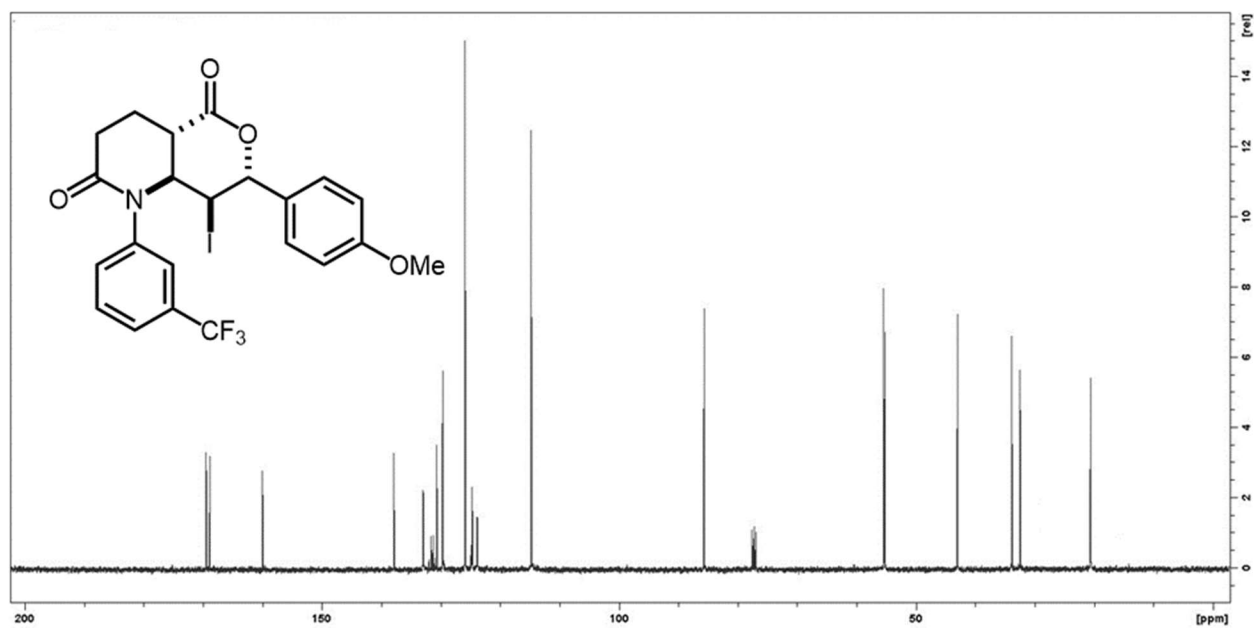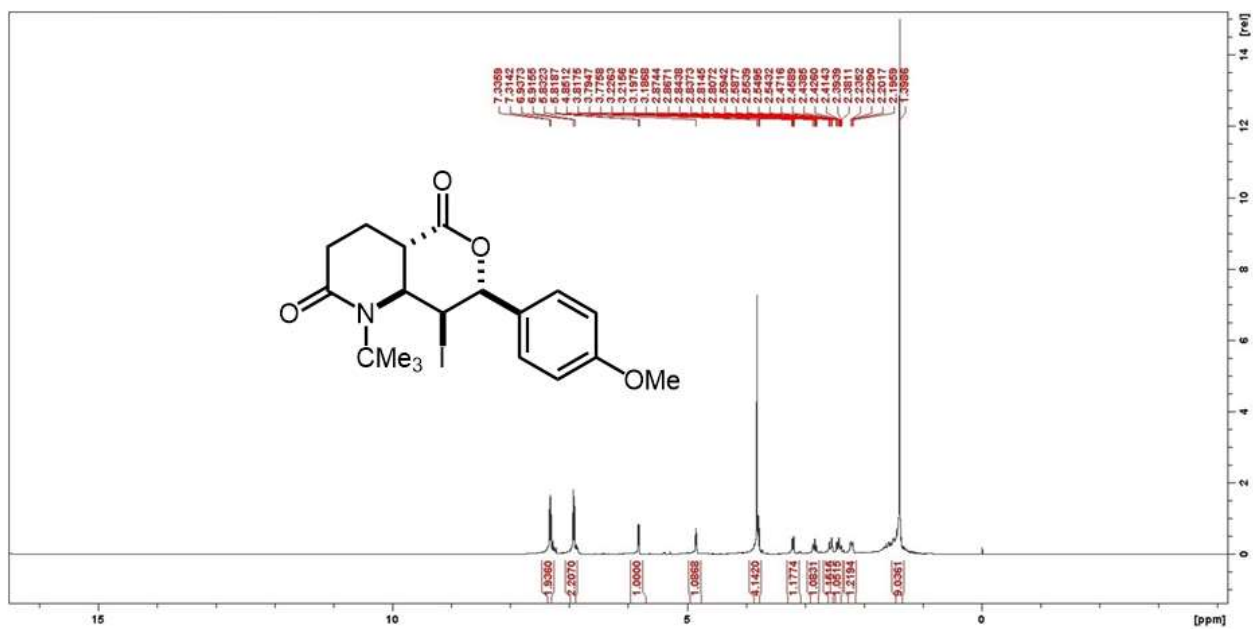
Spectra 3-7. ^{1}H-NMR spectrum for structure **9c**
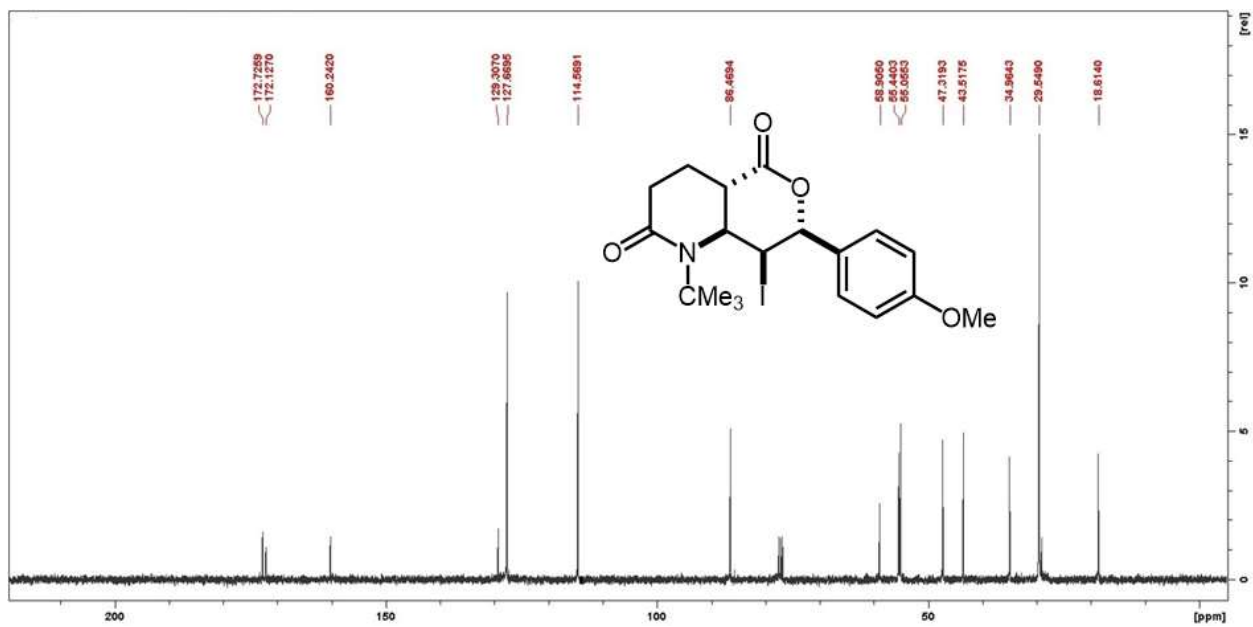
Spectra 3-8. ^{13}C-NMR spectrum of structure **9c**

68
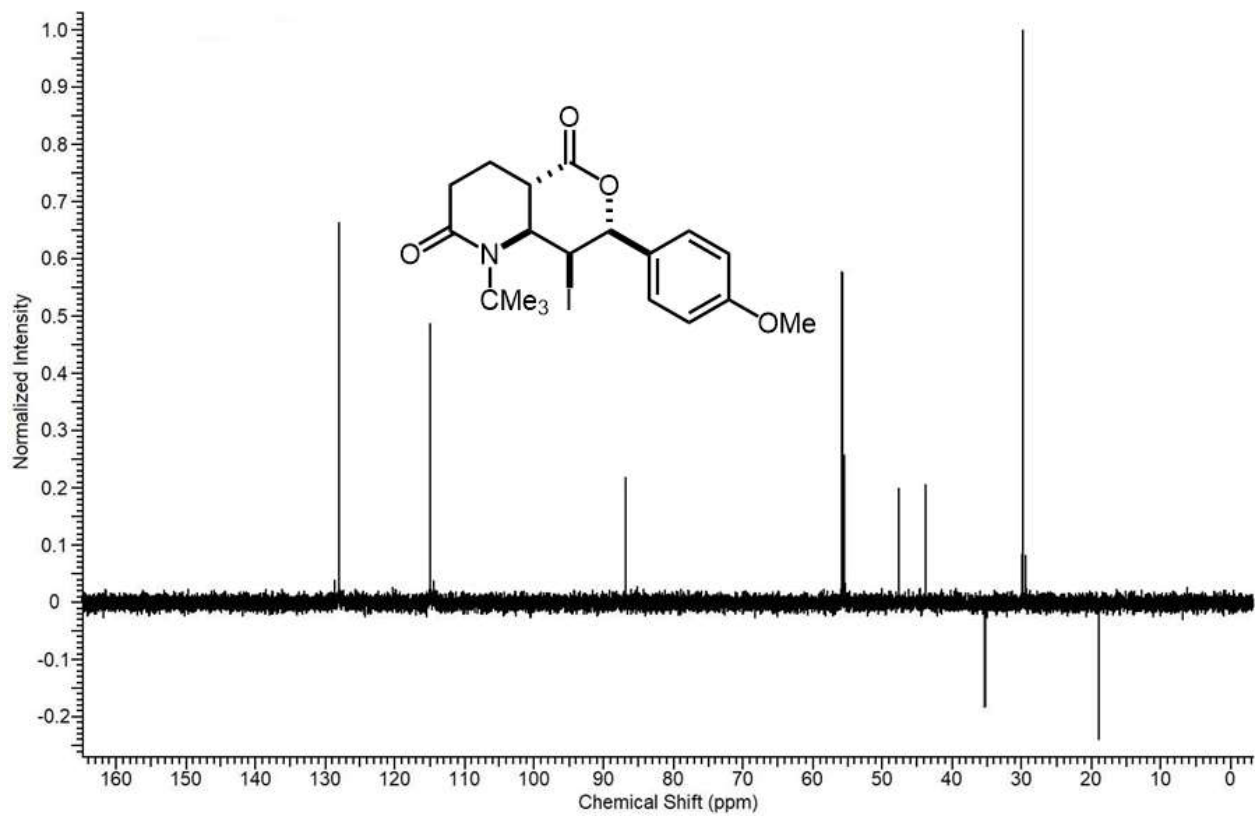
Spectra 3-9. DEPT-NMR spectrum of structure **9c**
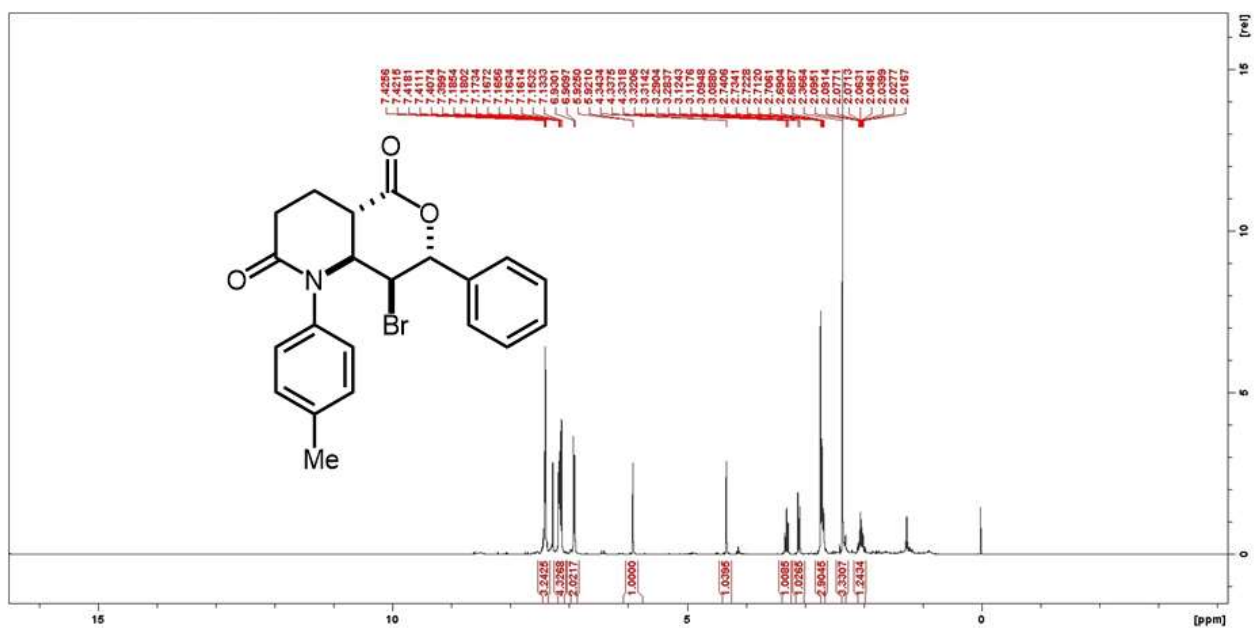
Spectra 3-10. ^{1}H-NMR spectrum for structure **9d**

69
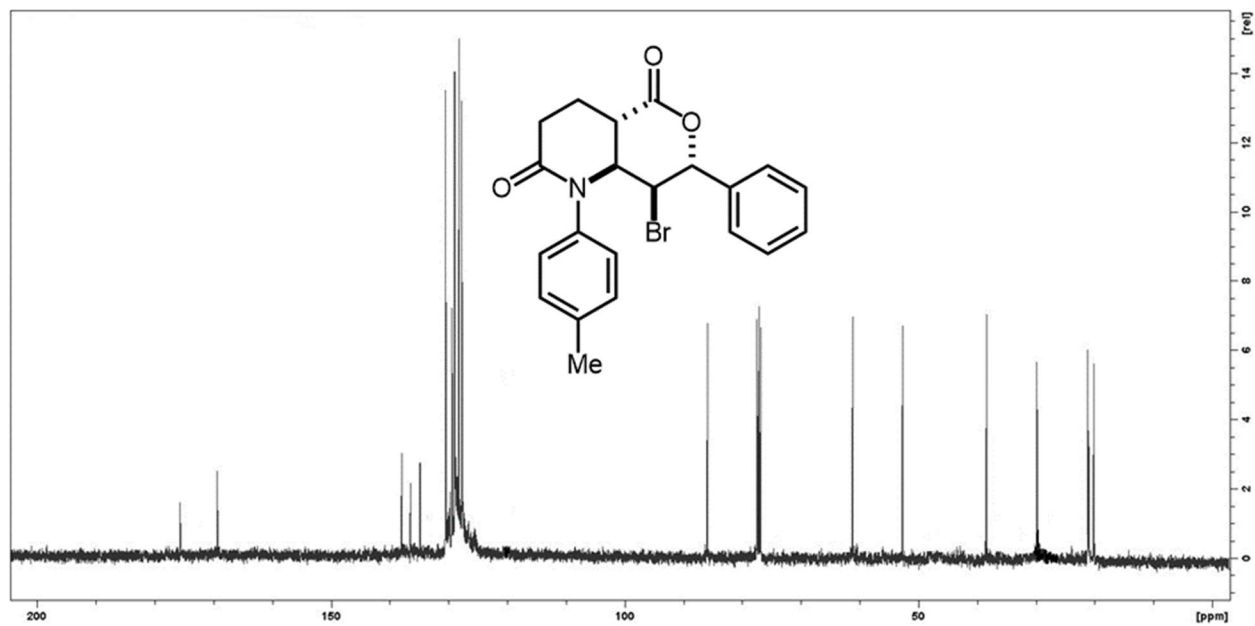
Spectra 3-11. ^{13}C-NMR spectrum of structure **9d**
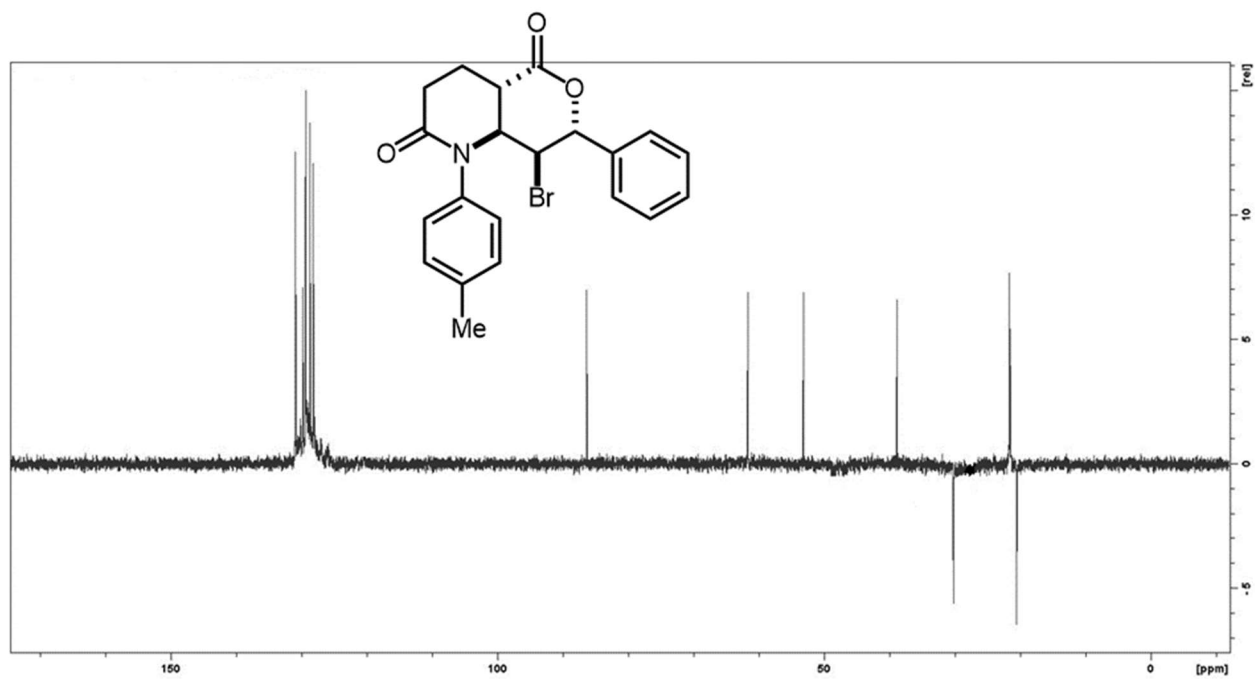
Spectra 3-12. DEPT-NMR spectrum of structure **9d**
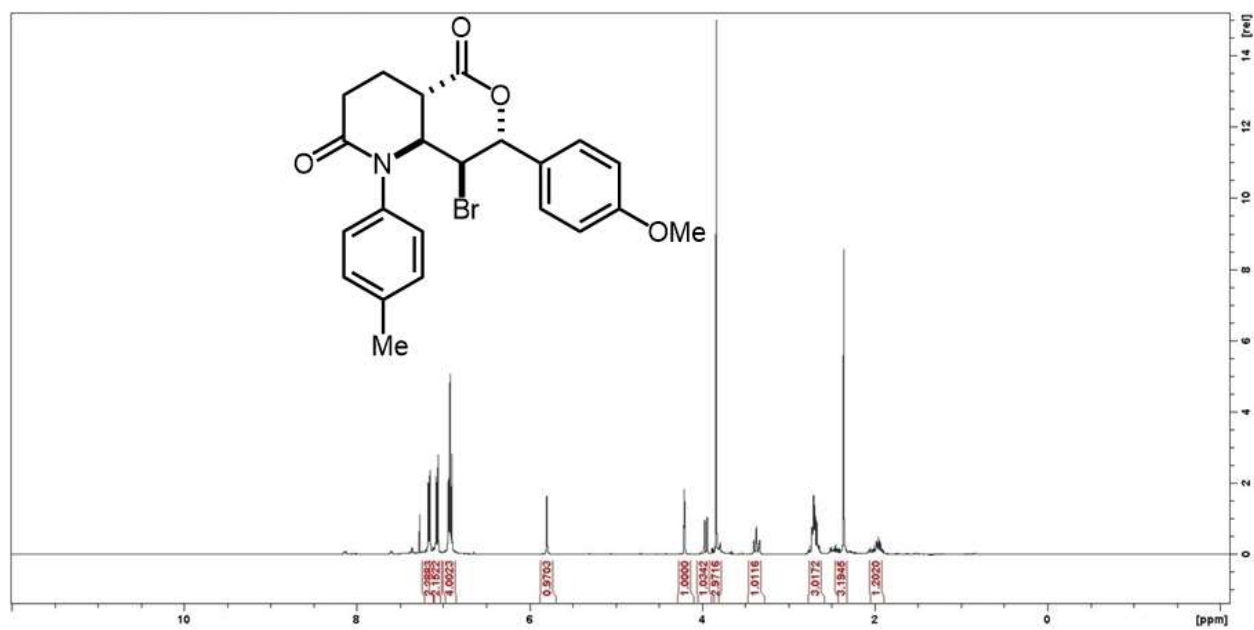
Spectra 3-13. ^{1}H-NMR spectrum for structure **9e**
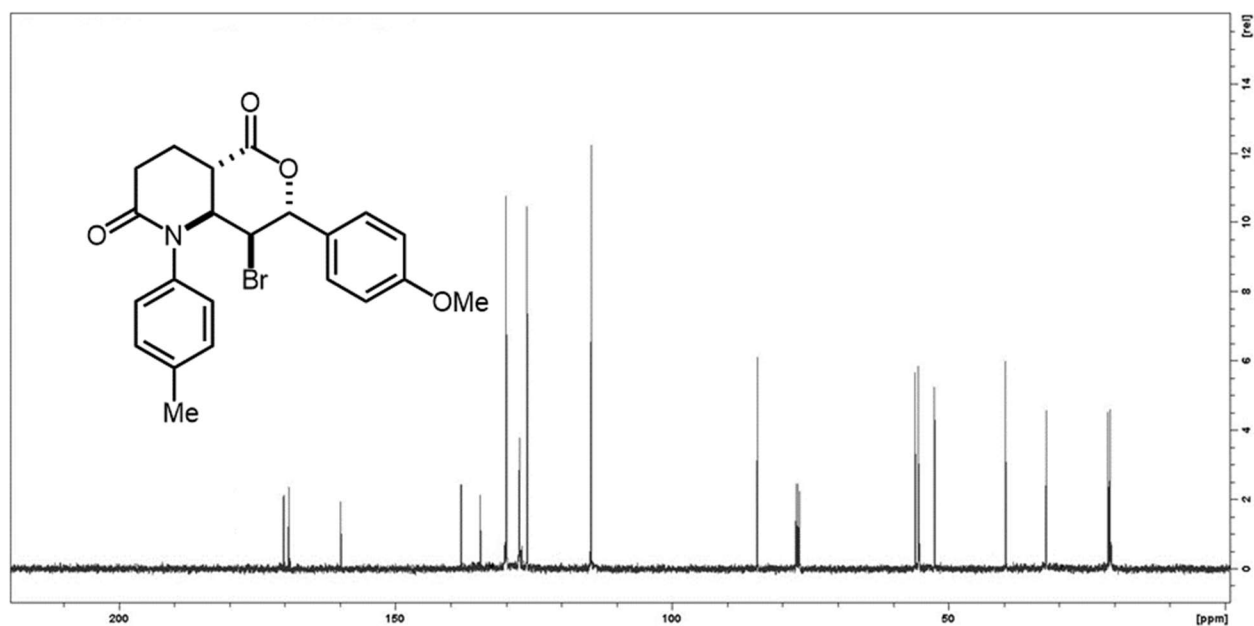
Spectra 3-14. ^{13}C-NMR spectrum of structure **9e**
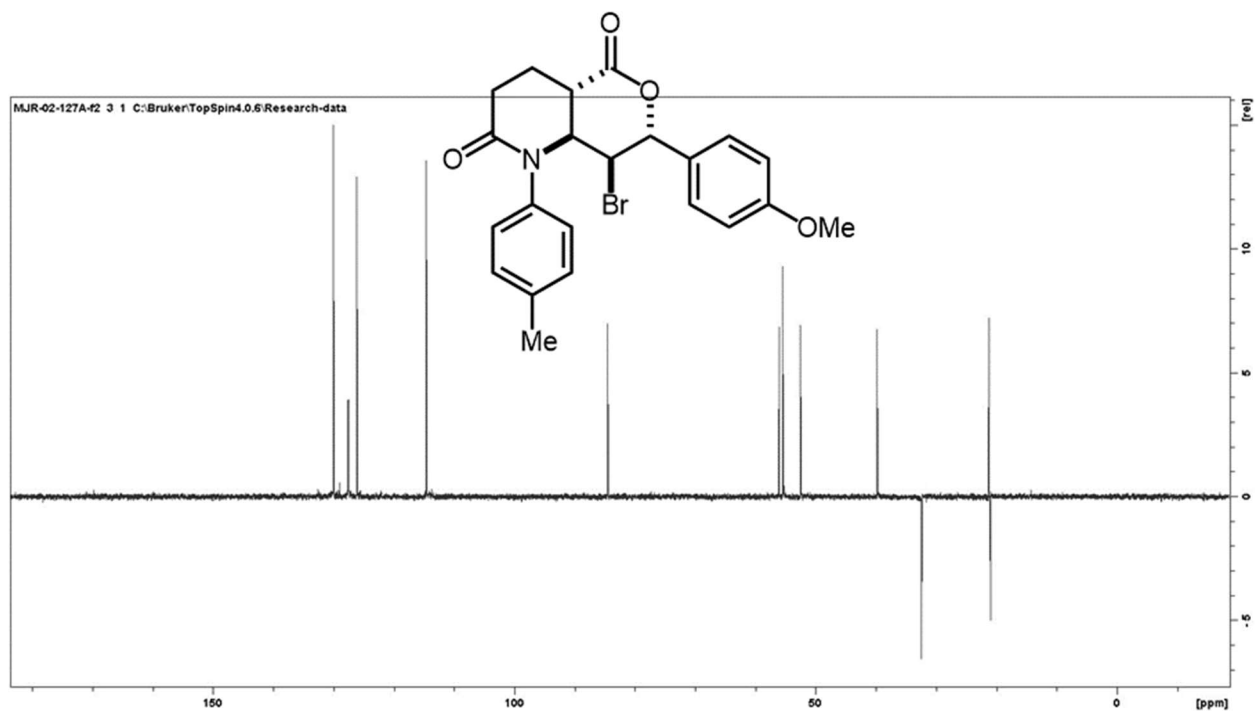
Spectra 3-15. DEPT-NMR spectrum of structure **9e**
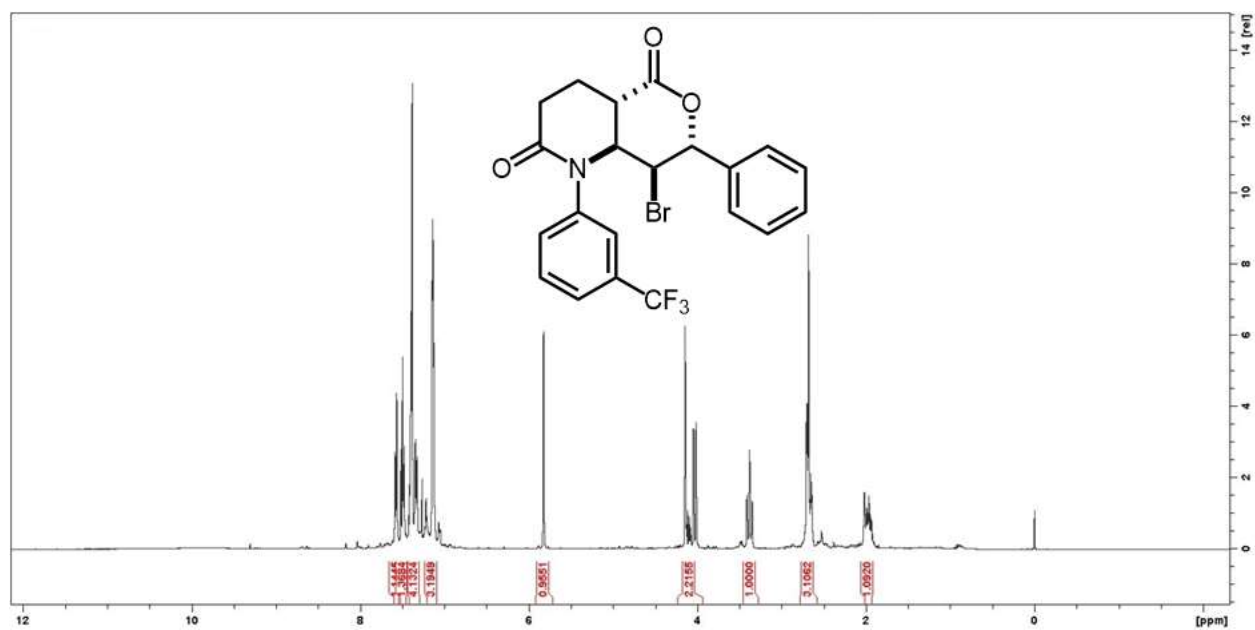
Spectra 3-16. ¹H-NMR spectrum for structure **9f**

Spectra 3-17. ^{13}C-NMR spectrum of structure **9f**

Spectra 3-18. DEPT-NMR spectrum of structure **9f**
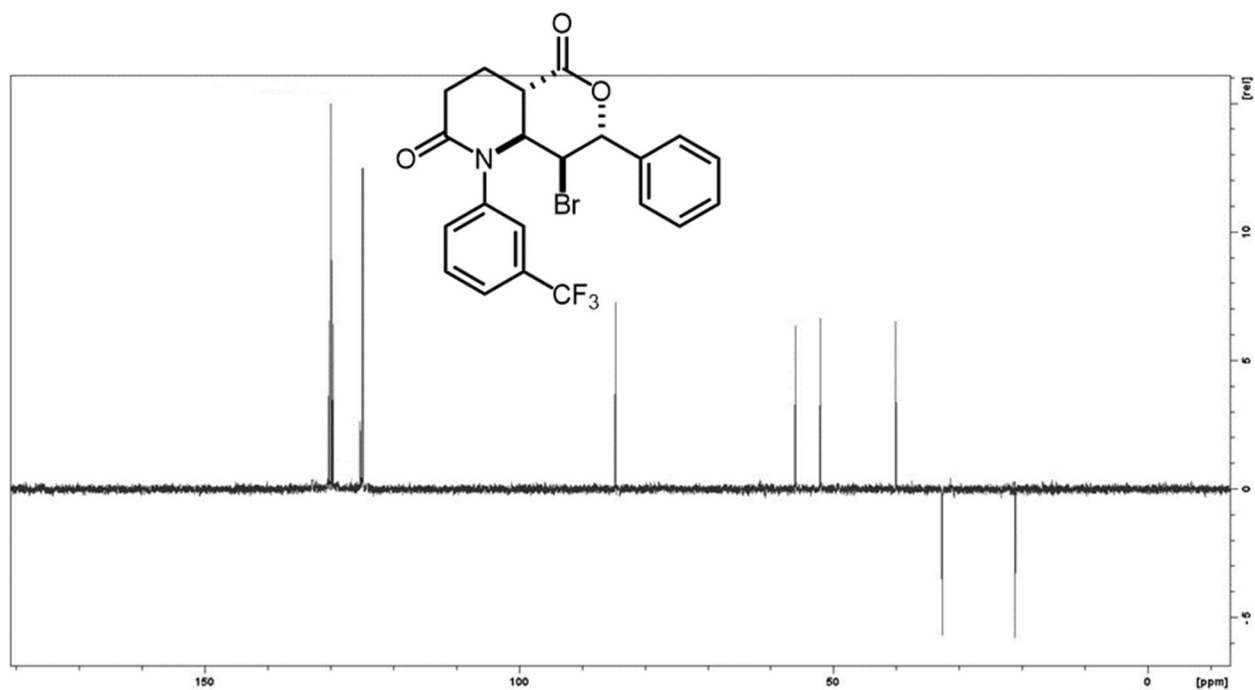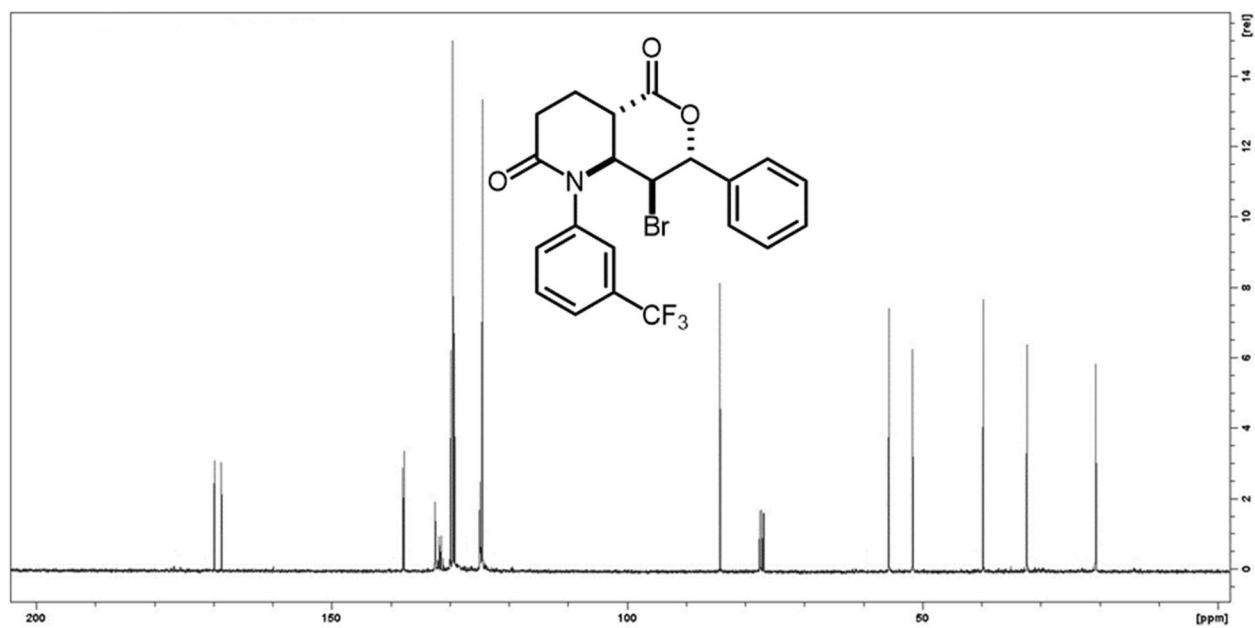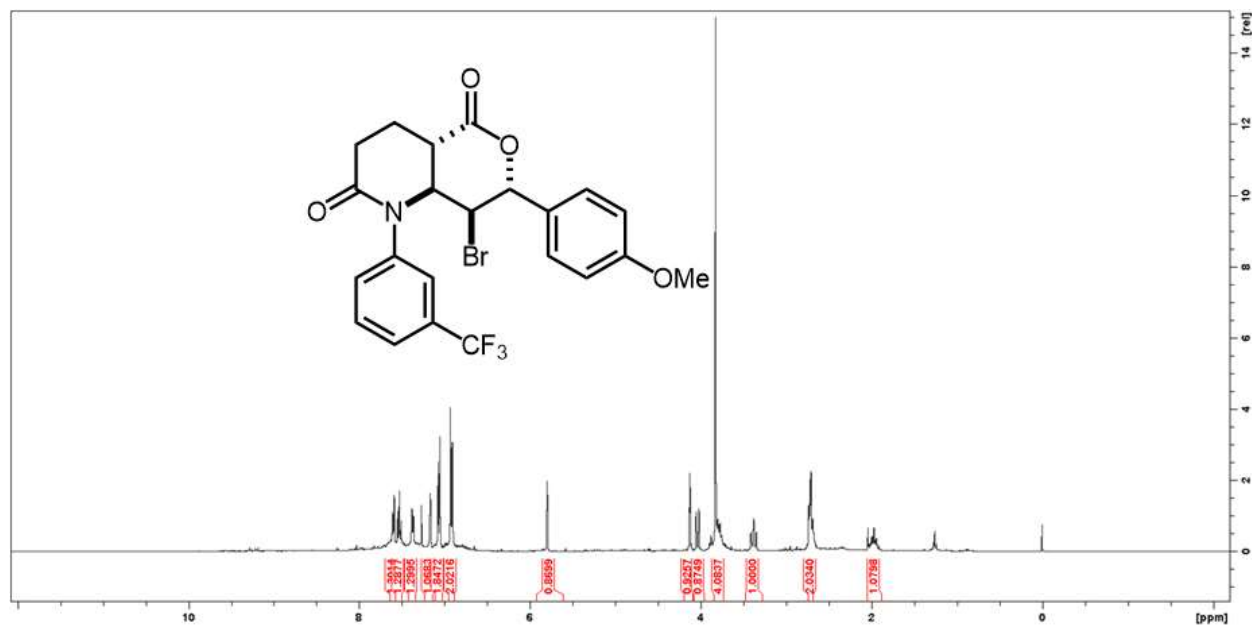
Spectra 3-19. ^{1}H-NMR spectrum for structure **9g**
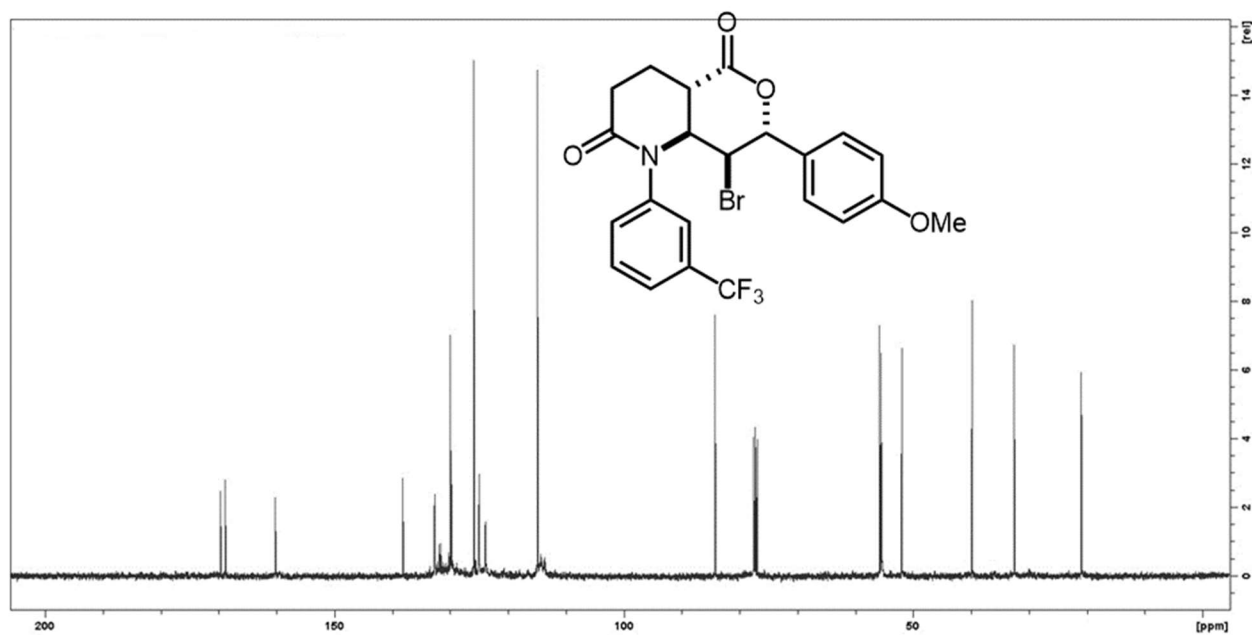
Spectra 3-20. ^{13}C-NMR spectrum of structure **9g**

74
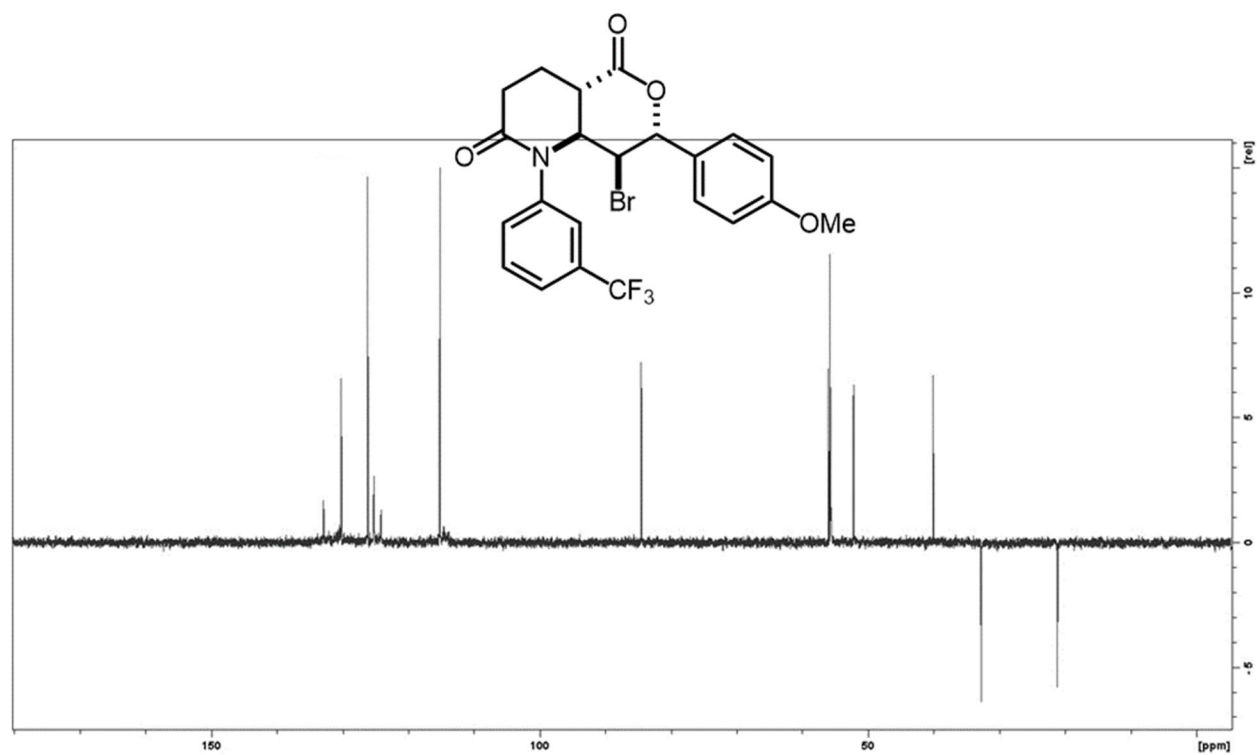
Spectra 3-21. DEPT-NMR spectrum of structure **9g**
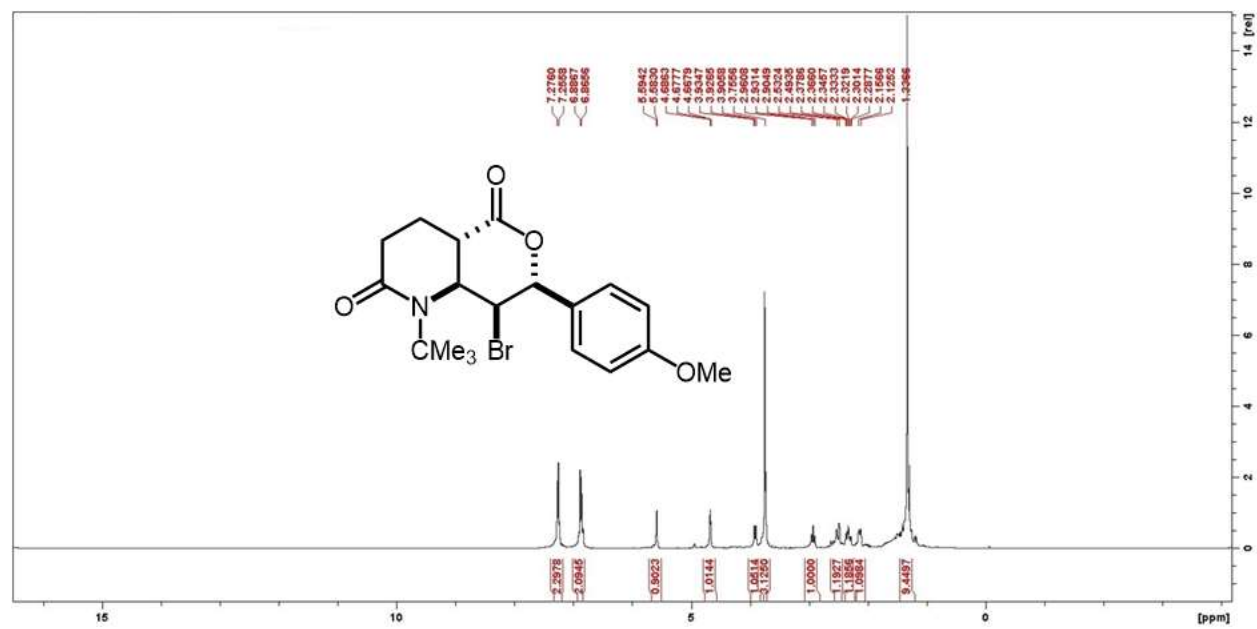
Spectra 3-22. ^{1}H-NMR spectrum for structure **9h**
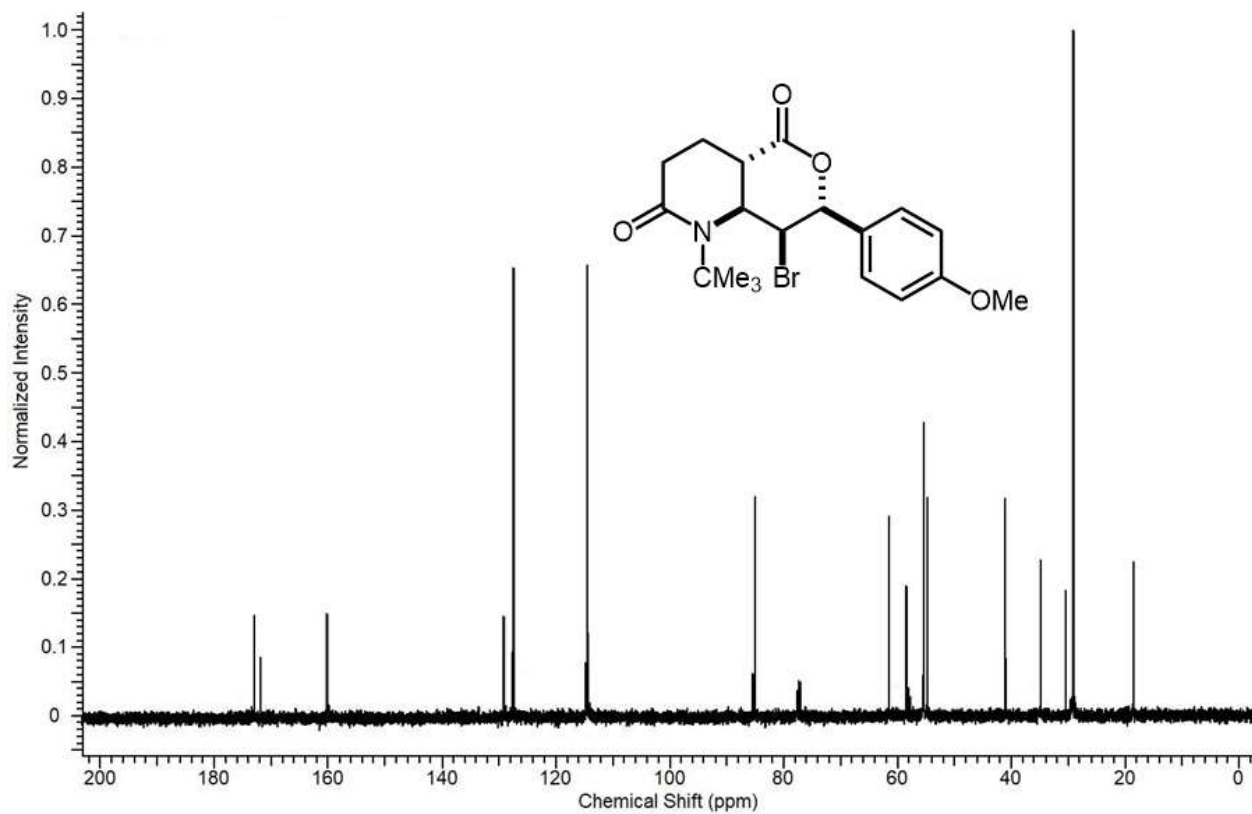
Spectra 3-23. ^{13}C-NMR spectrum of structure **9h**
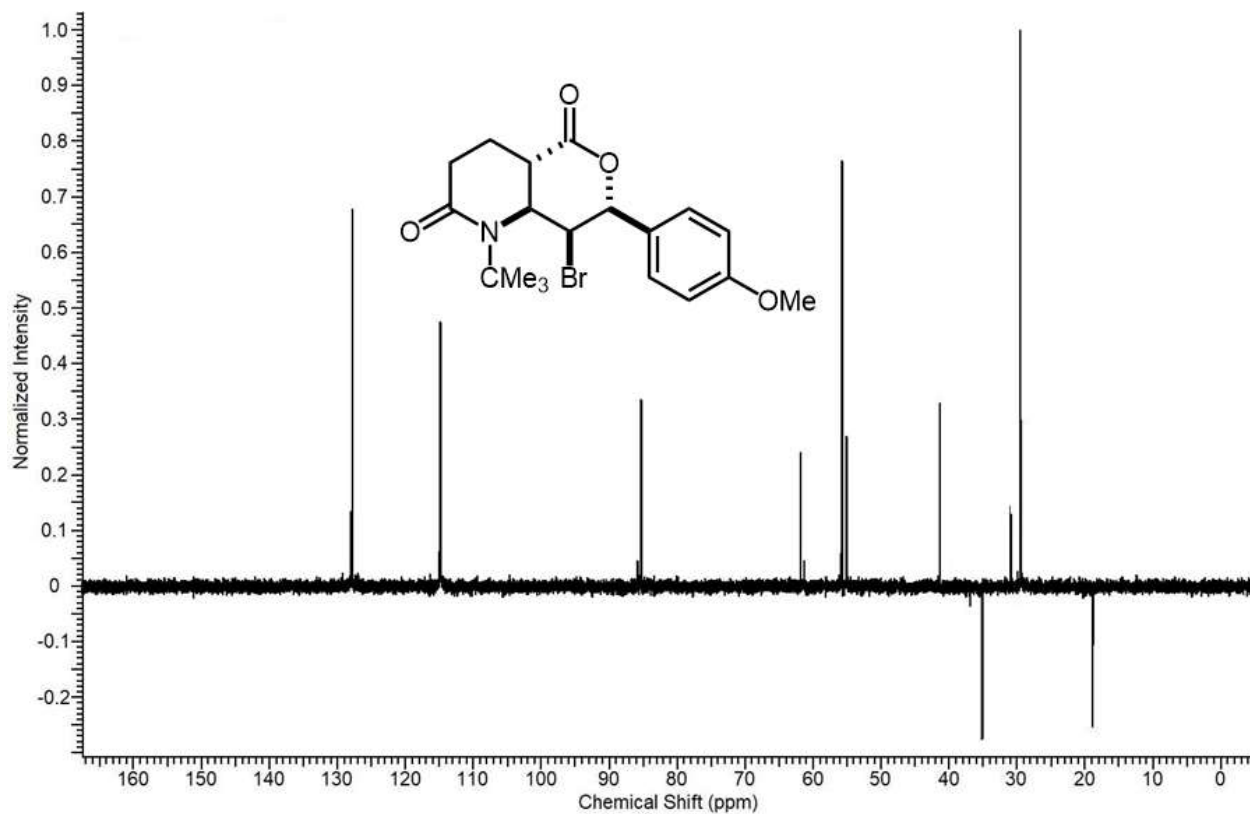
Spectra 3-24. DEPT-NMR spectrum of structure **9h**
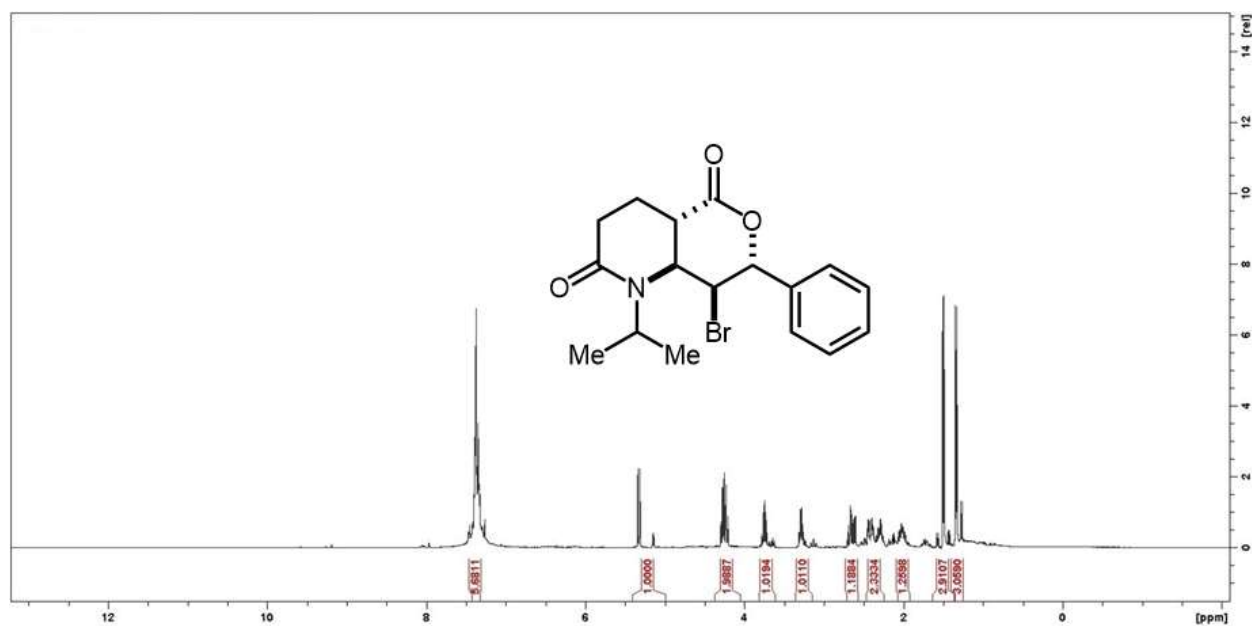
Spectra 3-25. ¹H-NMR spectrum for structure **9i**
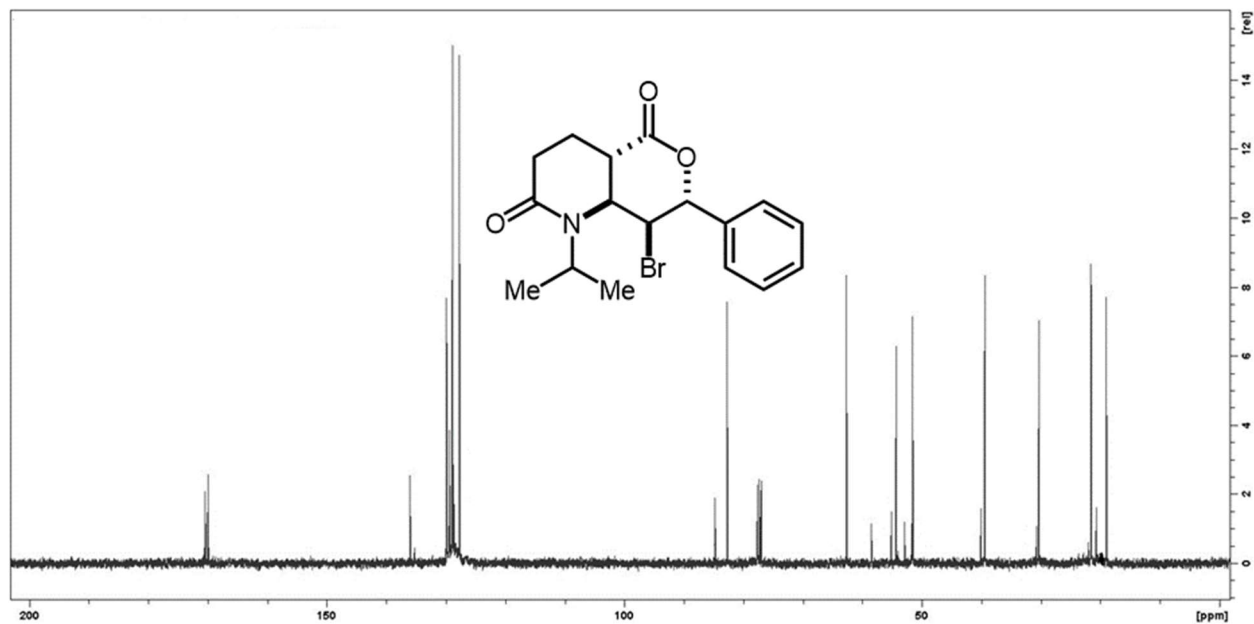
Spectra 3-26. ^{13}C-NMR spectrum of structure **9i**
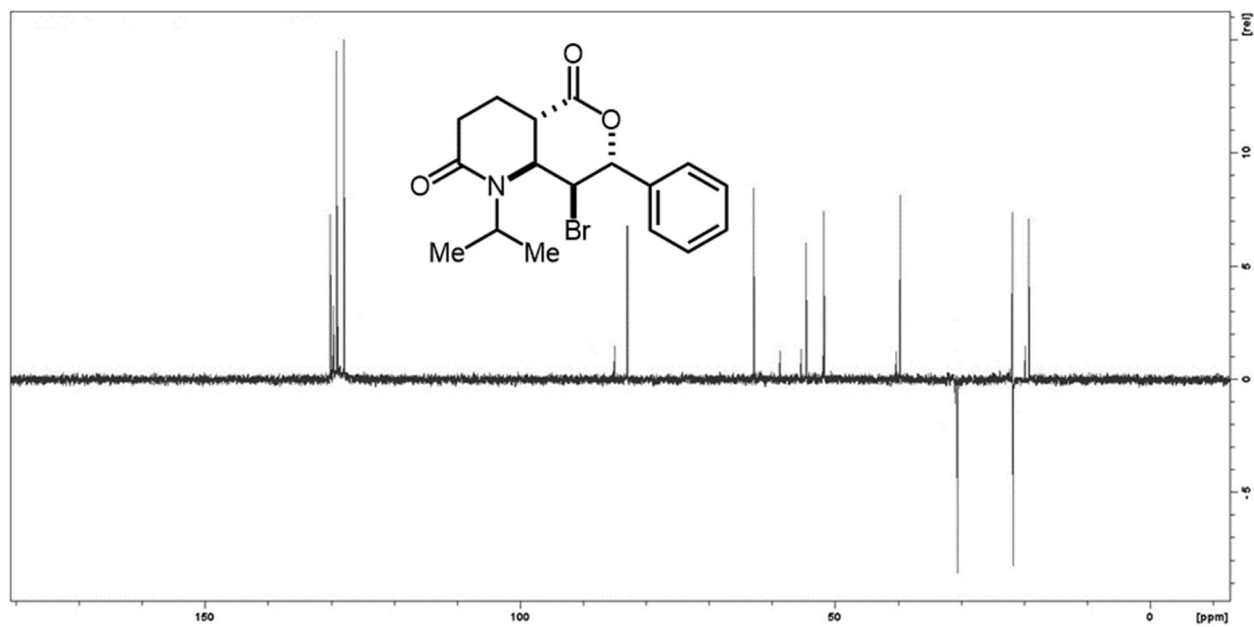
Spectra 3-27. DEPT-NMR spectrum of structure **9i**
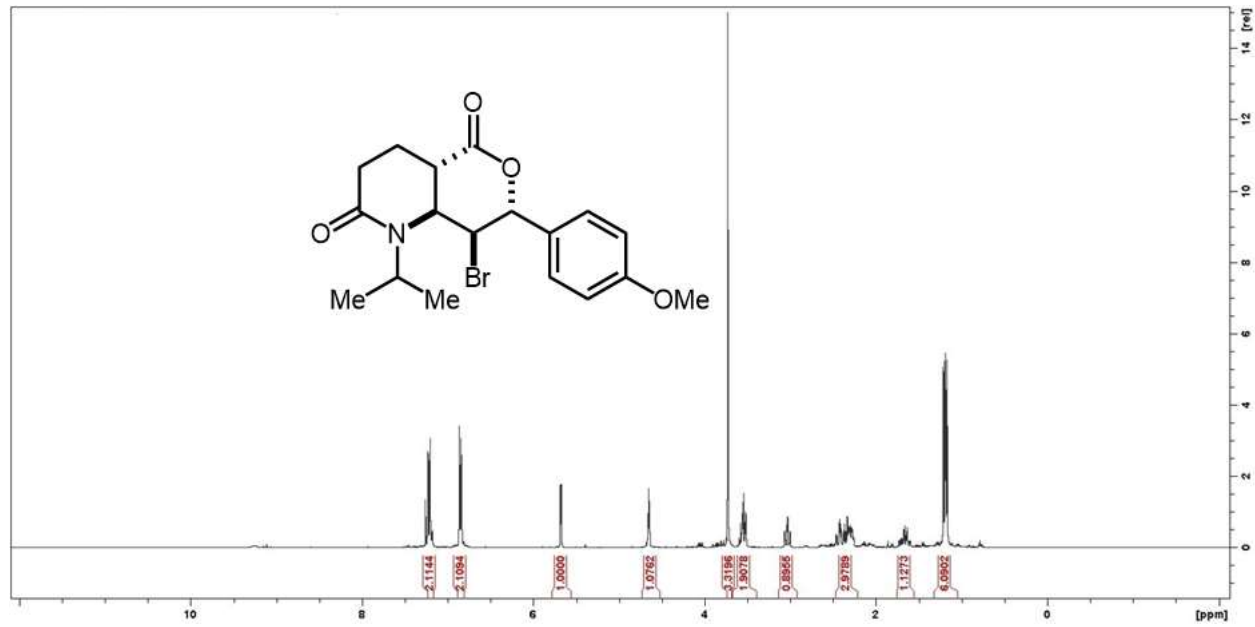
Spectra 3-28. ^{1}H-NMR spectrum for structure **9j**
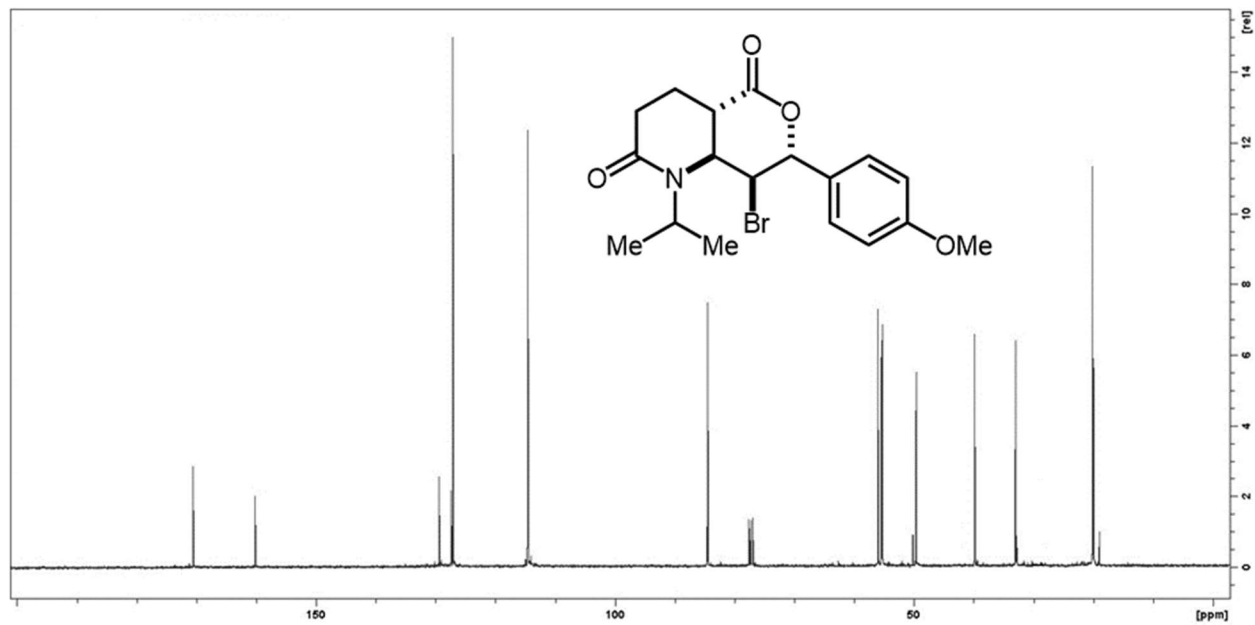
Spectra 3-29. ^{13}C-NMR spectrum of structure **9j**
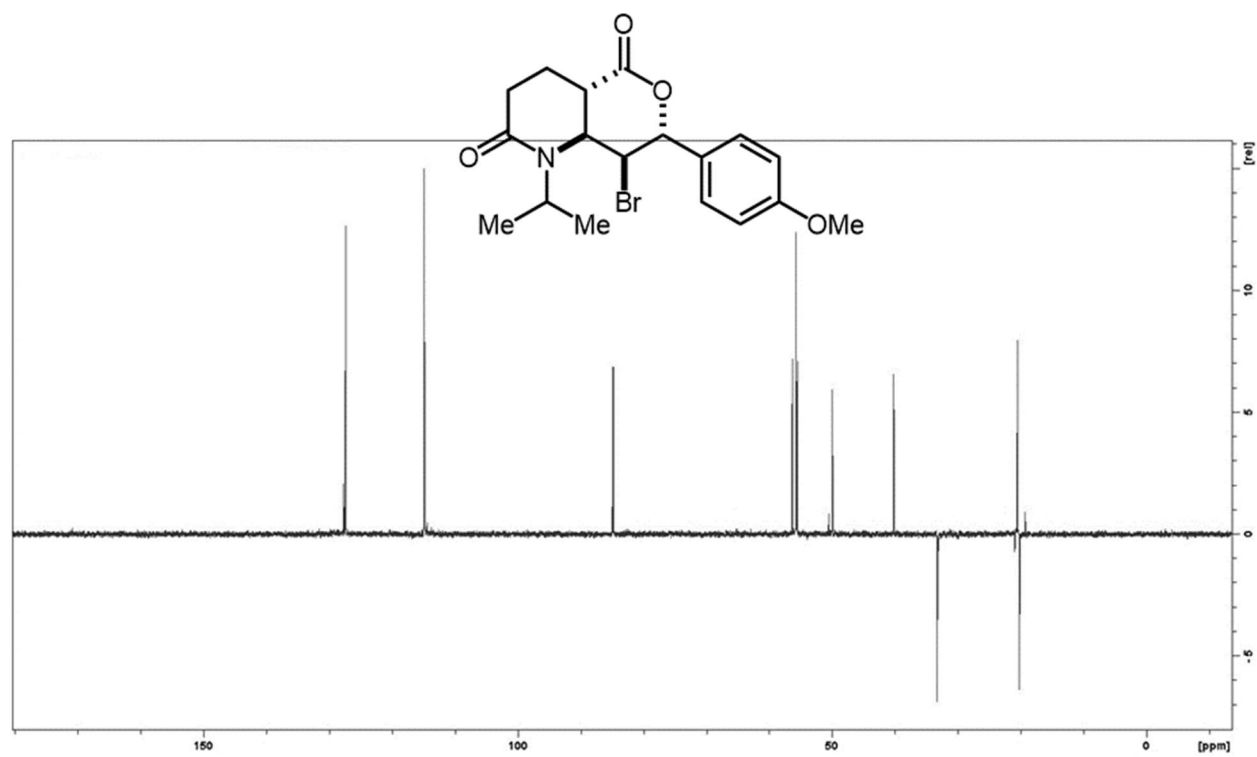
Spectra 3-30. DEPT-NMR spectrum of structure **9j**
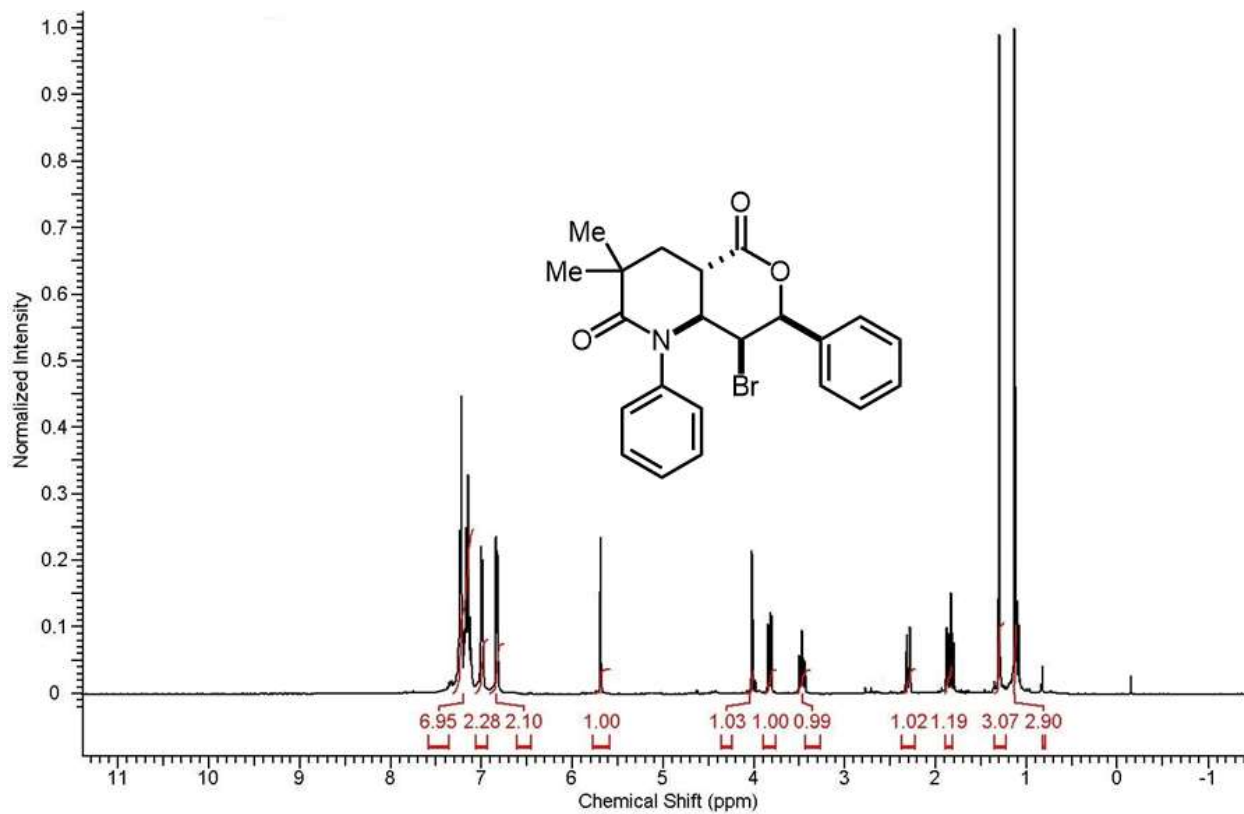
Spectra 3-31. ^{1}H-NMR spectrum for structure **9k**
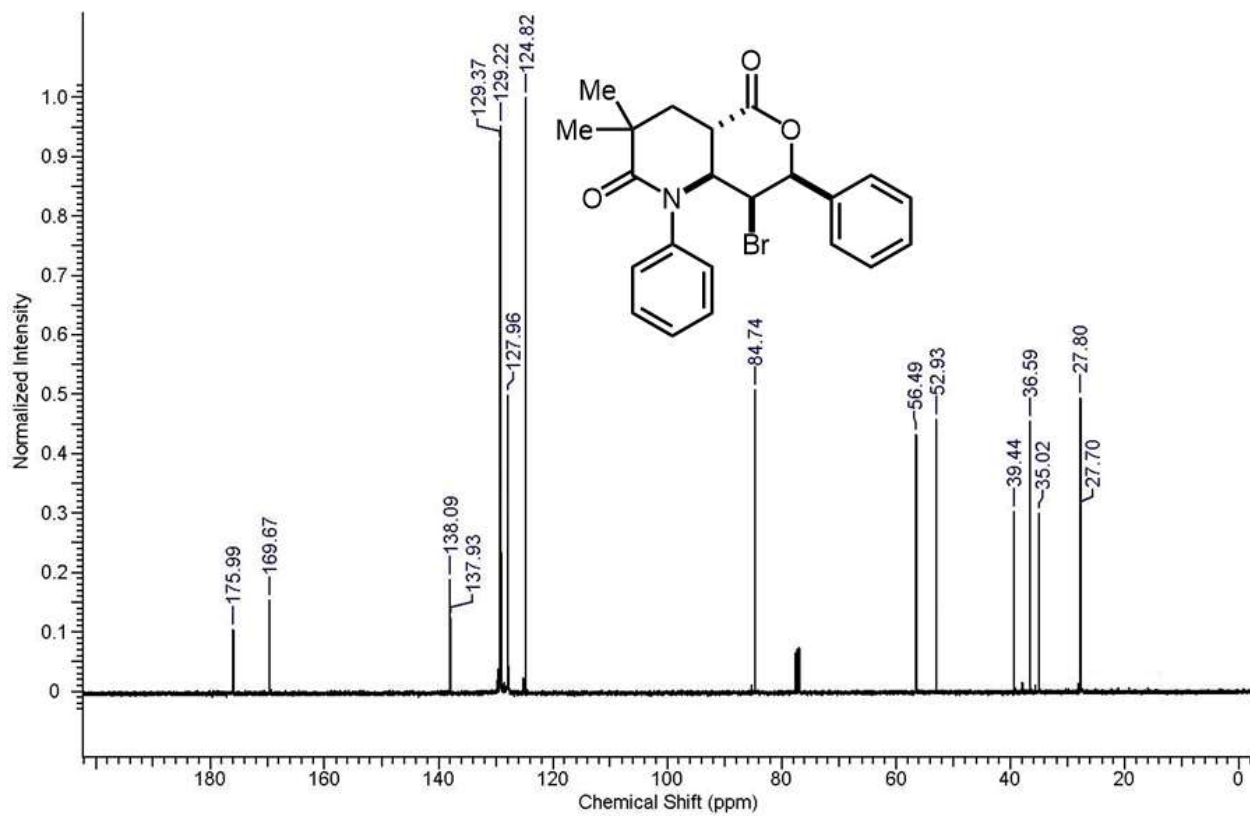
Spectra 3-32. ^{13}C-NMR spectrum of structure **9k**
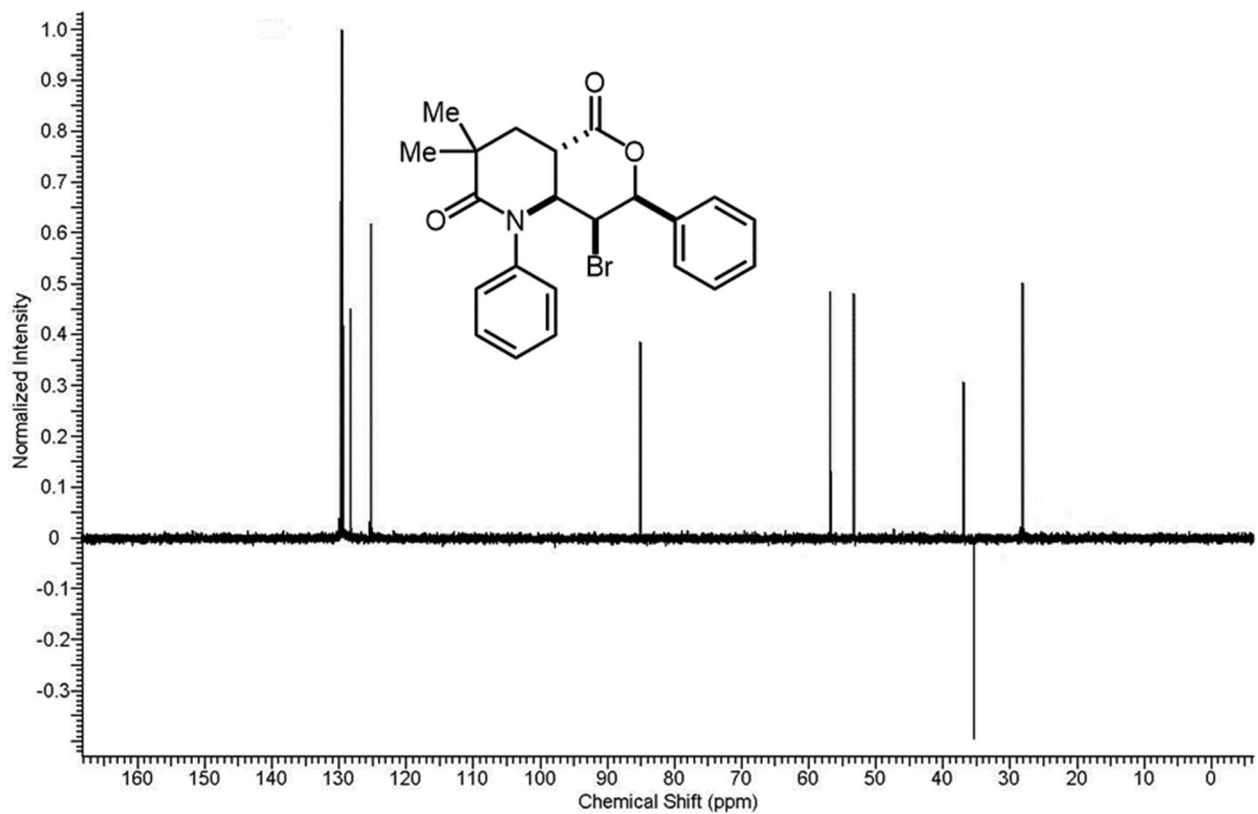
Spectra 3-33. DEPT-NMR spectrum of structure **9k**
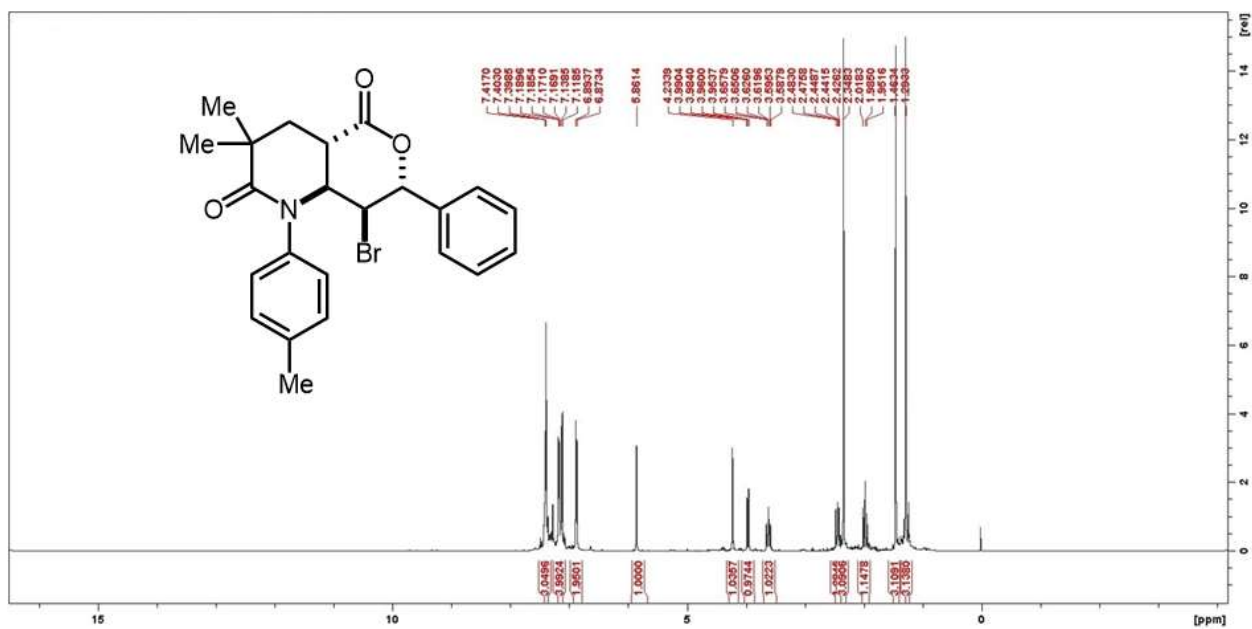
Spectra 3-34. ^{1}H-NMR spectrum for structure **9l**
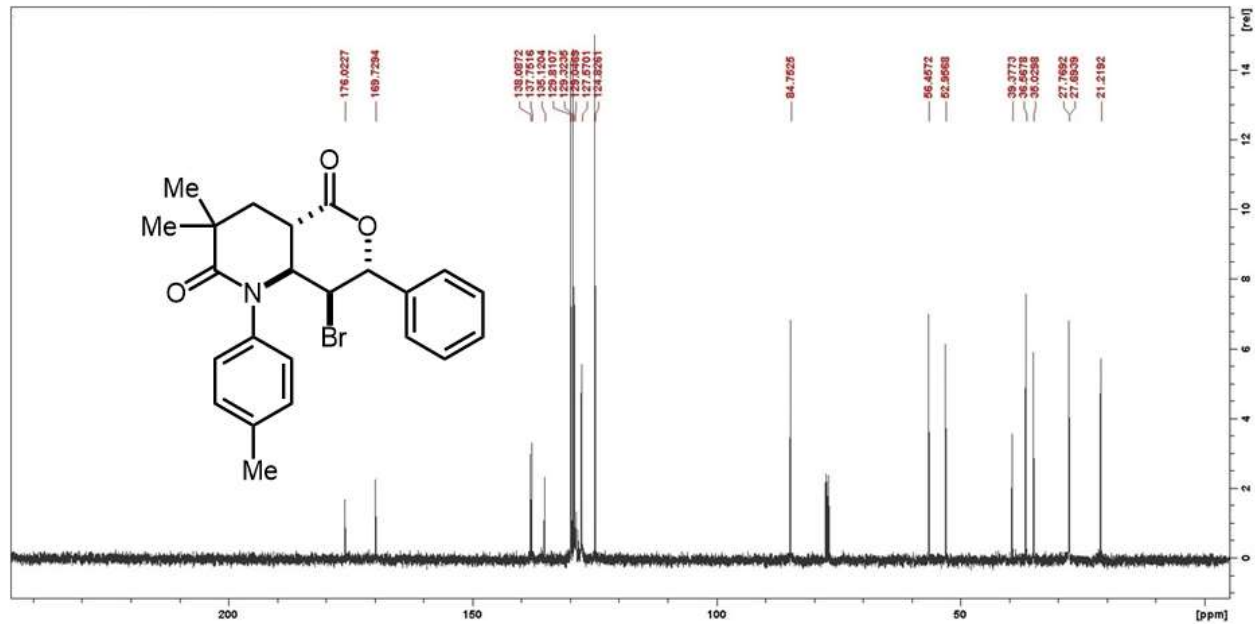
Spectra 3-35. ^{13}C-NMR spectrum of structure **9l**
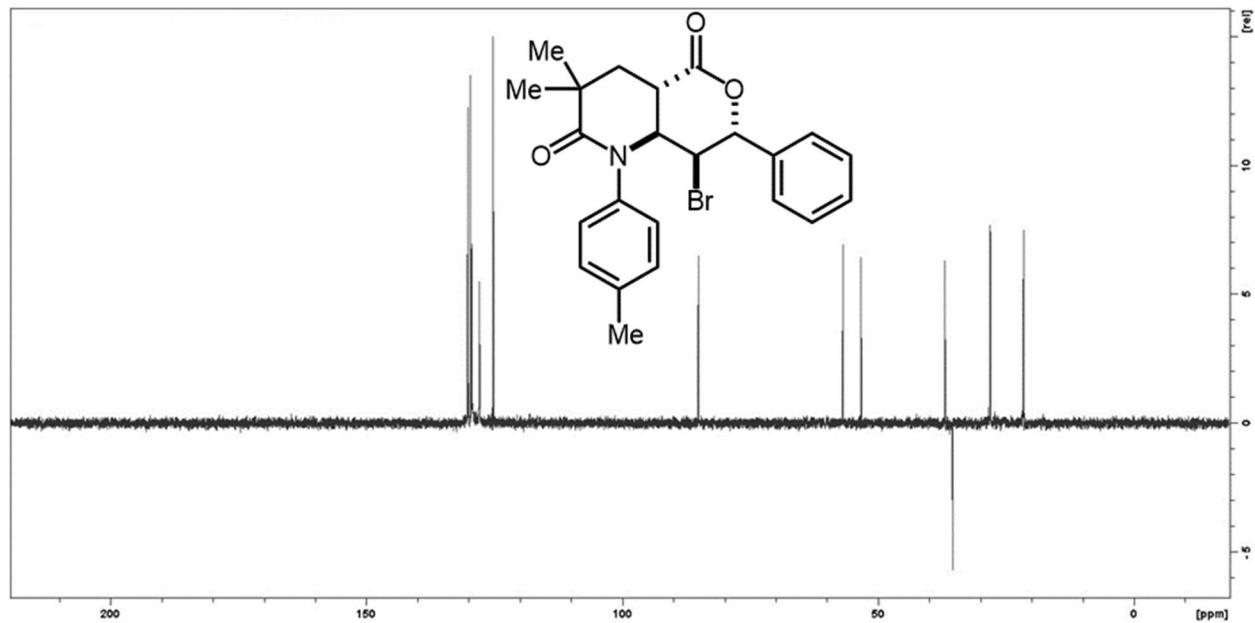
Spectra 3-36. DEPT-NMR spectrum of structure **9l**

3.2 Pyrrolidinones
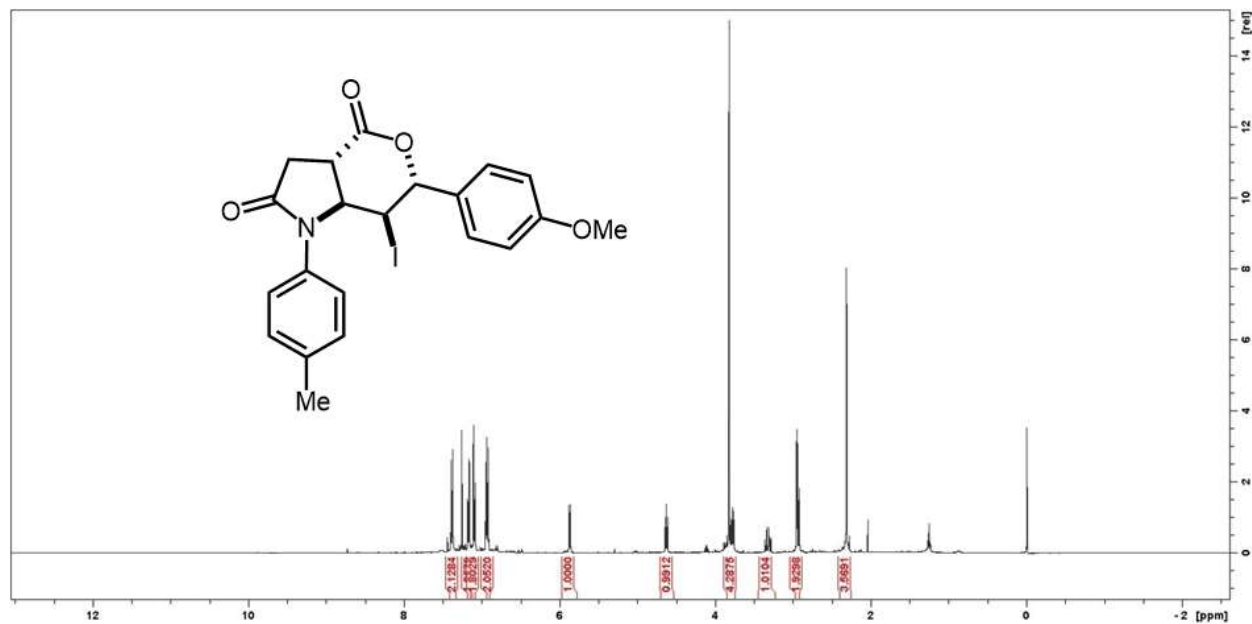
Spectra 3-37. ^{1}H-NMR spectrum for structure **9m**
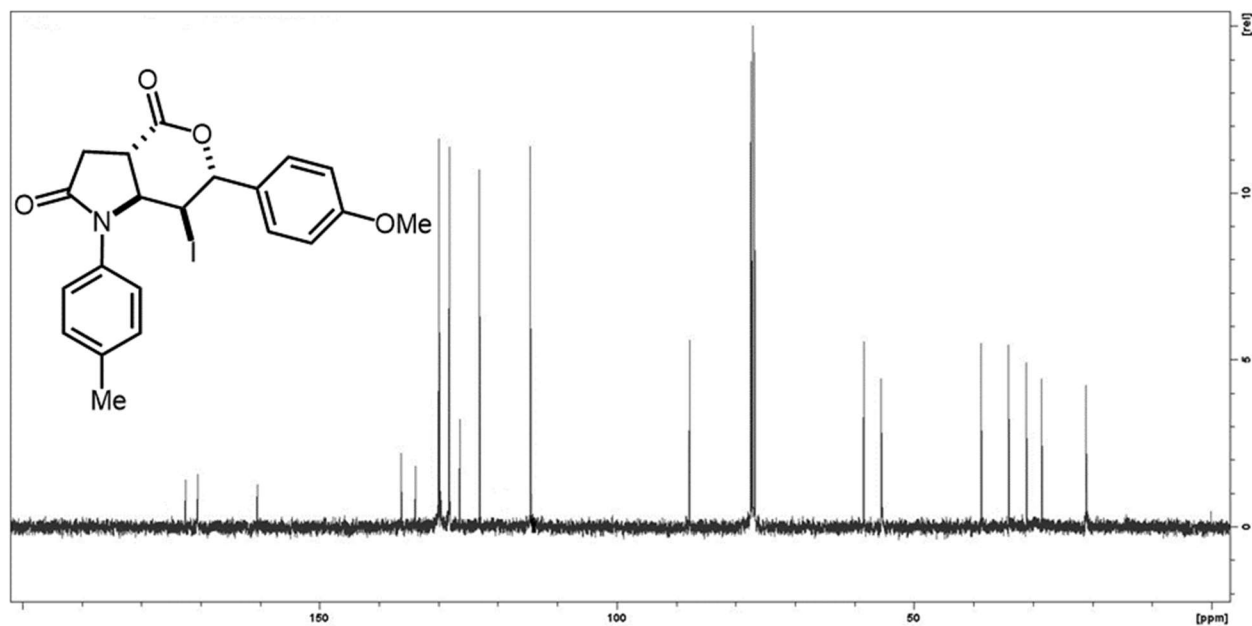
Spectra 3-38. ^{13}C-NMR spectrum of structure **9m**
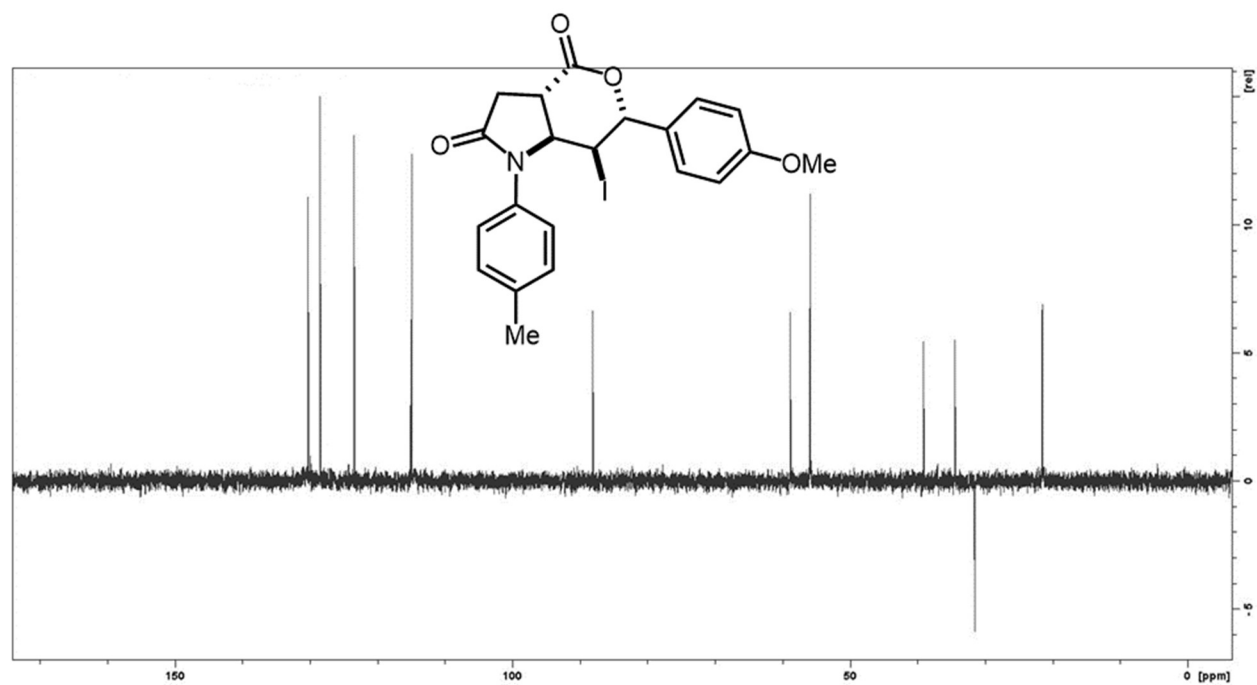
Spectra 3-39. DEPT-NMR spectrum of structure **9m**
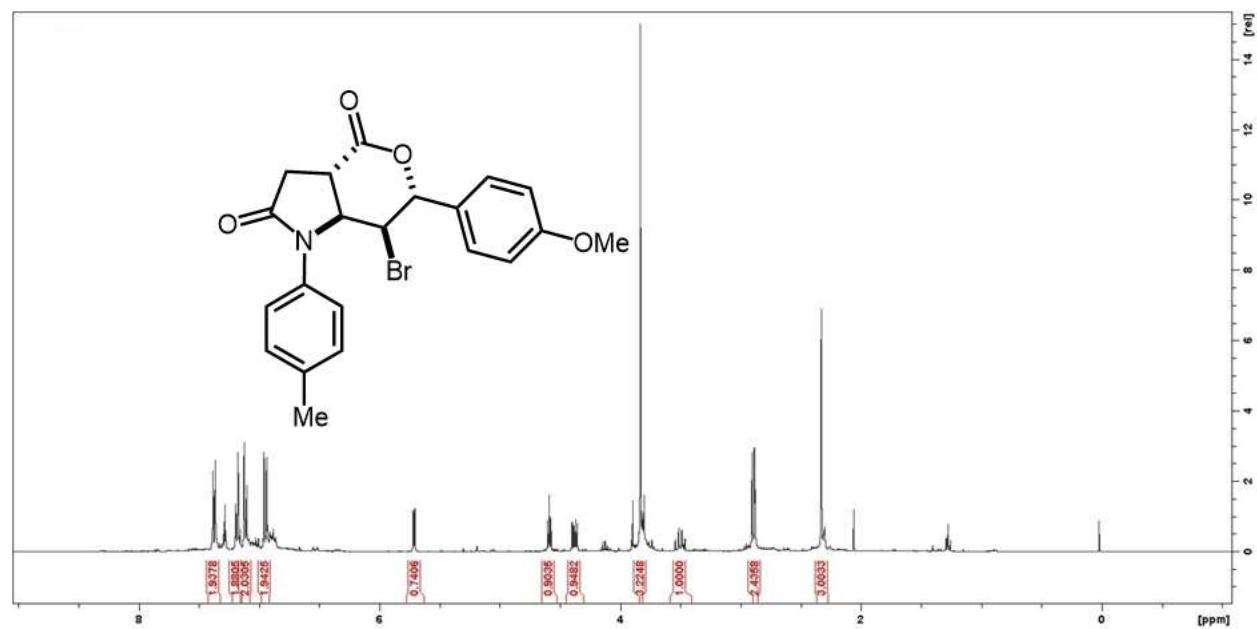
Spectra 3-40. ^{1}H-NMR spectrum for structure **9n**
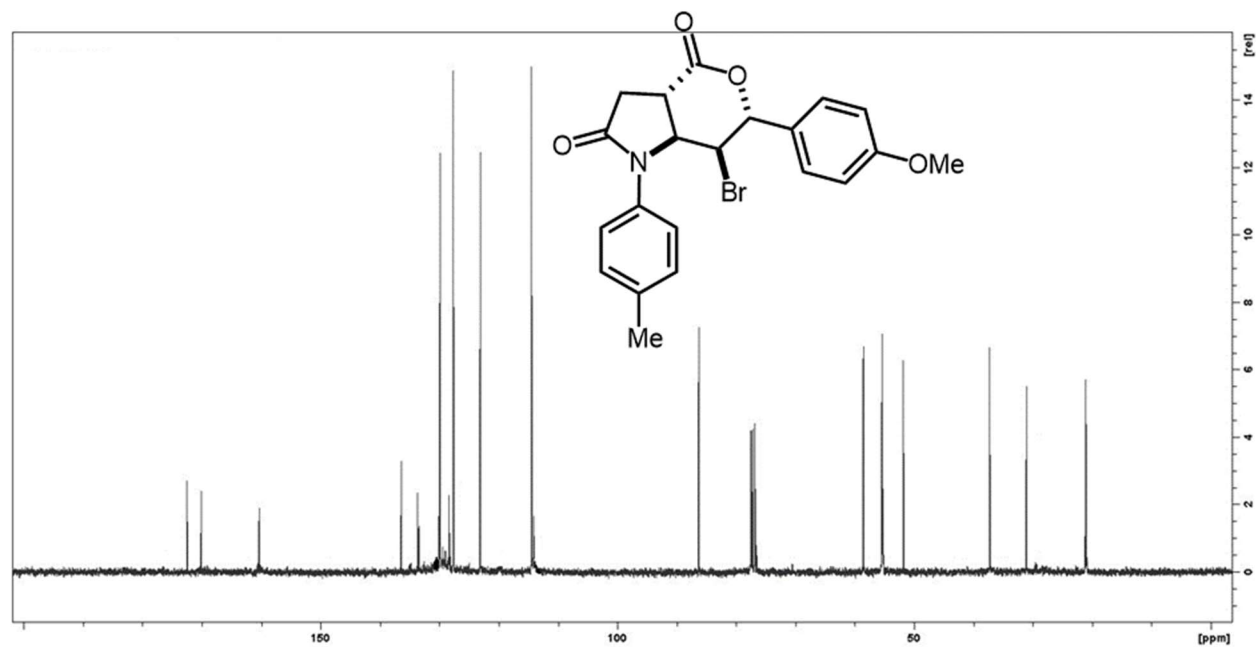
Spectra 3-41. ^{13}C-NMR spectrum of structure **9n**
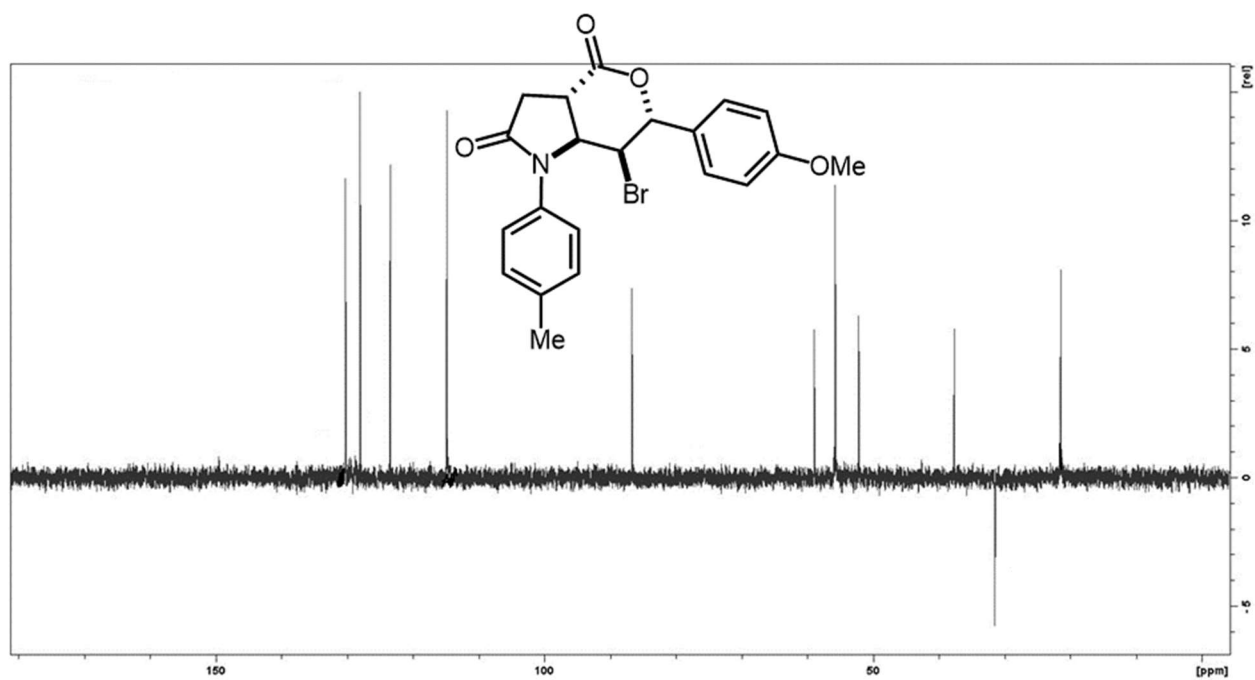
Spectra 3-42. DEPT-NMR spectrum of structure **9n**
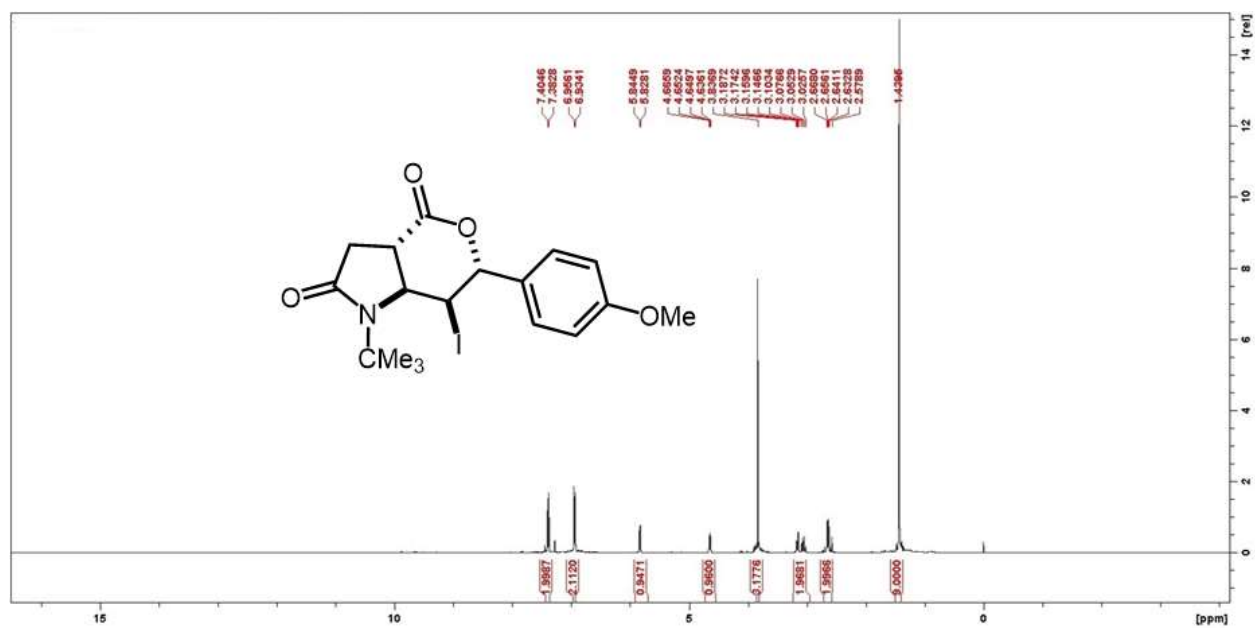
Spectra 3-43. ^{1}H-NMR spectrum for structure **9o**
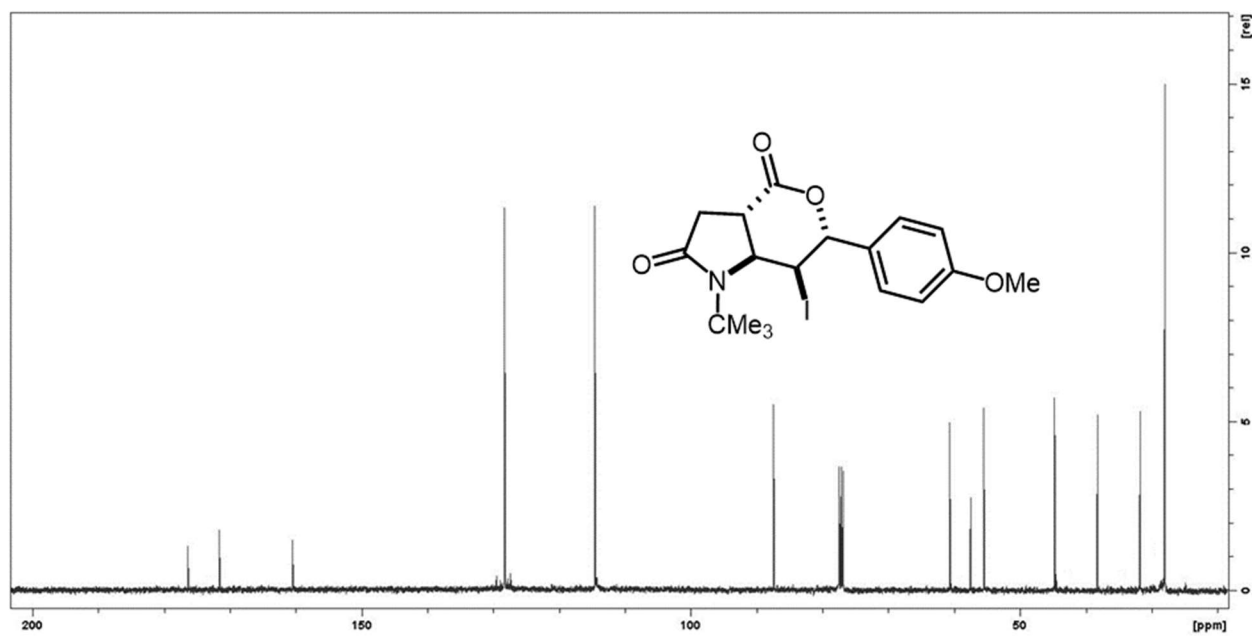
Spectra 3-44. ^{13}C-NMR spectrum of structure **9o**
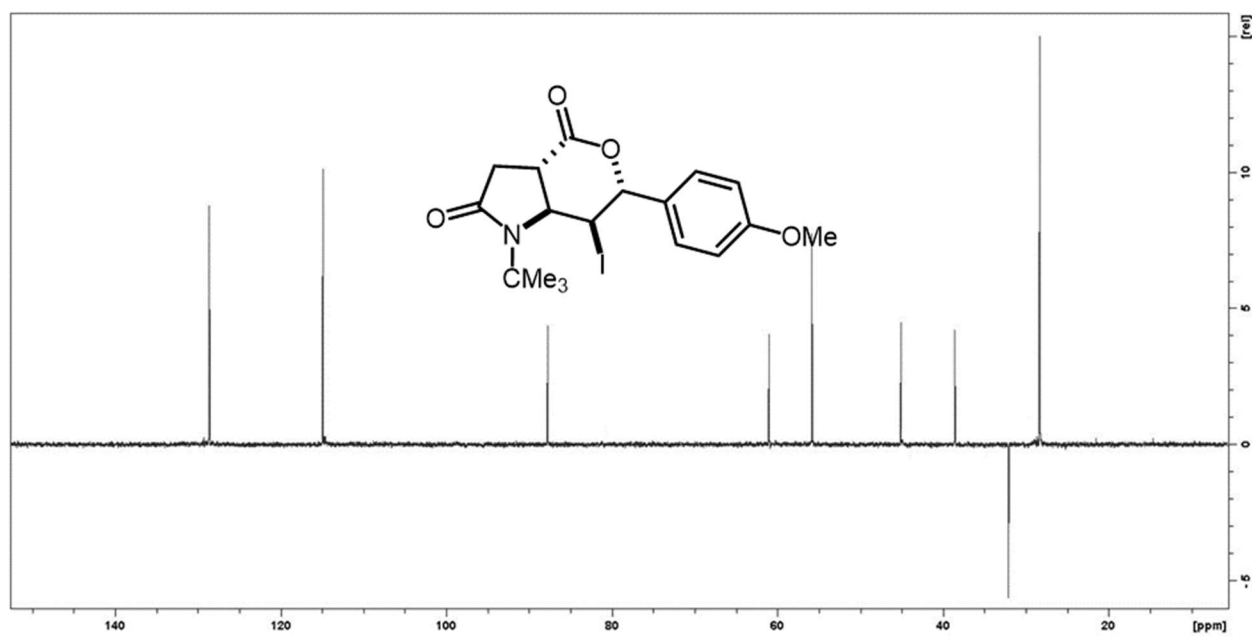
Spectra 3-45. DEPT-NMR spectrum of structure **9o**

89
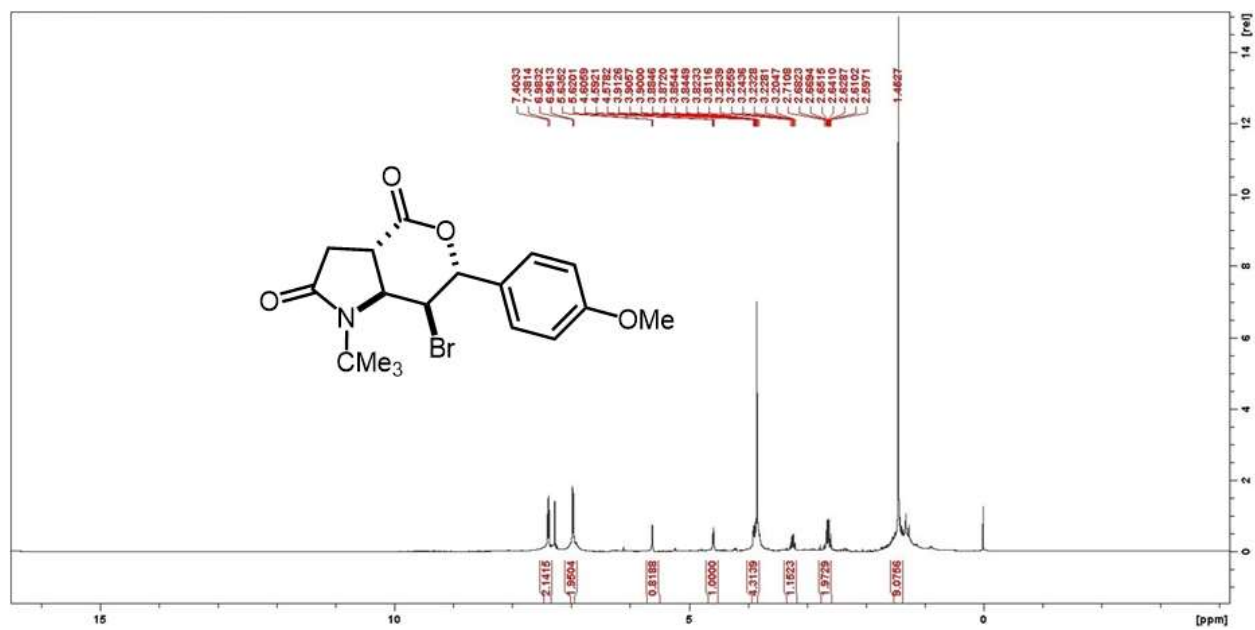
Spectra 3-46. ^{1}H-NMR spectrum for structure **9p**
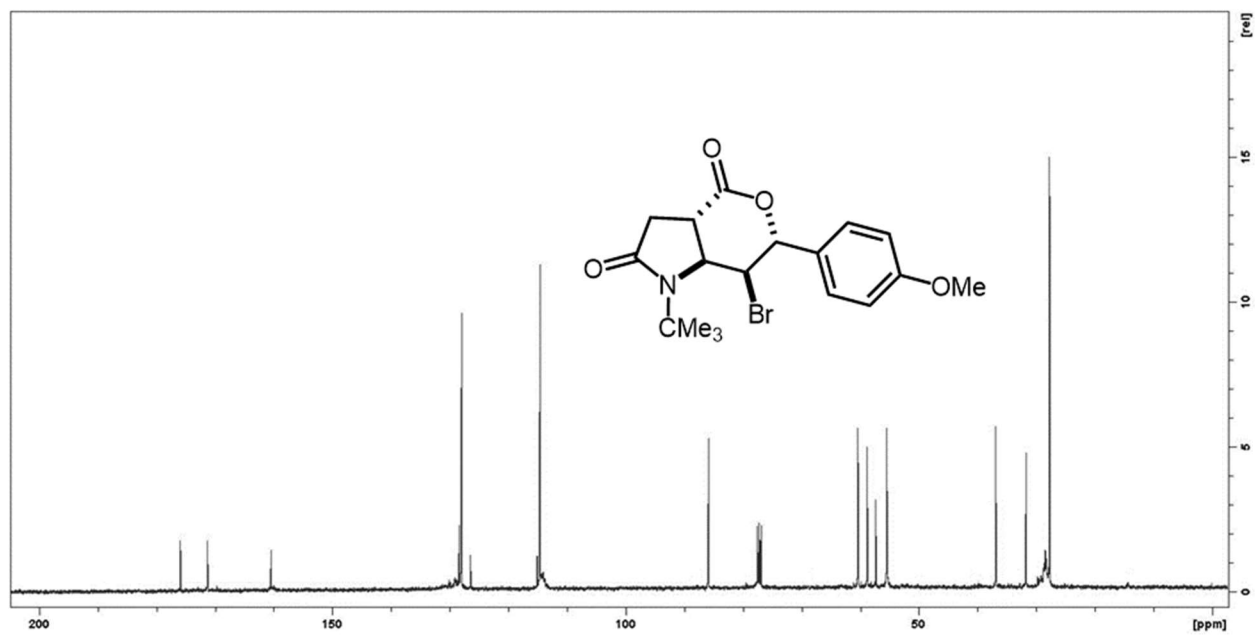
Spectra 3-47. ^{13}C-NMR spectrum of structure **9p**
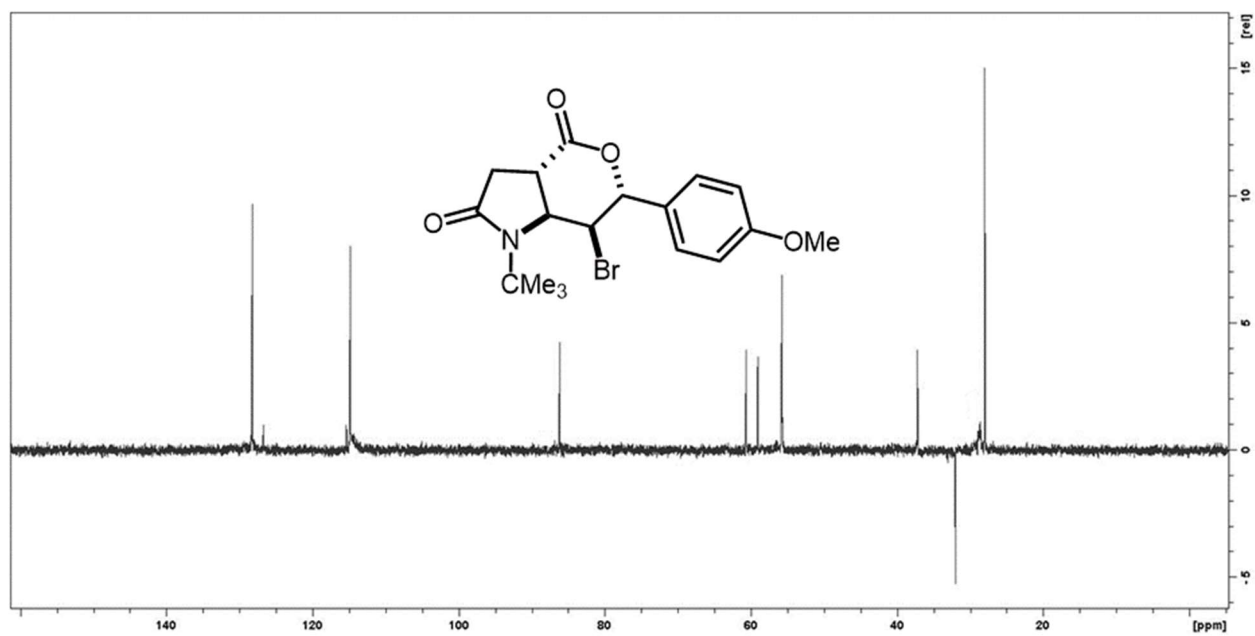
Spectra 3-48. DEPT-NMR spectrum of structure **9p**
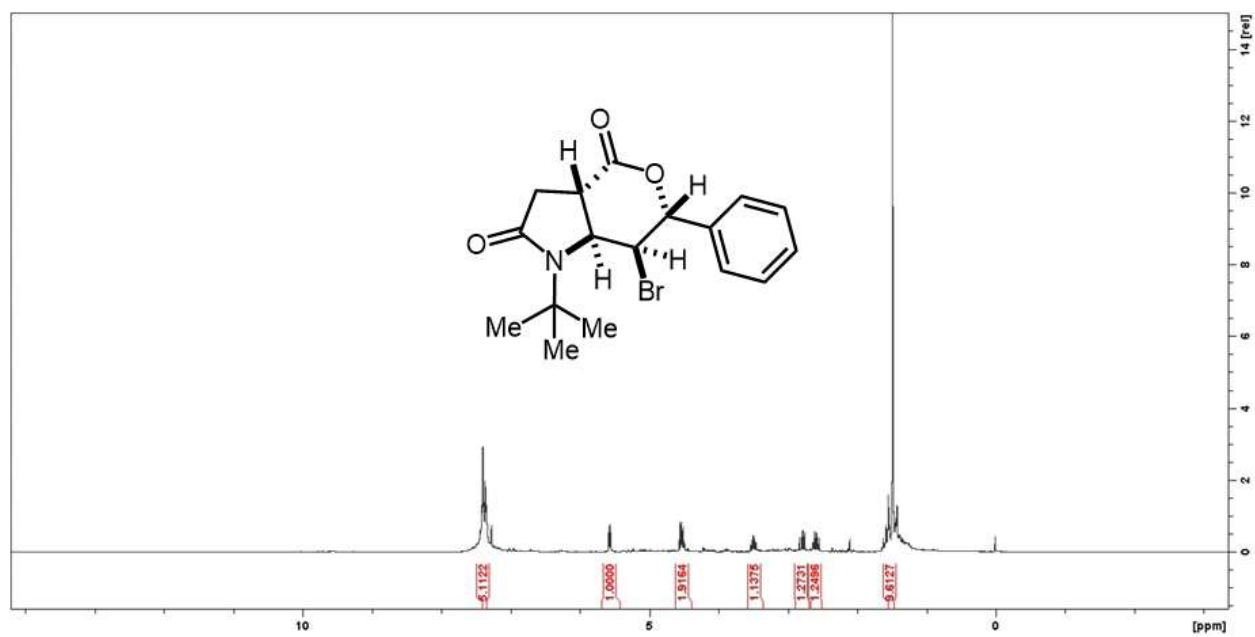
Spectra 3-49. ^{1}H-NMR spectrum for structure **9q**
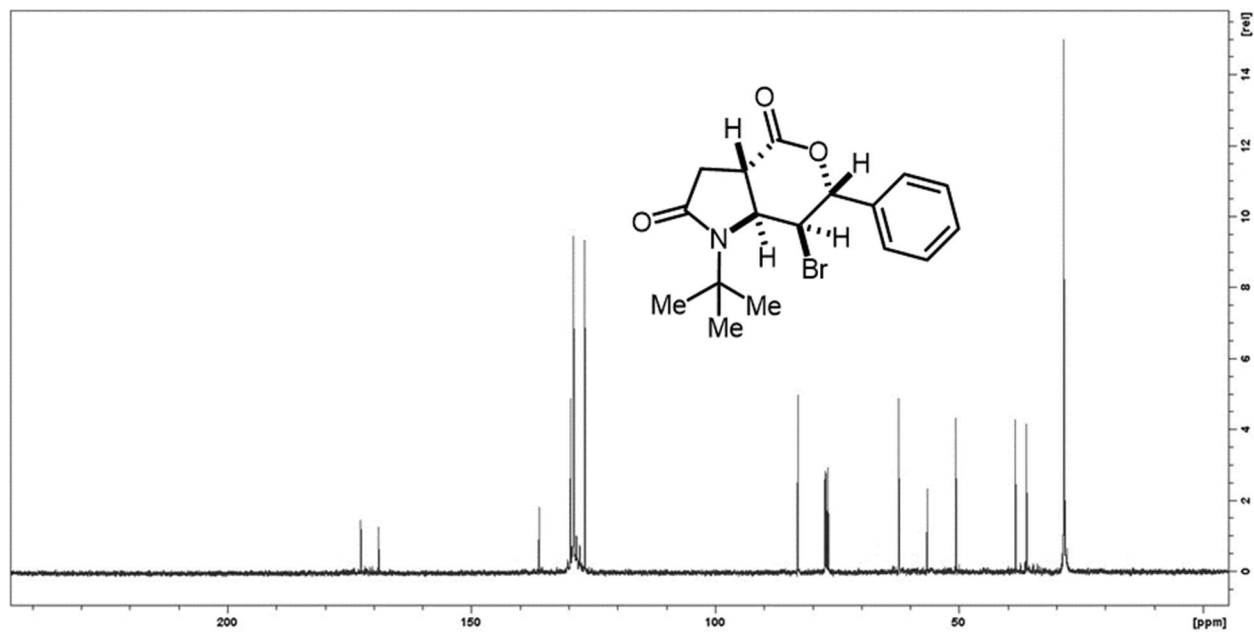
Spectra 3-50. ^{13}C-NMR spectrum of structure **9q**
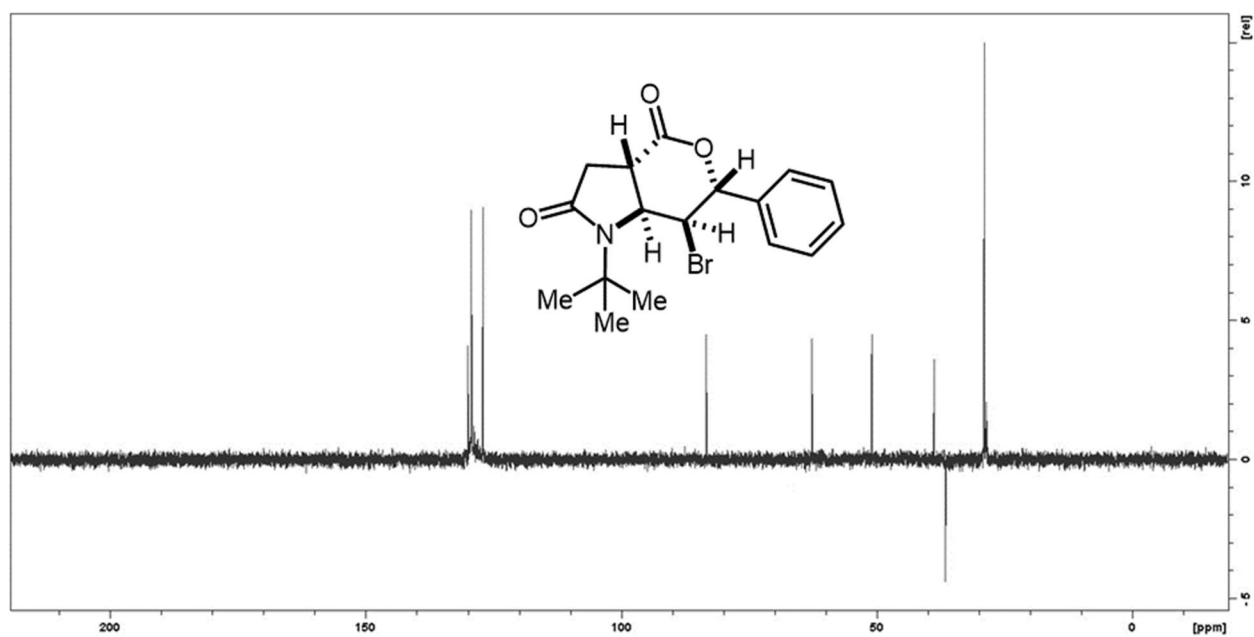
Spectra 3-51. DEPT-NMR spectrum of structure **9q**
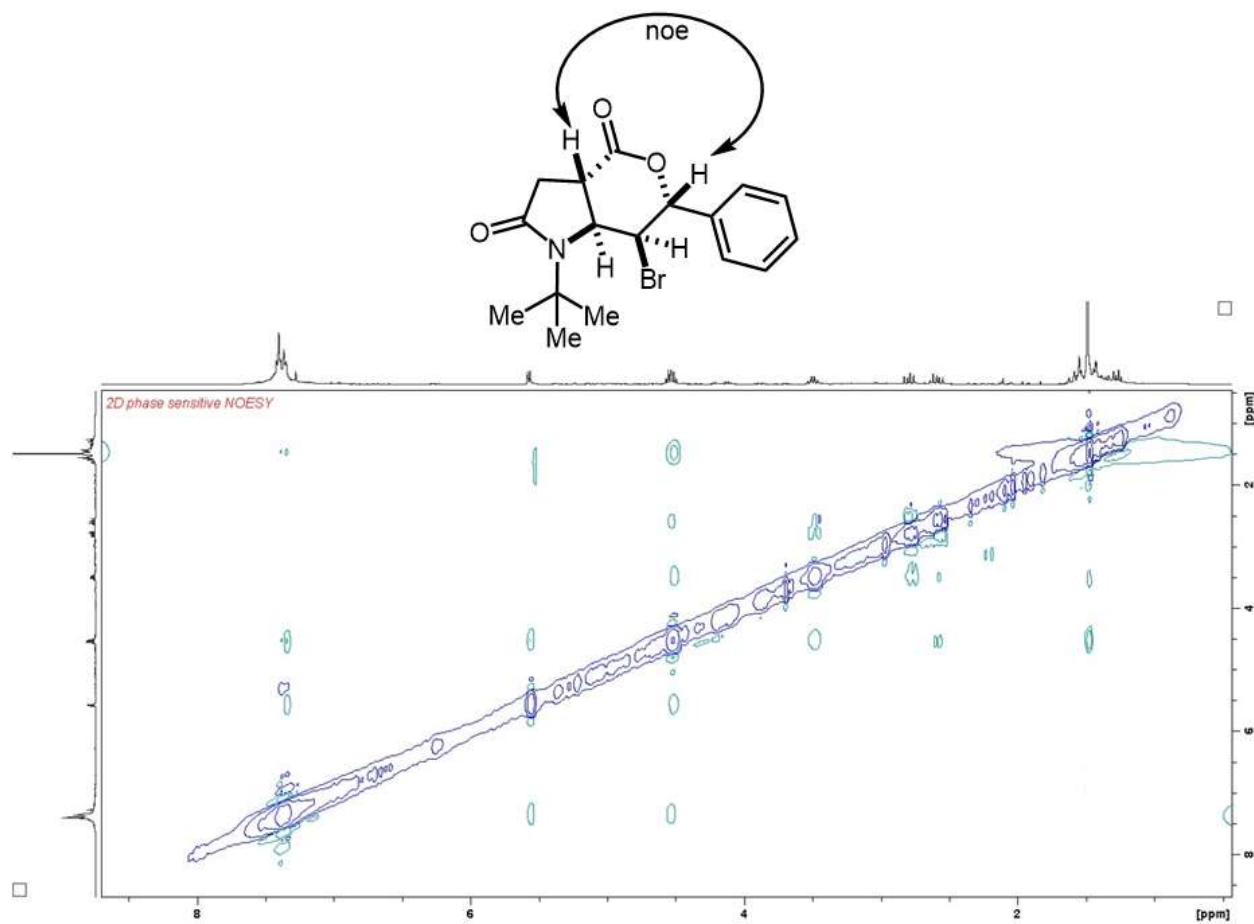
Spectra 3-52. NOESY spectrum of **9q**
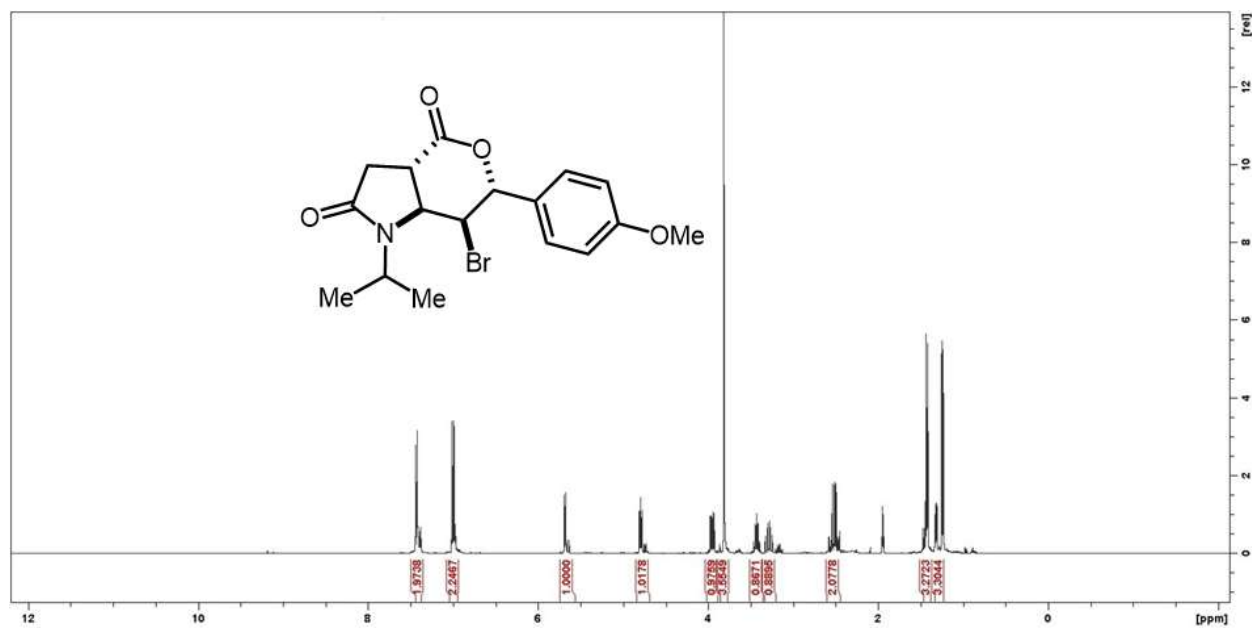
Spectra 3-53. ^{1}H-NMR spectrum for structure **9r**
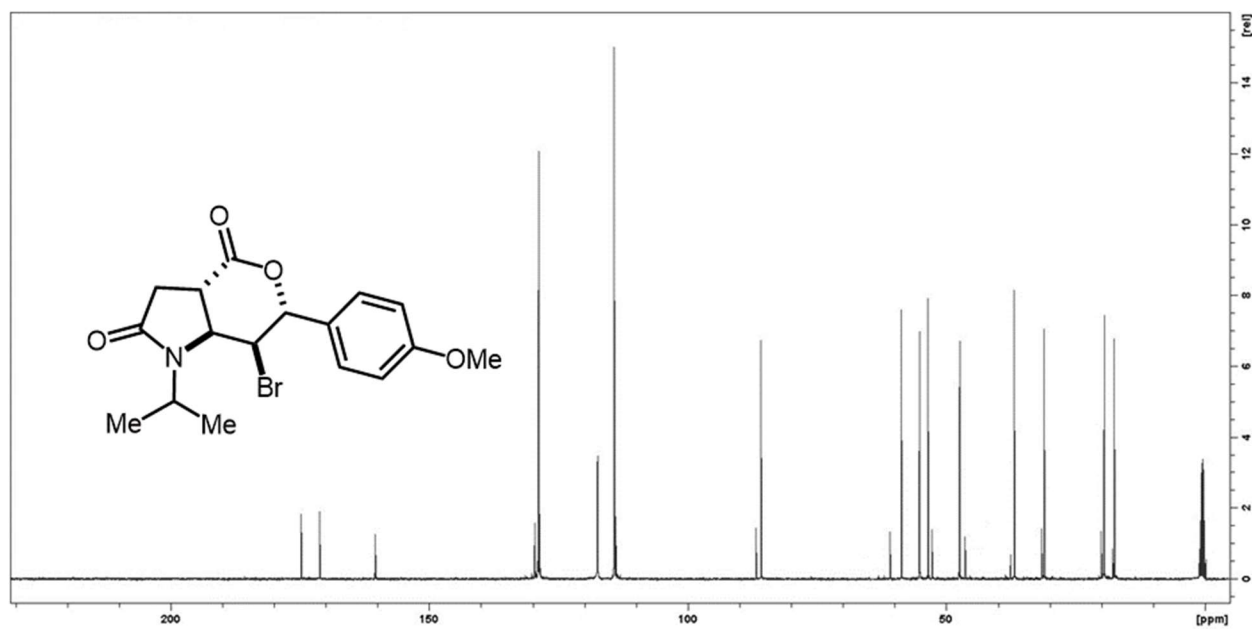
Spectra 3-54. ^{13}C-NMR spectrum of structure **9r**
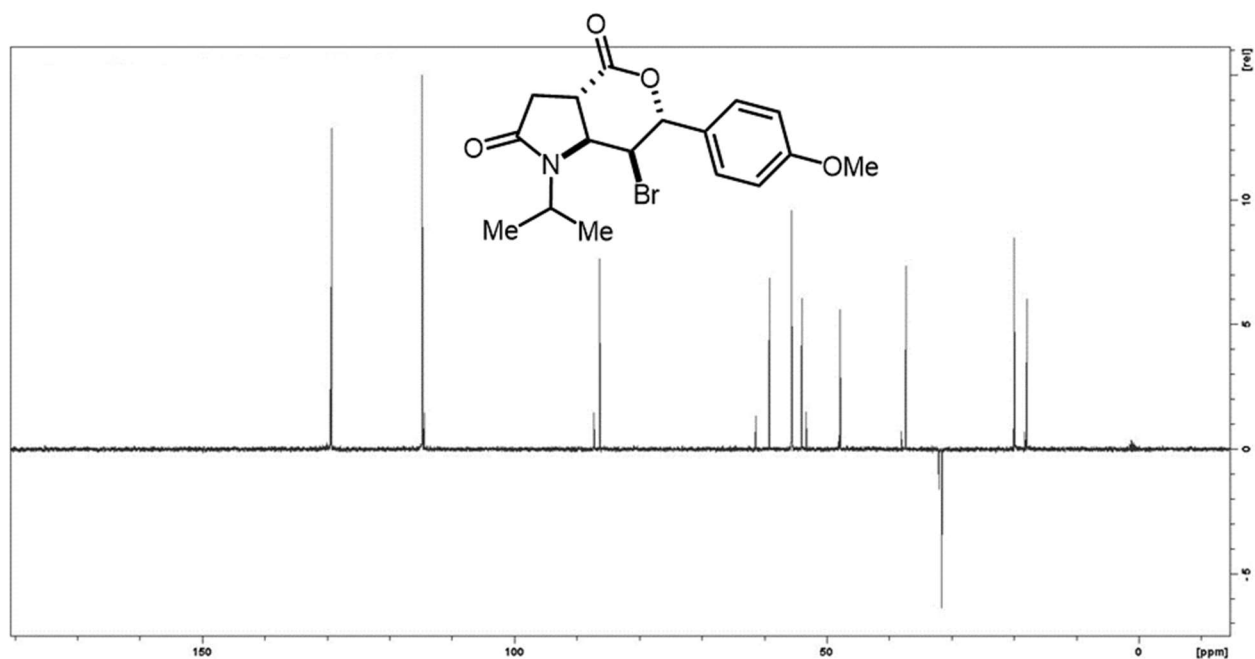
Spectra 3-55. DEPT-NMR spectrum of structure **9r**

3.3 Morpholinones
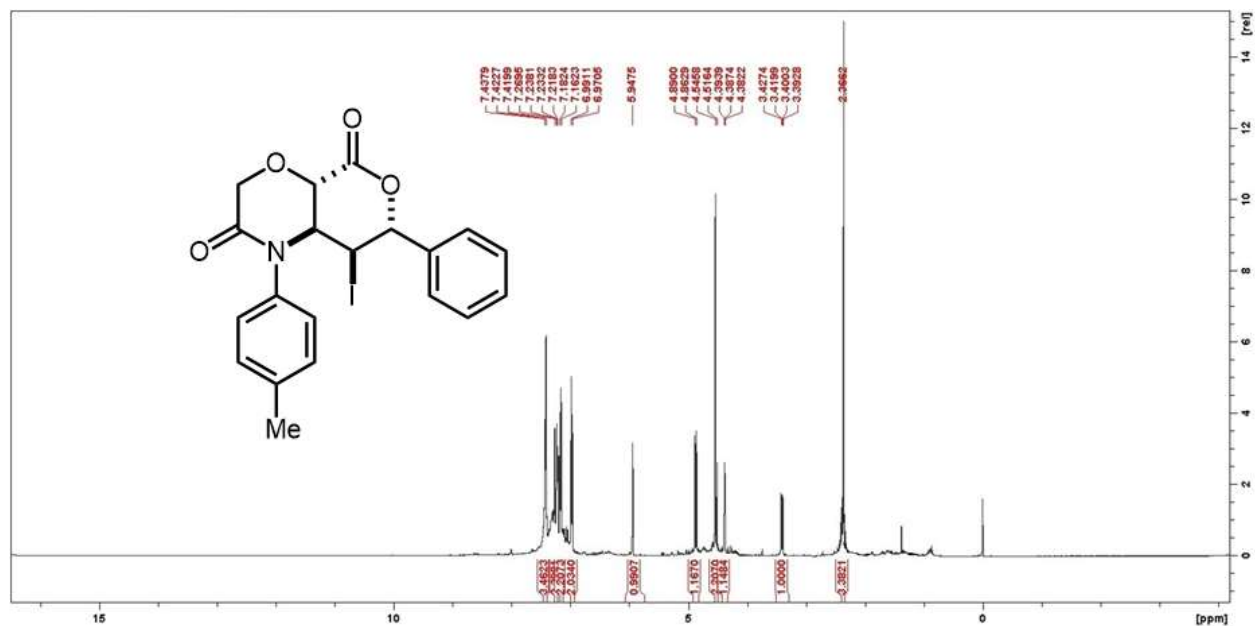
Spectra 3-56. ¹H-NMR spectrum for structure **9s**
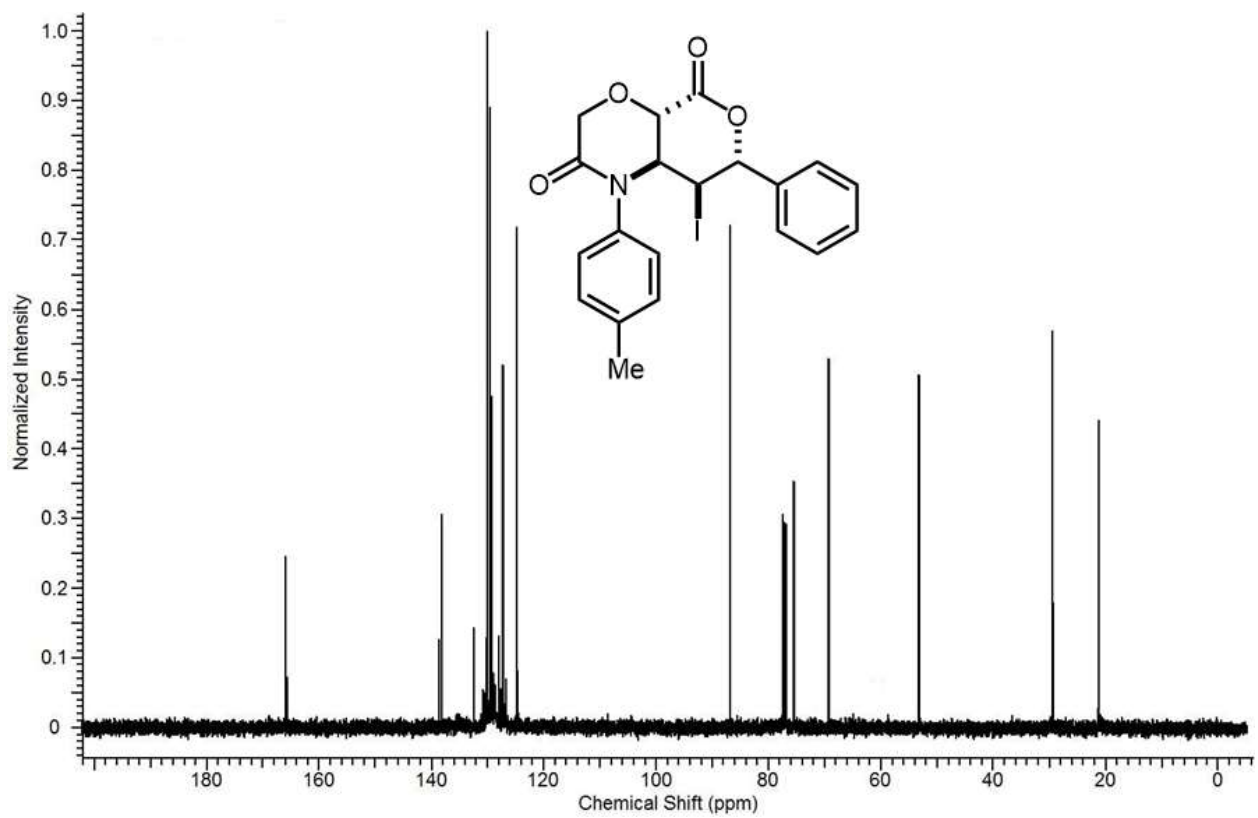
Spectra 3-57. ^{13}C-NMR spectrum of structure **9s**

Spectra 3-58. DEPT-NMR spectrum of structure **9s**

Spectra 3-59. ^{1}H-NMR spectrum for structure **9t**
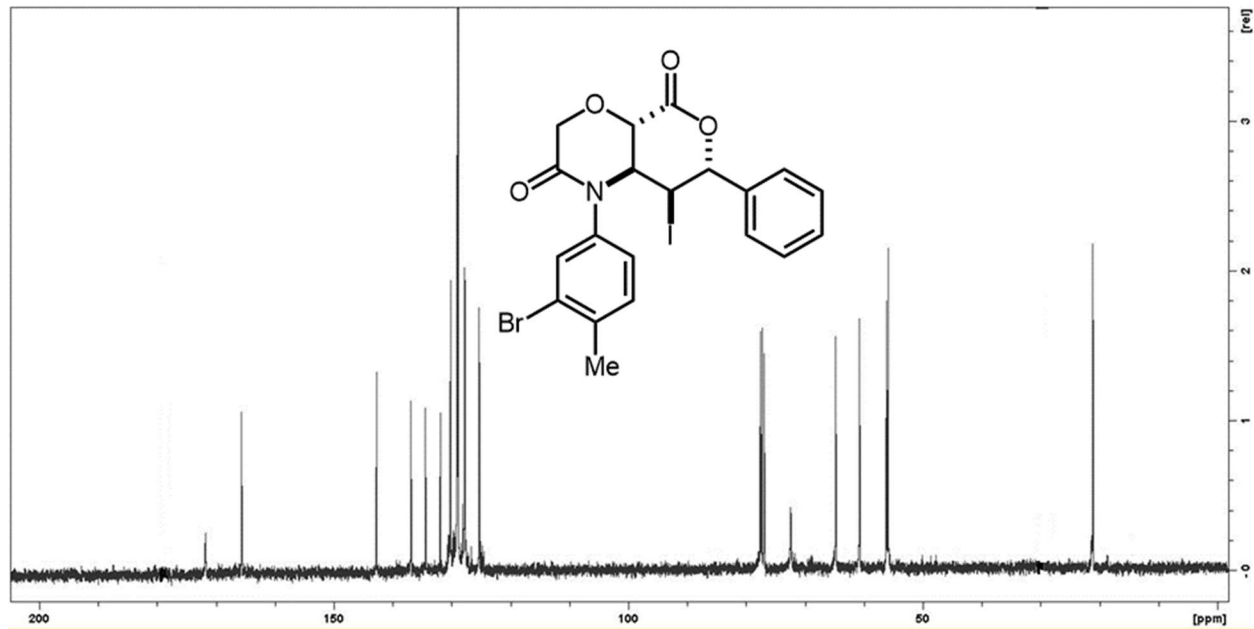
Spectra 3-60. ^{13}C-NMR spectrum of structure **9t**
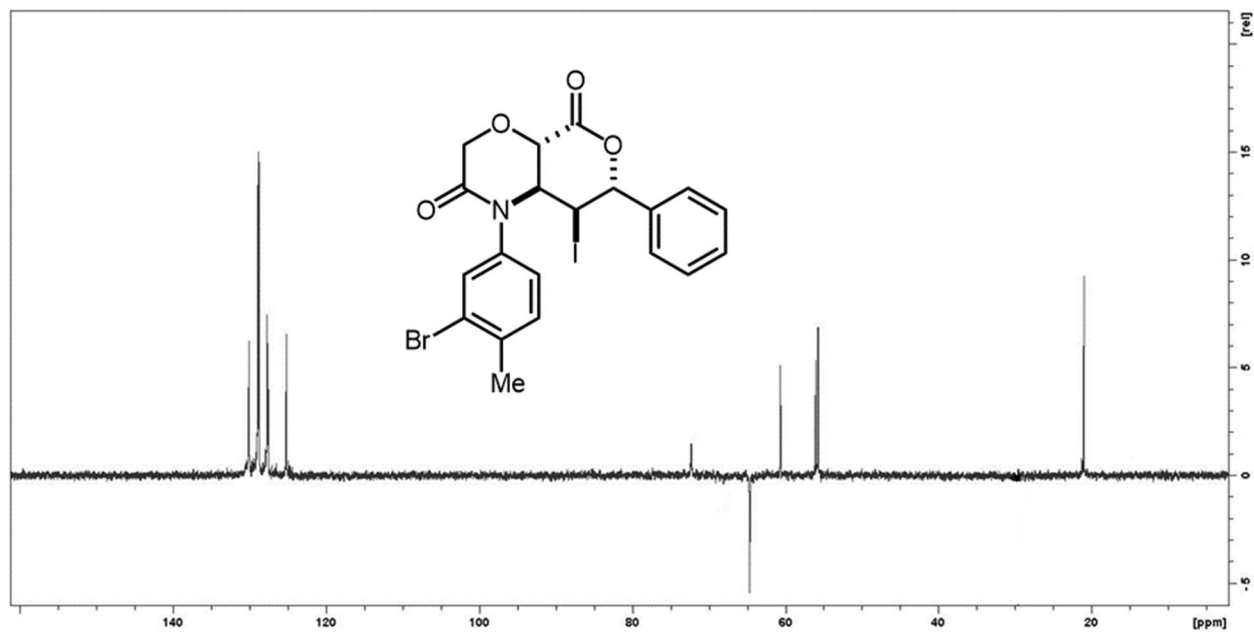
Spectra 3-61. DEPT-NMR spectrum of structure **9t**
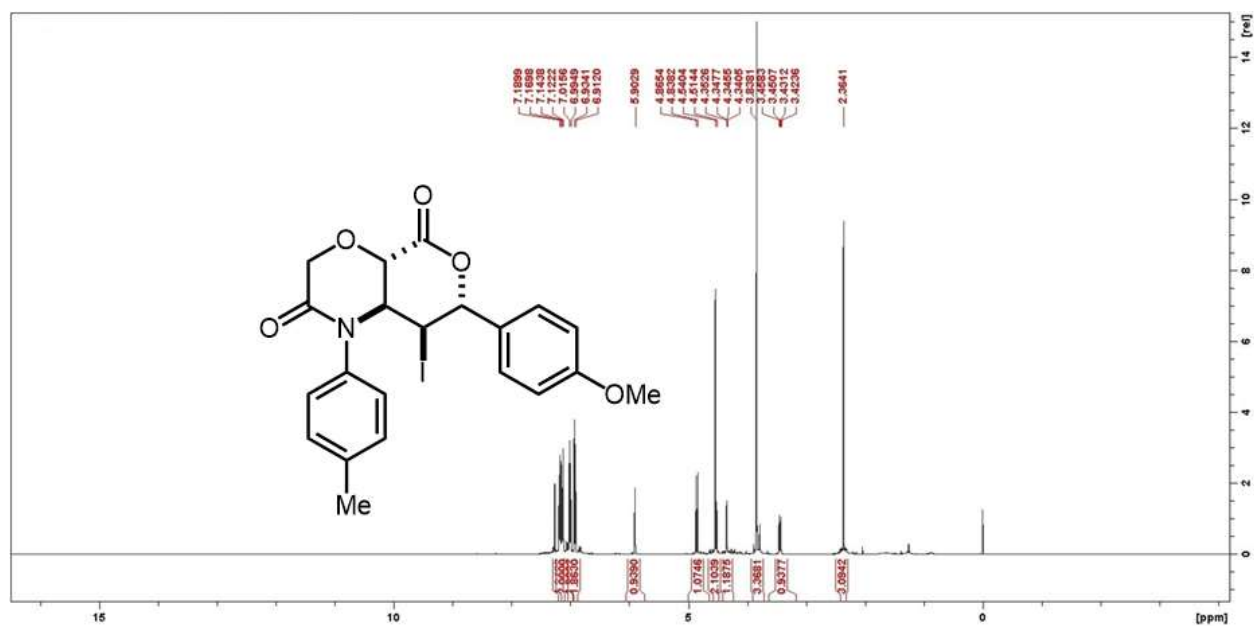
Spectra 3-62. ^{1}H-NMR spectrum for structure **9u**
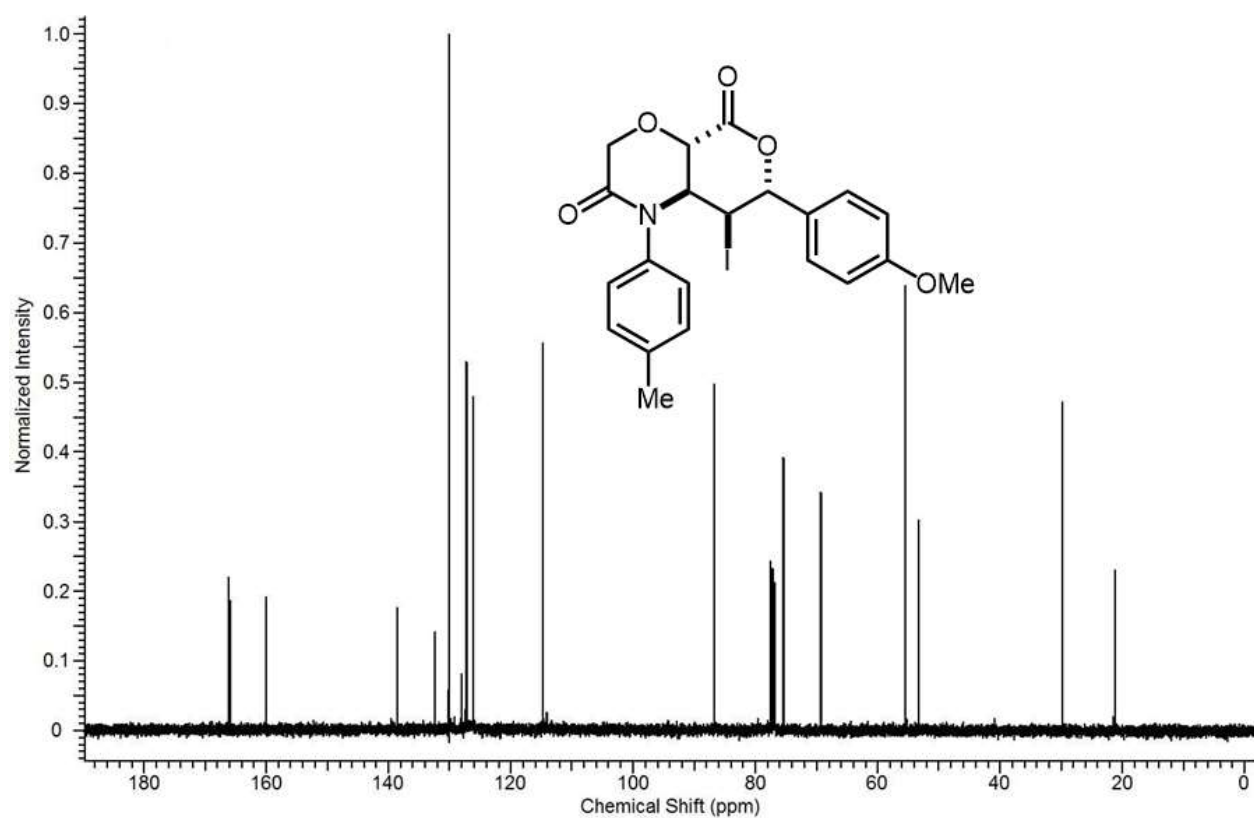
Spectra 3-63. ^{13}C-NMR spectrum of structure **9u**

99
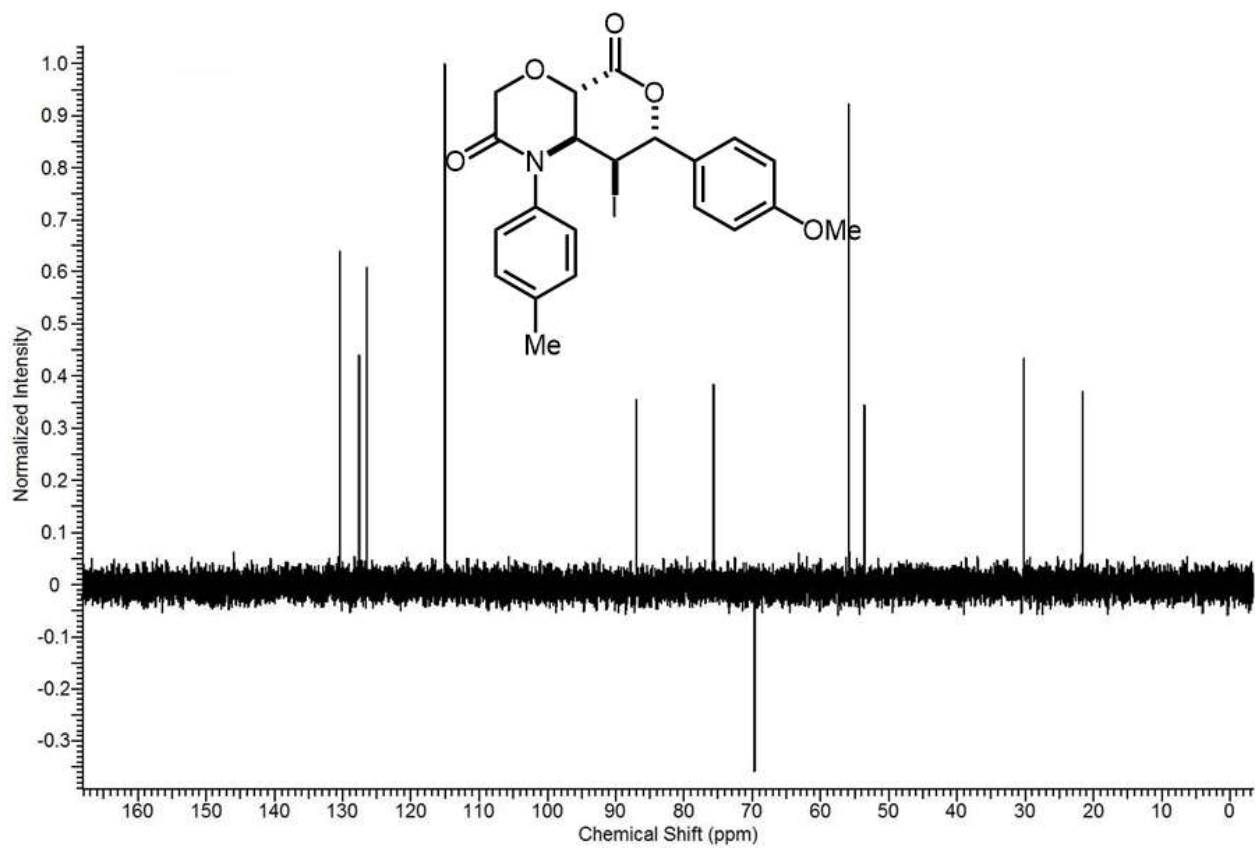
Spectra 3-64. DEPT-NMR spectrum of structure **9u**
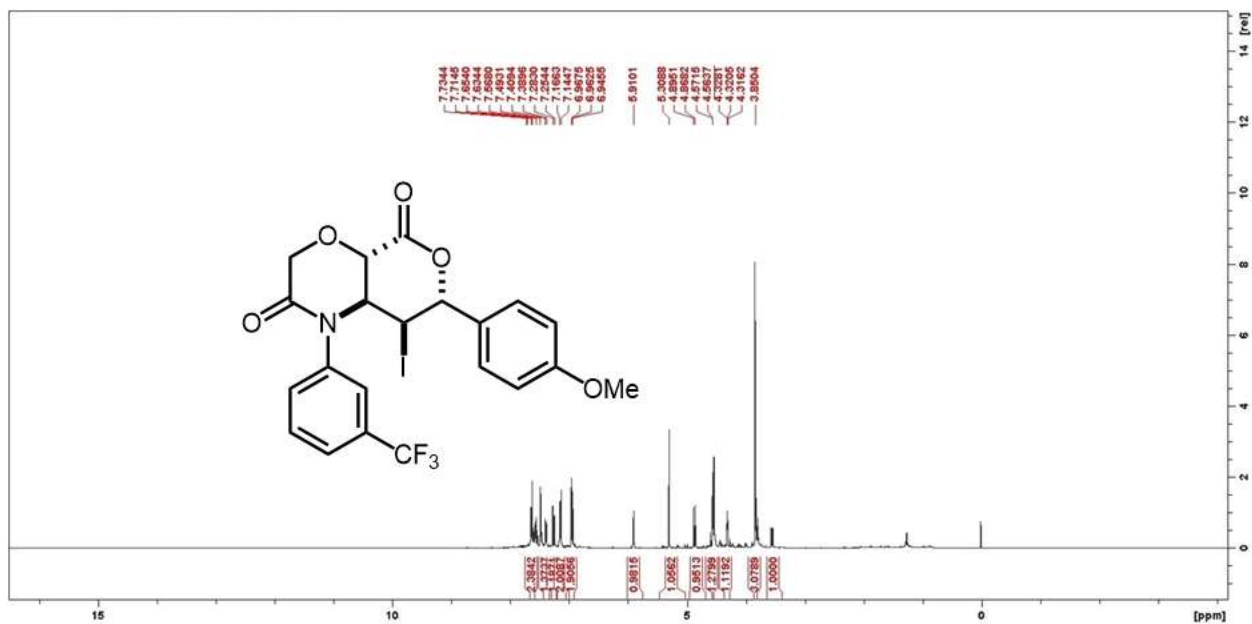
Spectra 3-65. ^{1}H-NMR spectrum for structure **9v**
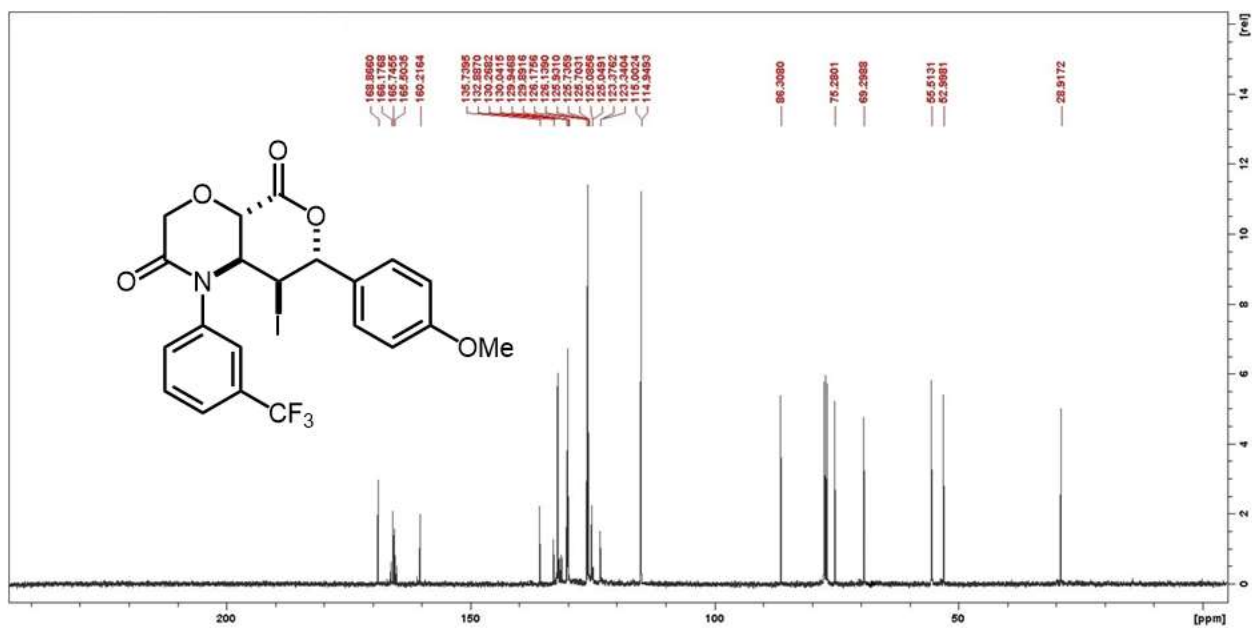
Spectra 3-66. ^{13}C-NMR spectrum of structure **9v**
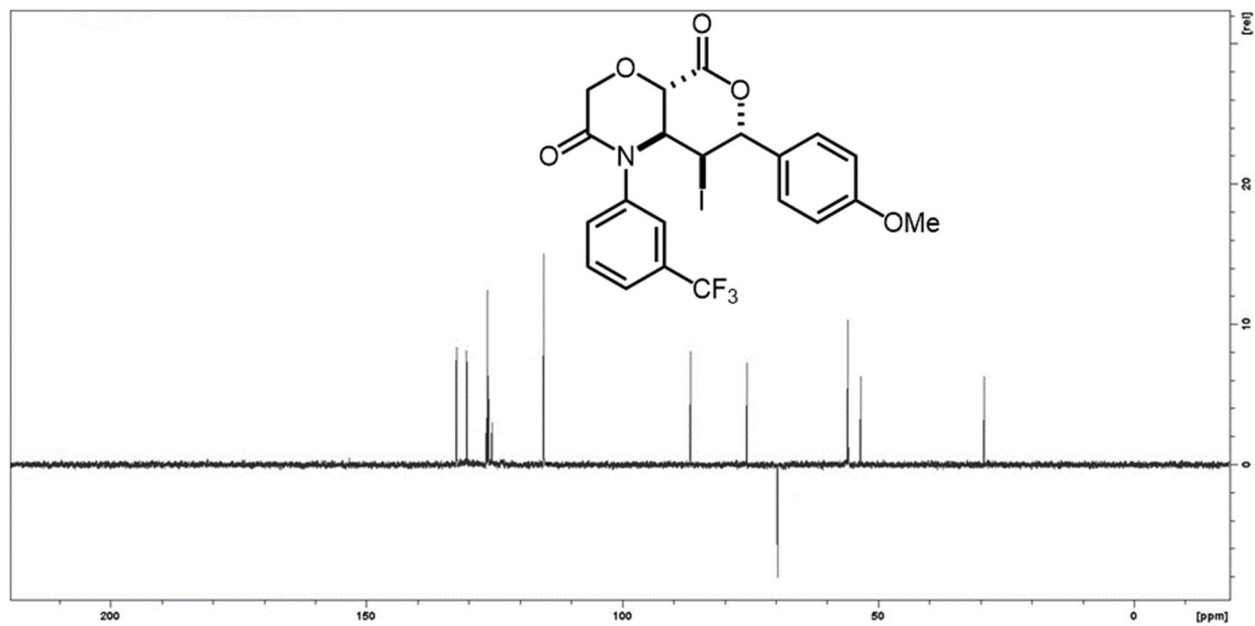
Spectra 3-67. DEPT-NMR spectrum of structure **9v**
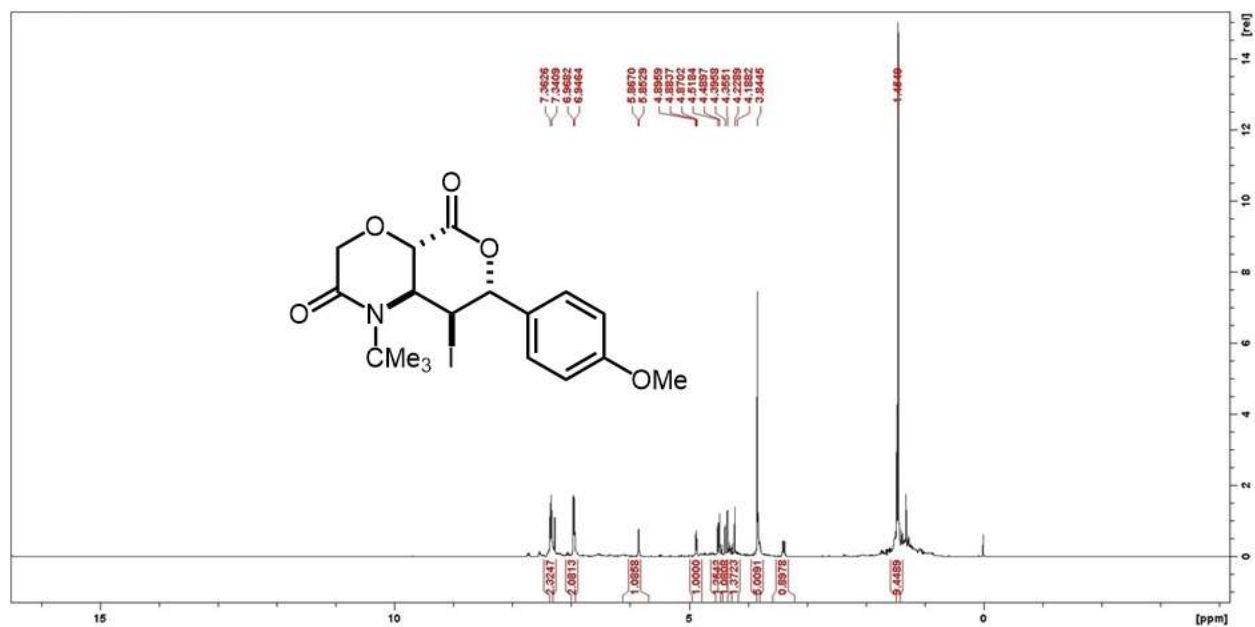
Spectra 3-68. ^{1}H-NMR spectrum for structure **9w**
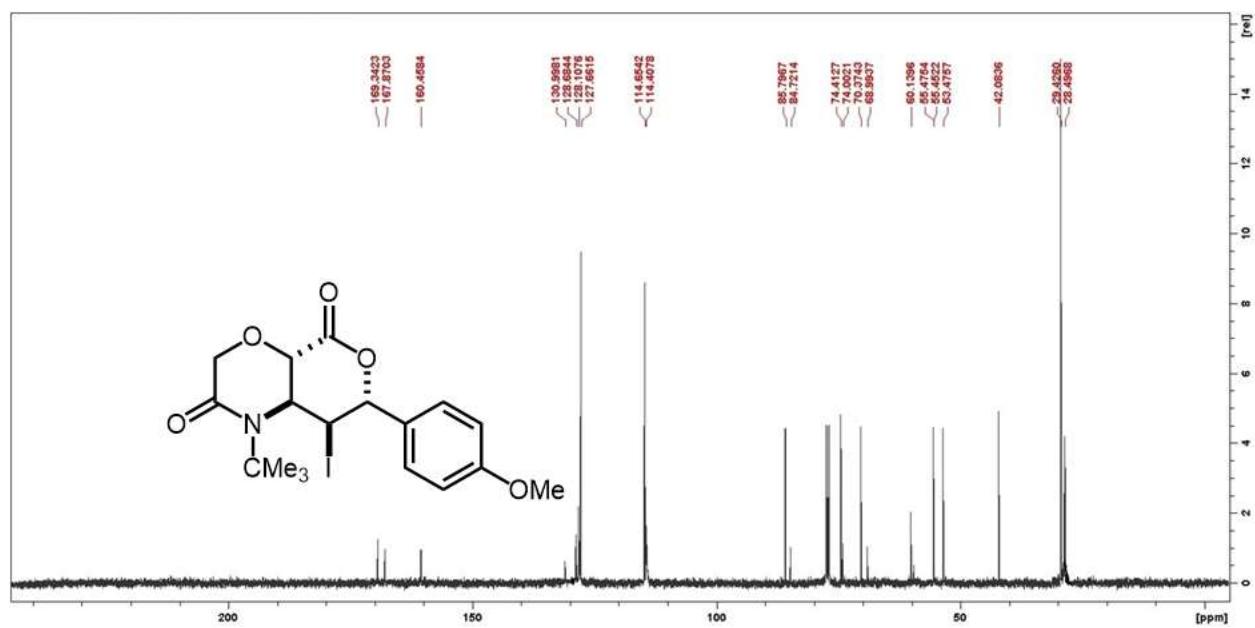
Spectra 3-69. ^{13}C-NMR spectrum of structure **9w**
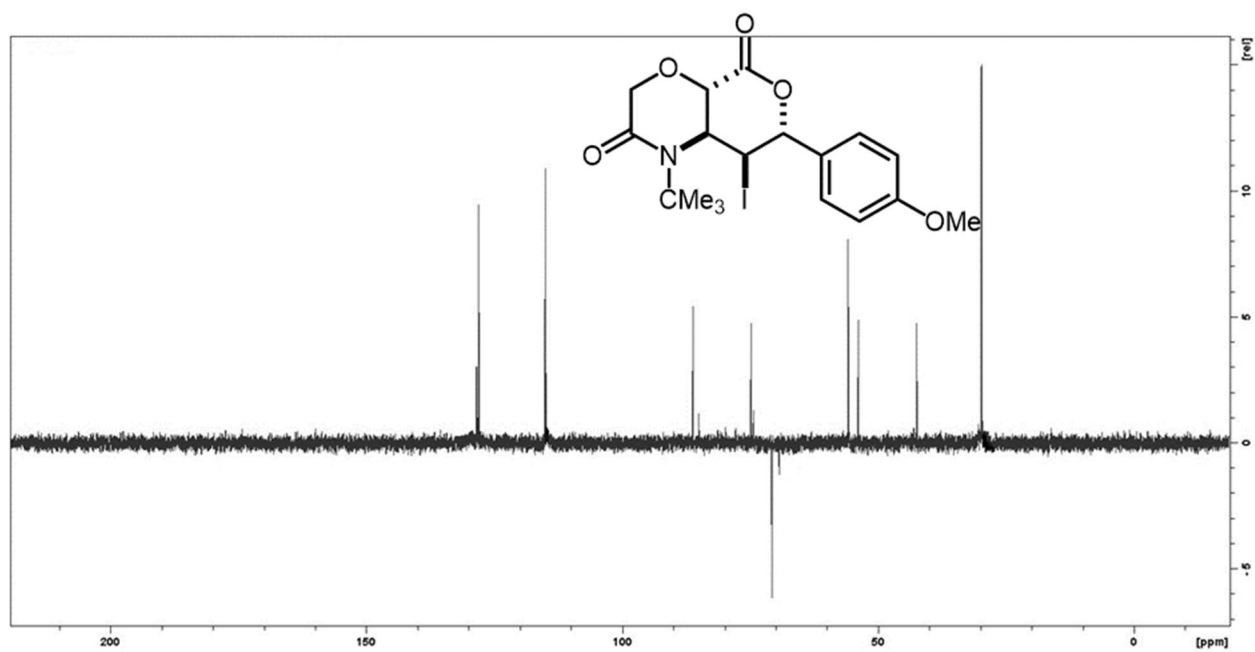
Spectra 3-70. DEPT-NMR spectrum of structure **9w**

103
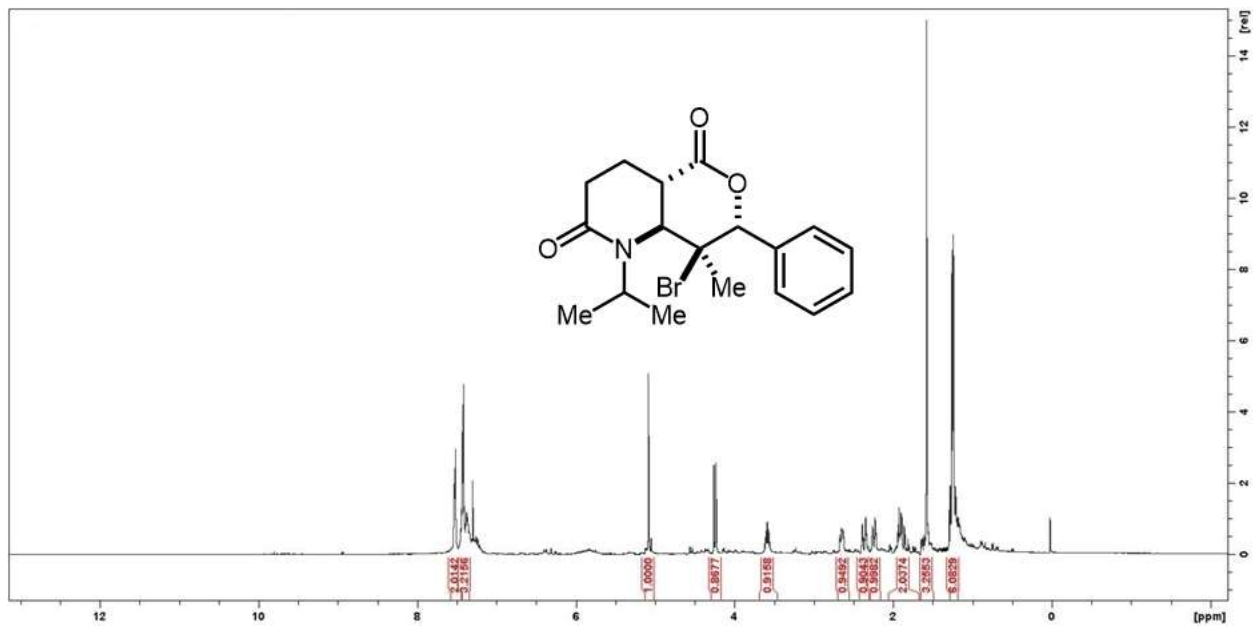
Spectra 3-71. [^1]H-NMR spectrum for structure **17a**
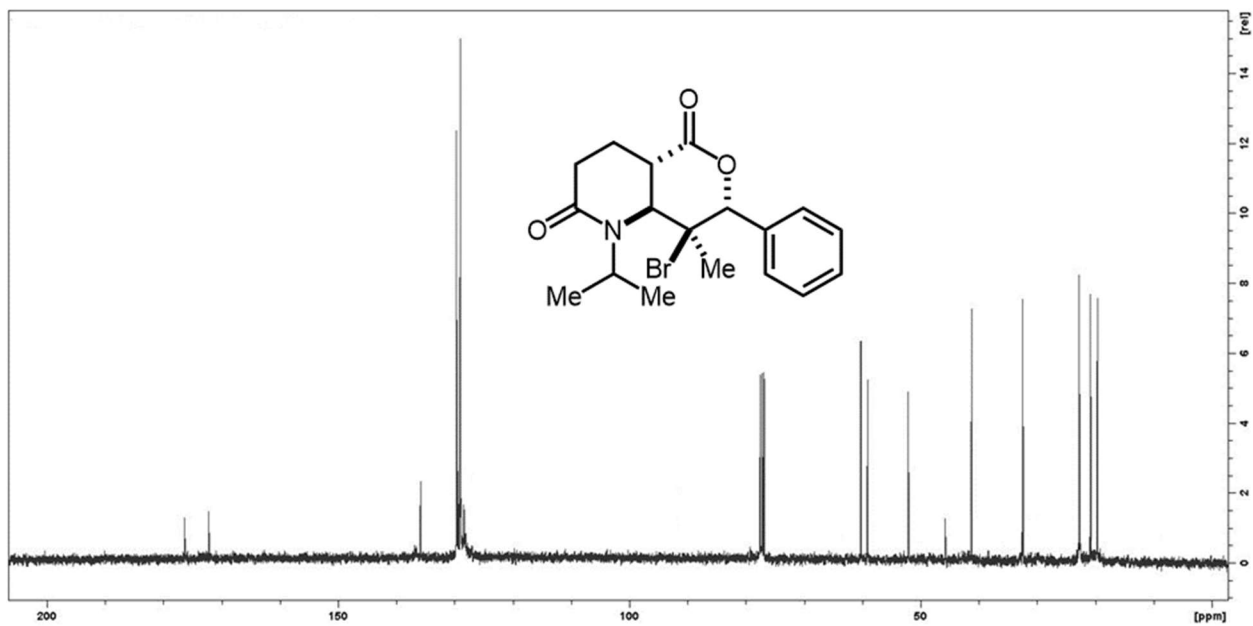
Spectra 3-72. [^13]C-NMR spectrum of structure **17a**
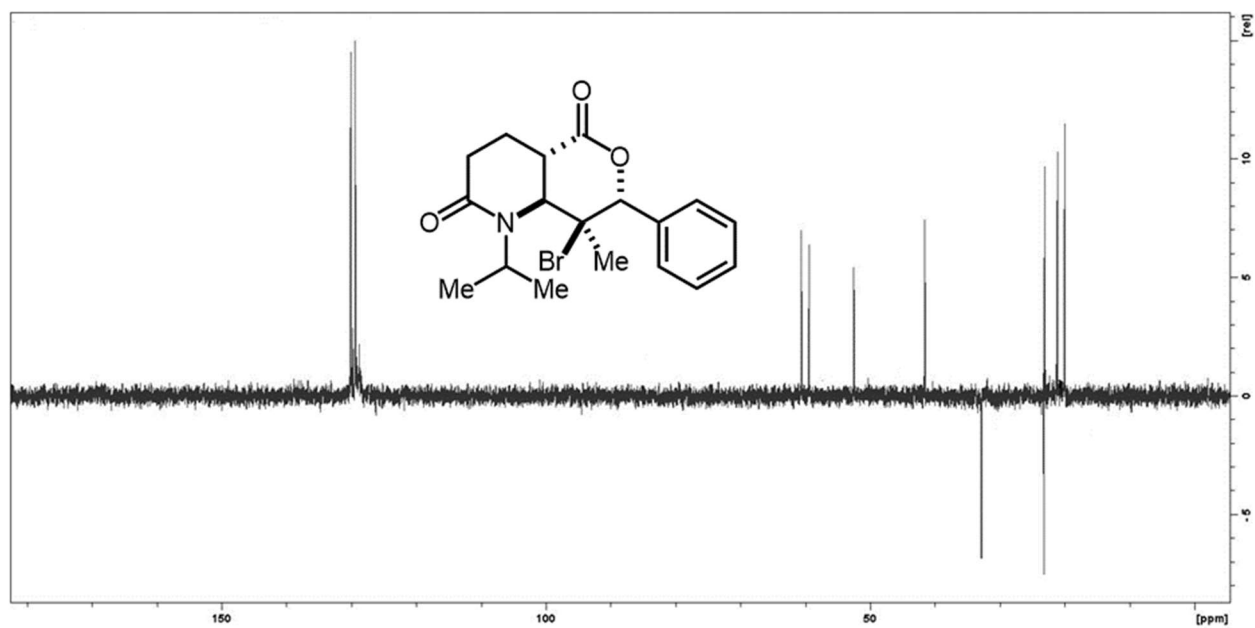
Spectra 3-73. DEPT-NMR spectrum of structure **17a**
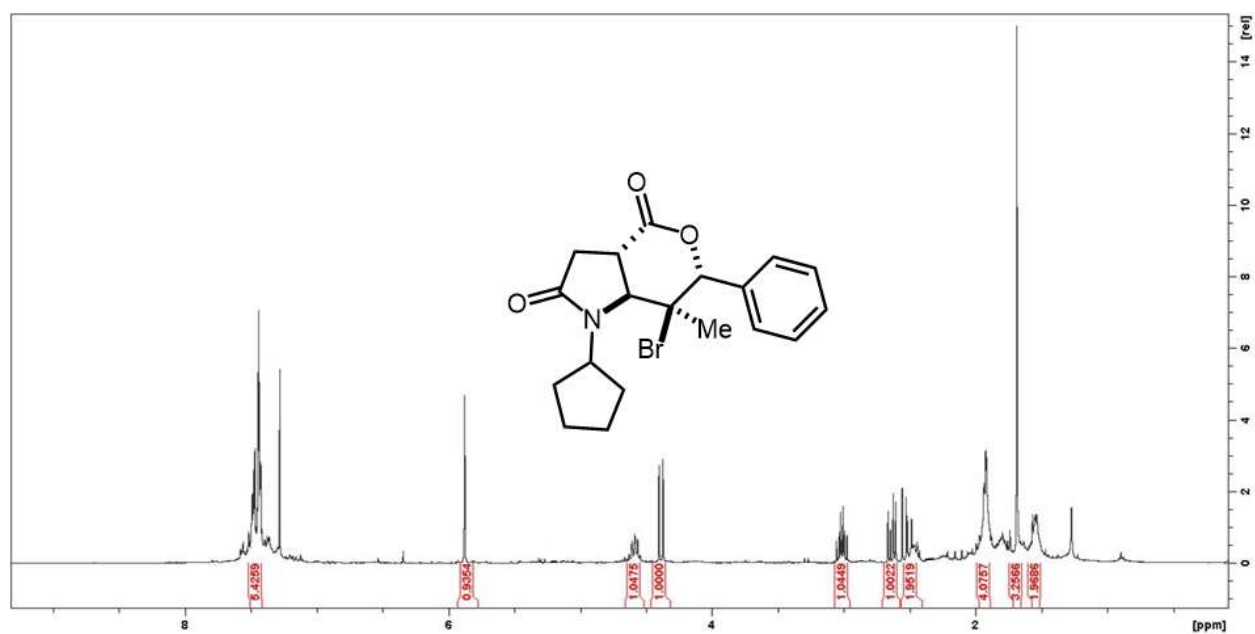
Spectra 3-74. ^{1}H-NMR spectrum for structure **17b**
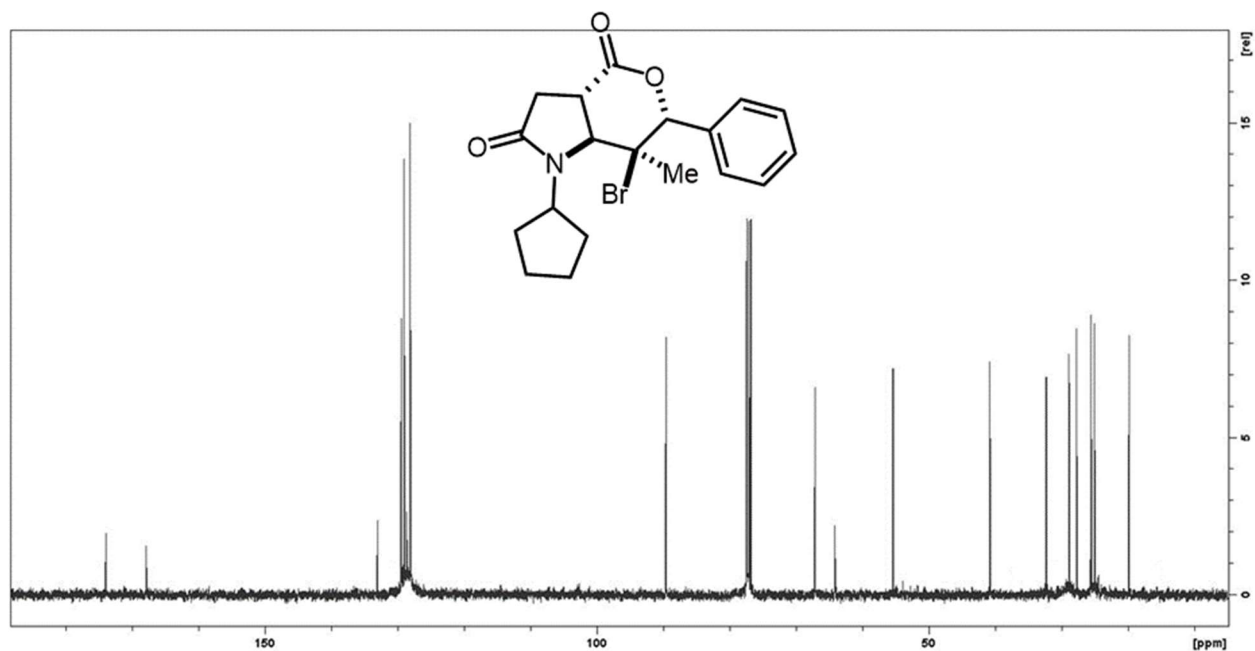
Spectra 3-75. ^{13}C-NMR spectrum of structure **17b**
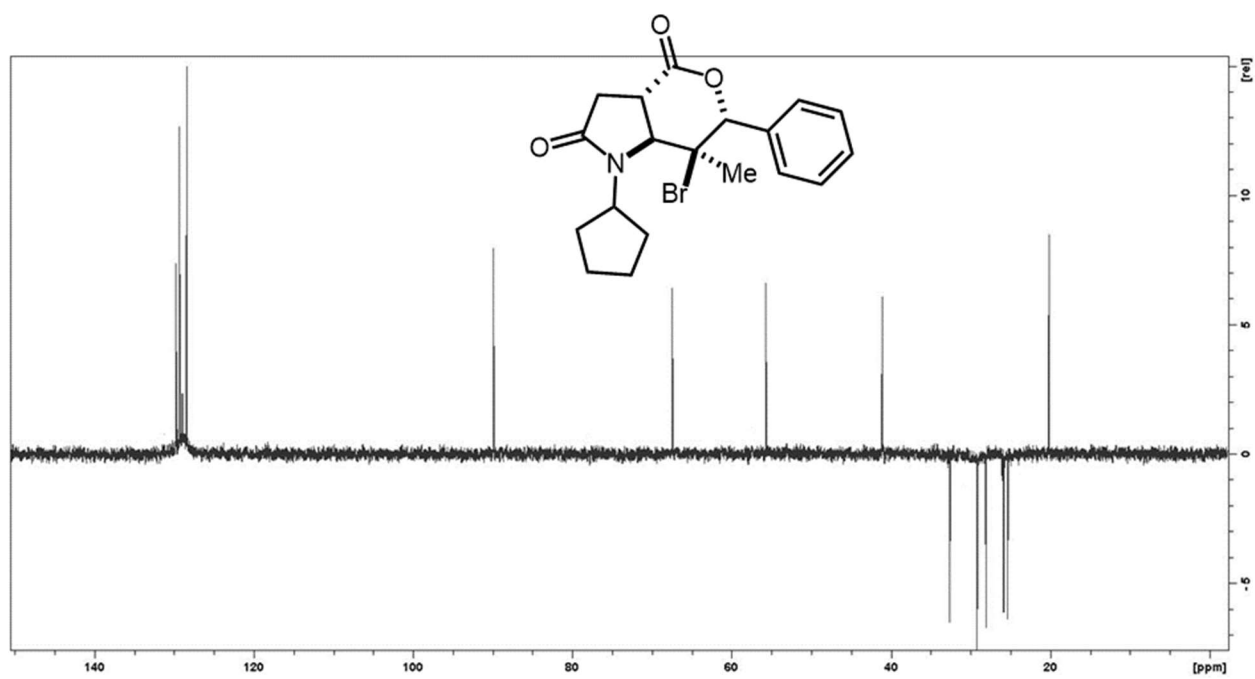
Spectra 3-76. DEPT-NMR spectrum of structure **17b**

106
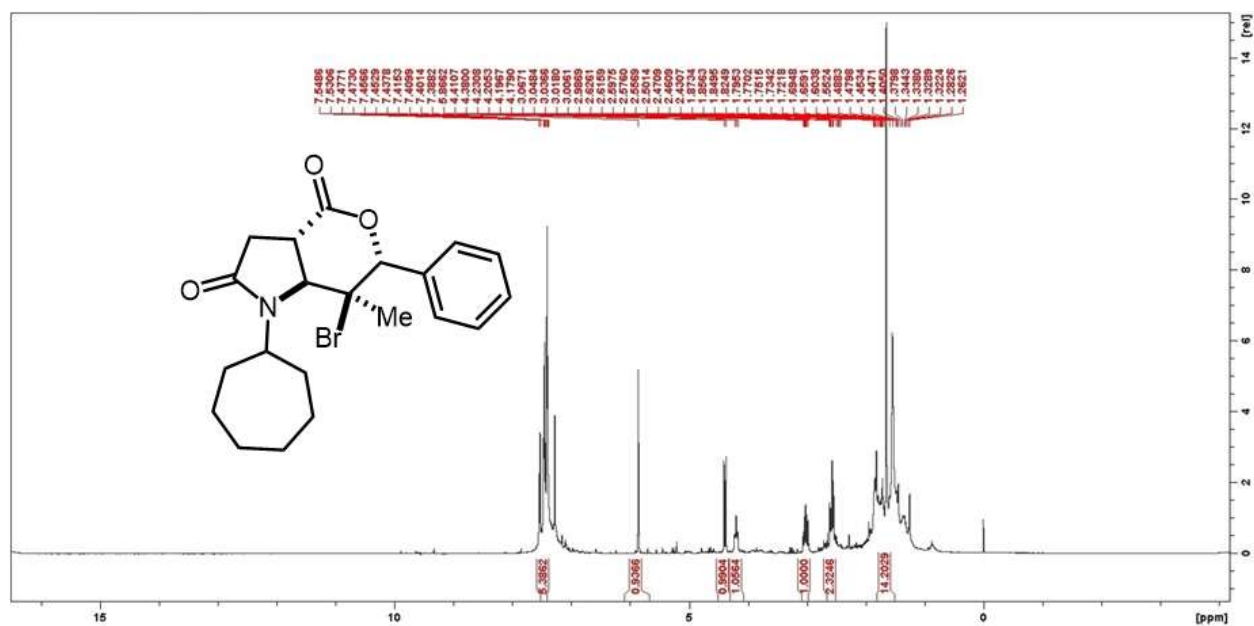
Spectra 3-77. ^{1}H-NMR spectrum for structure **17c**
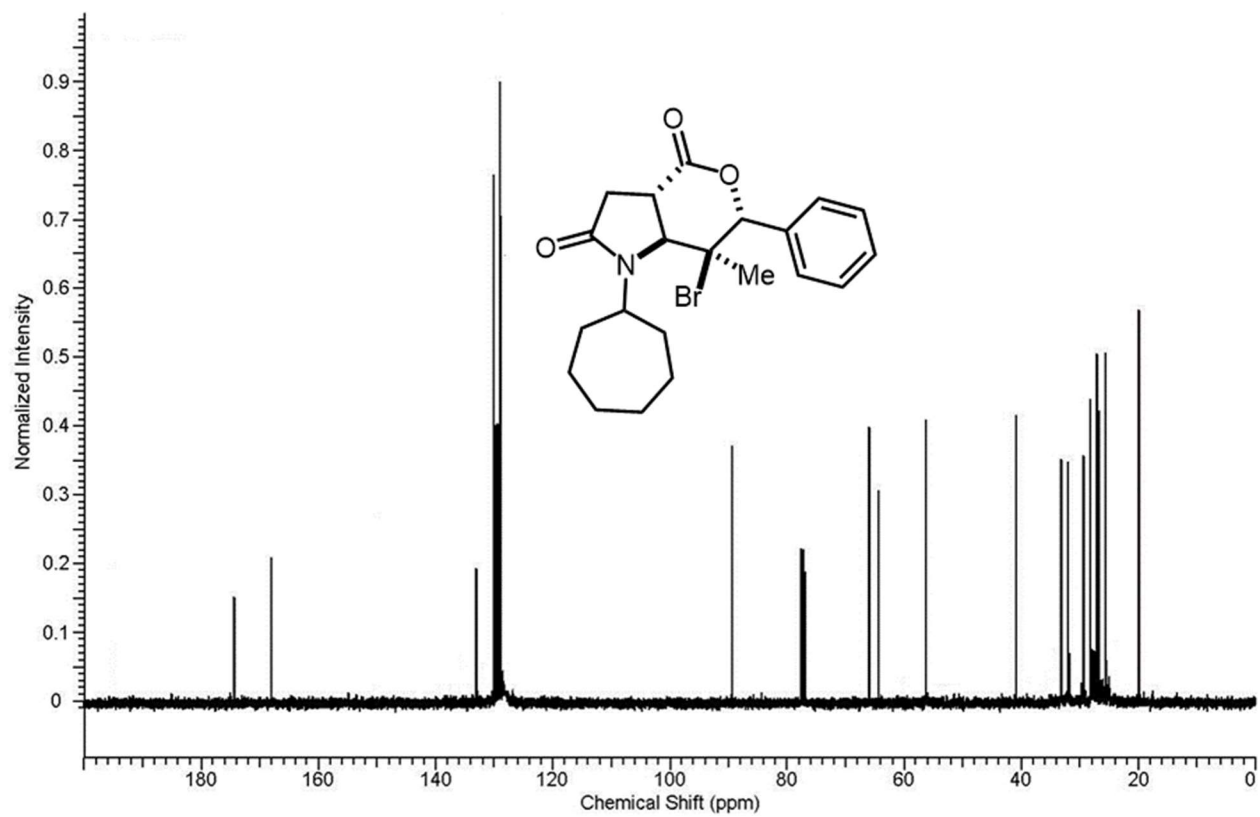
Spectra 3-78. ^{13}C-NMR spectrum of structure **17c**
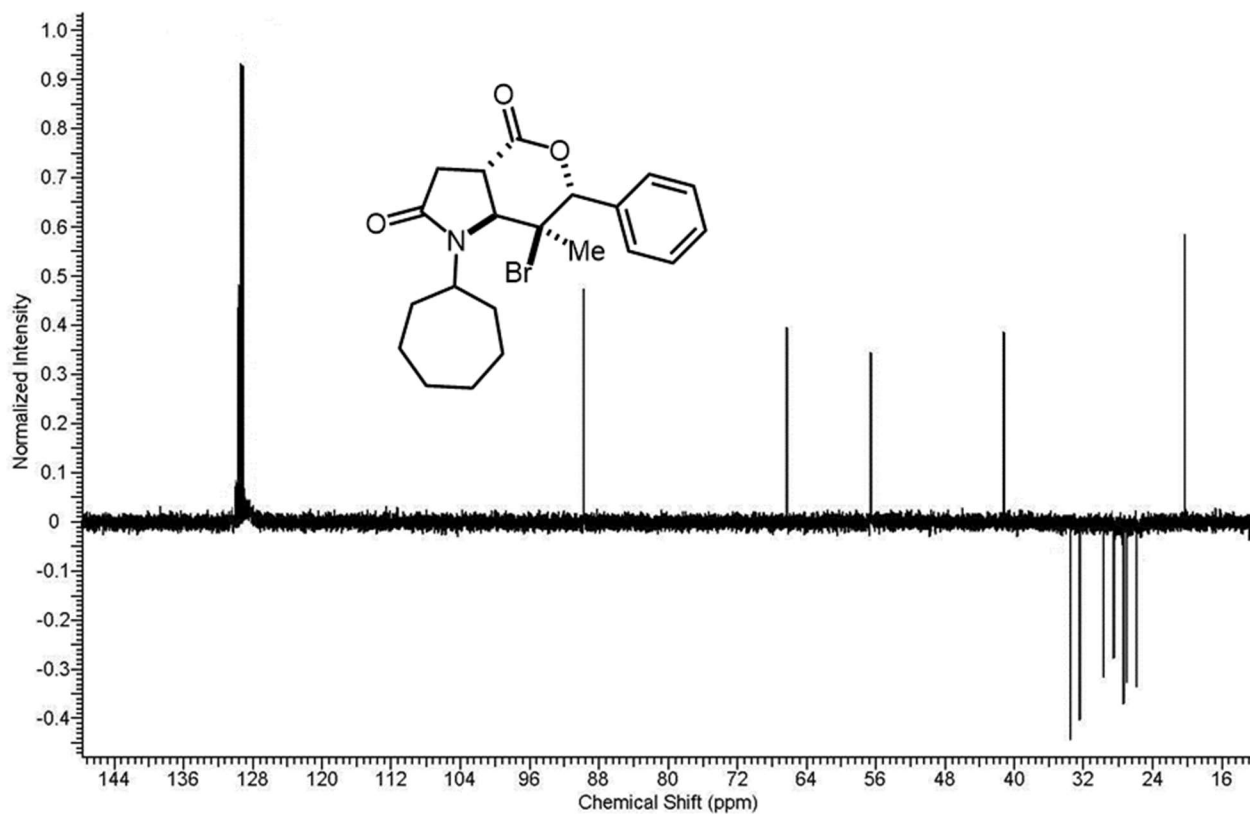
Spectra 3-79. DEPT-NMR spectrum of structure **17c**
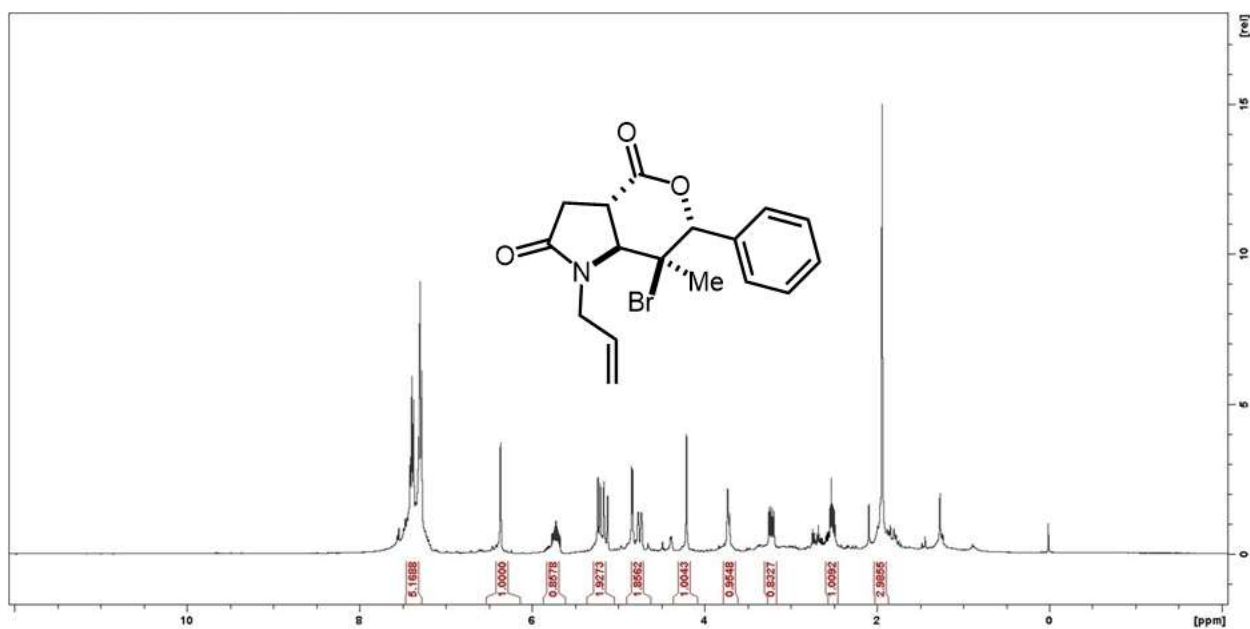
Spectra 3-80. ^{1}H-NMR spectrum for structure **17d**

108
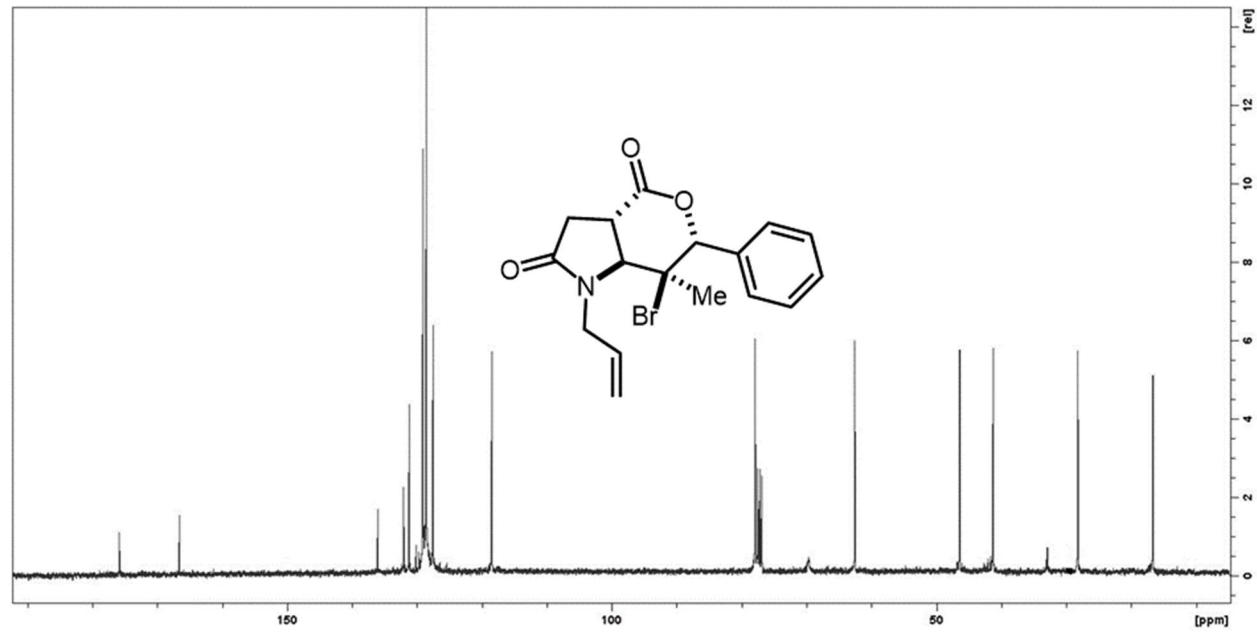
Spectra 3-81. ^{13}C-NMR spectrum of structure **17d**
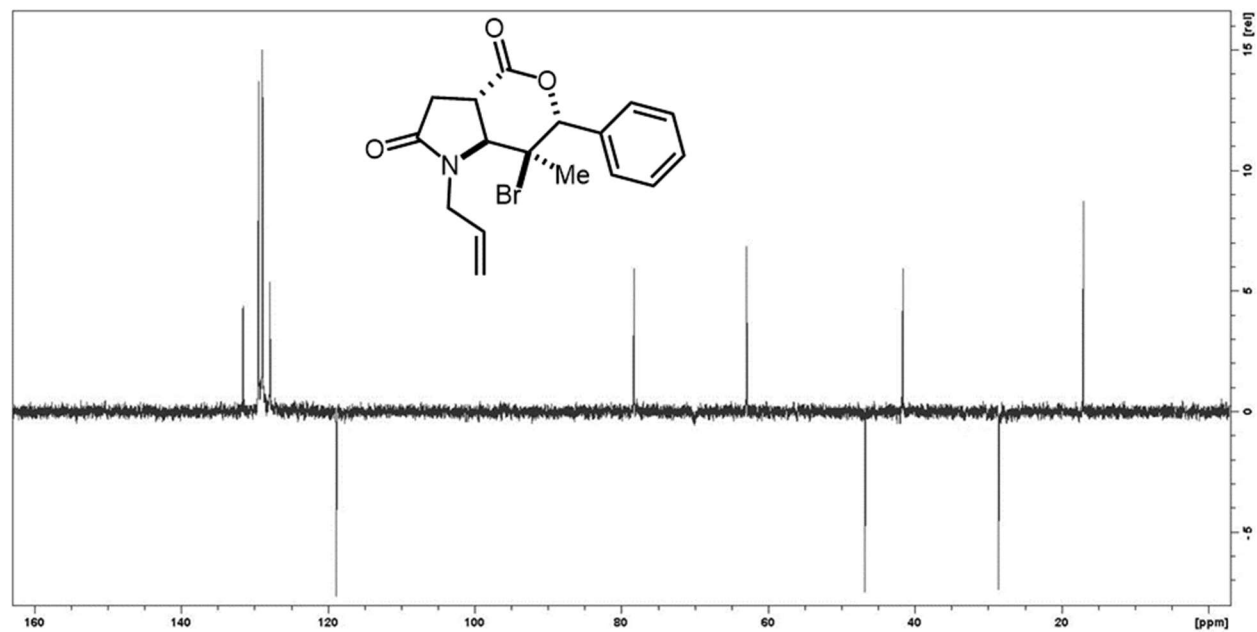
Spectra 3-82. DEPT-NMR spectrum of structure **17d**

Spectra 3-83. ^{1}H-NMR spectrum for structure **80e**

Spectra 3-83. ^{13}C-NMR spectrum of structure **17e**
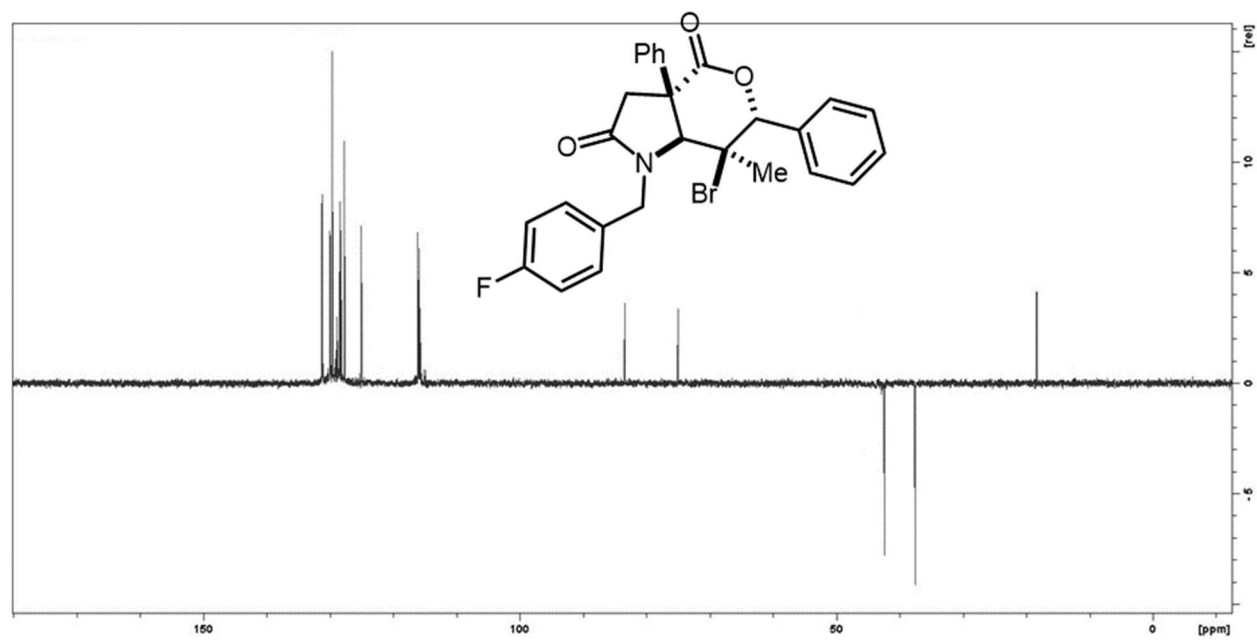
Spectra 3-84. DEPT-NMR spectrum of structure **17e**

3.4 Applications
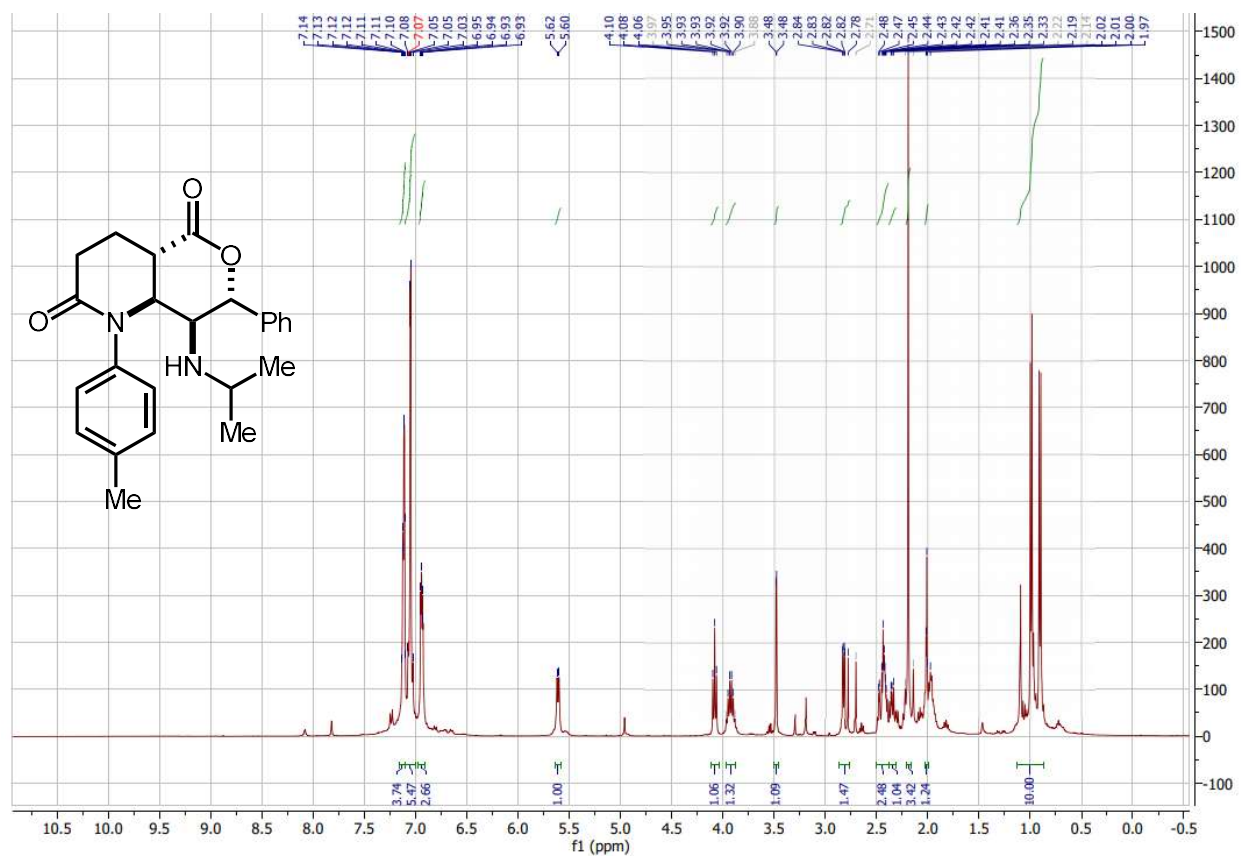
Spectra 3-85. ^{1}H-NMR spectra for **18a**
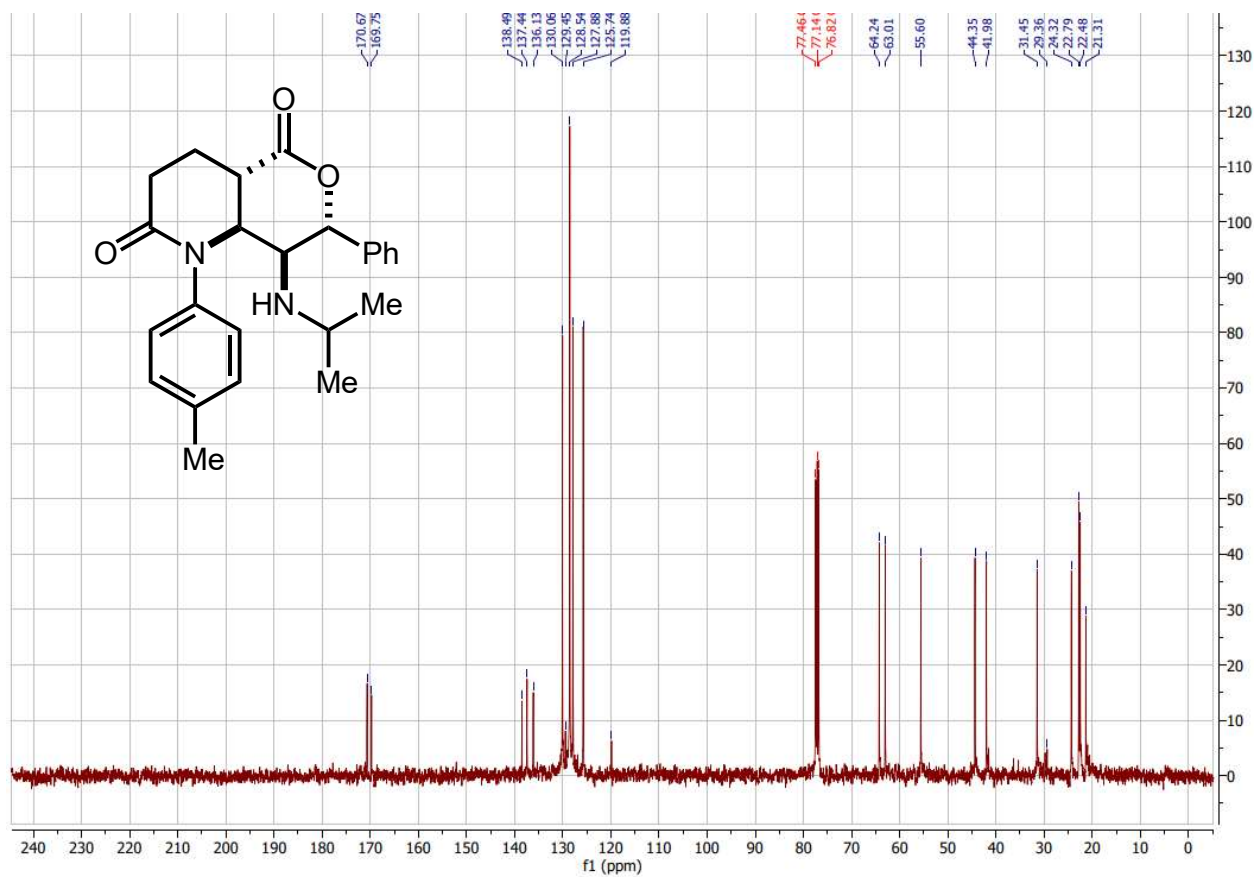
Spectra 3-86. ^{13}C-NMR spectra for **18a**
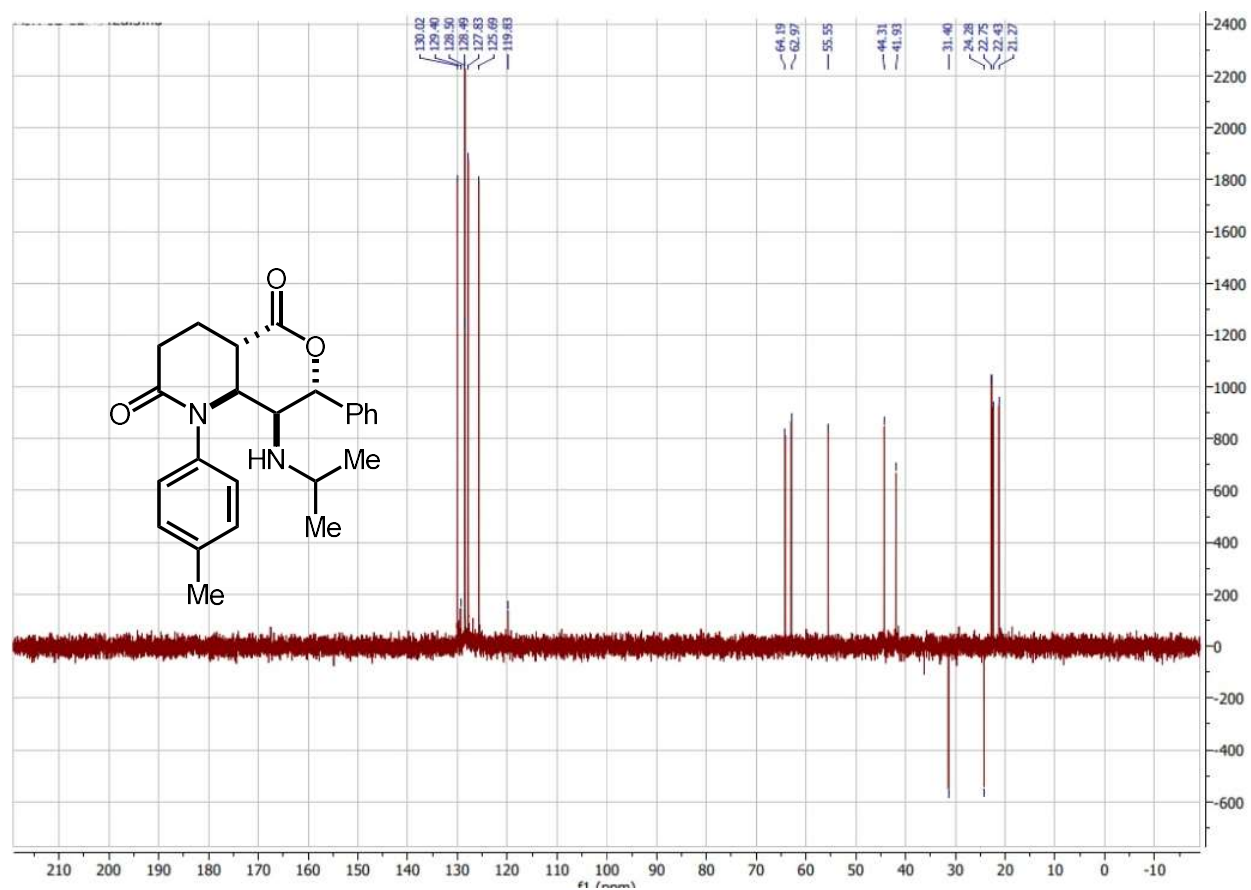
Spectra 3-87. DEPT-135 Spectra for **18a**
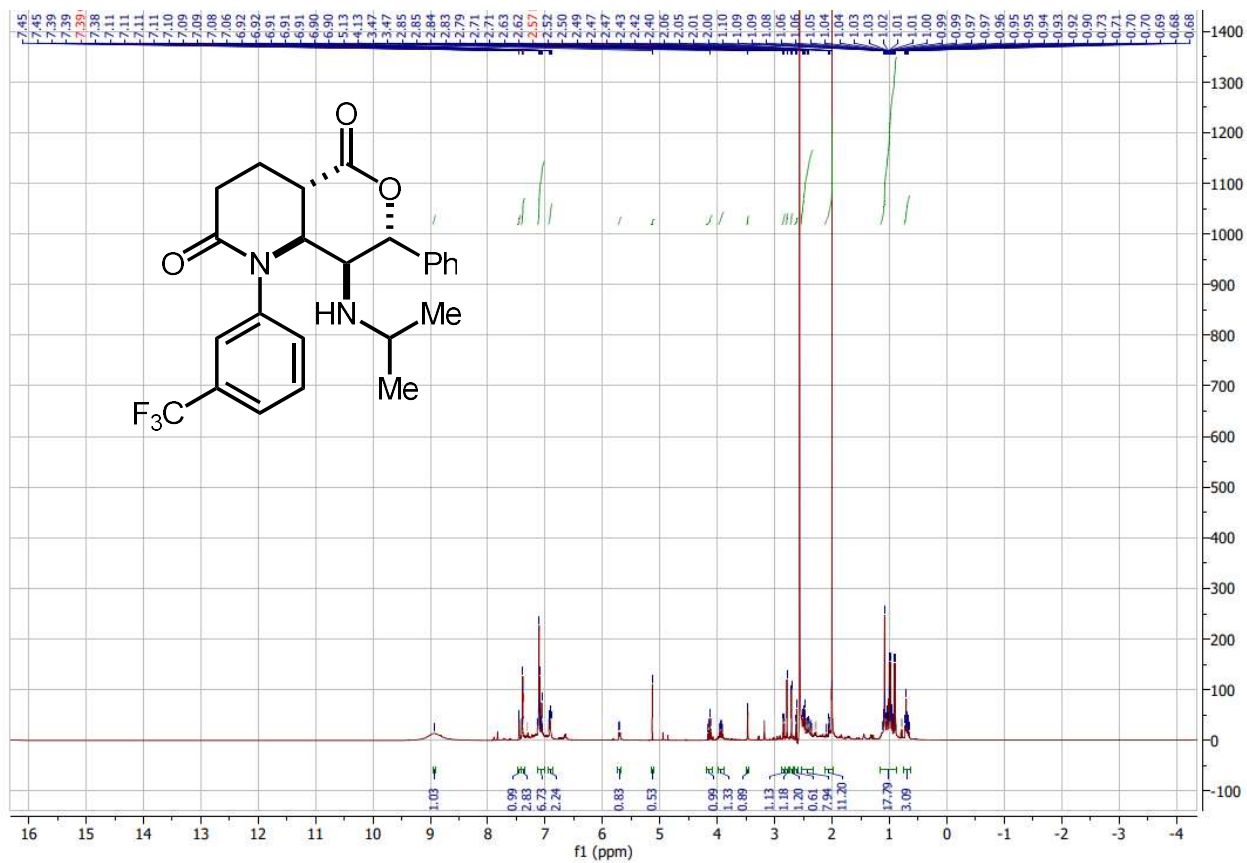
Spectra 3-88. ¹H-NMR spectra of **18b**
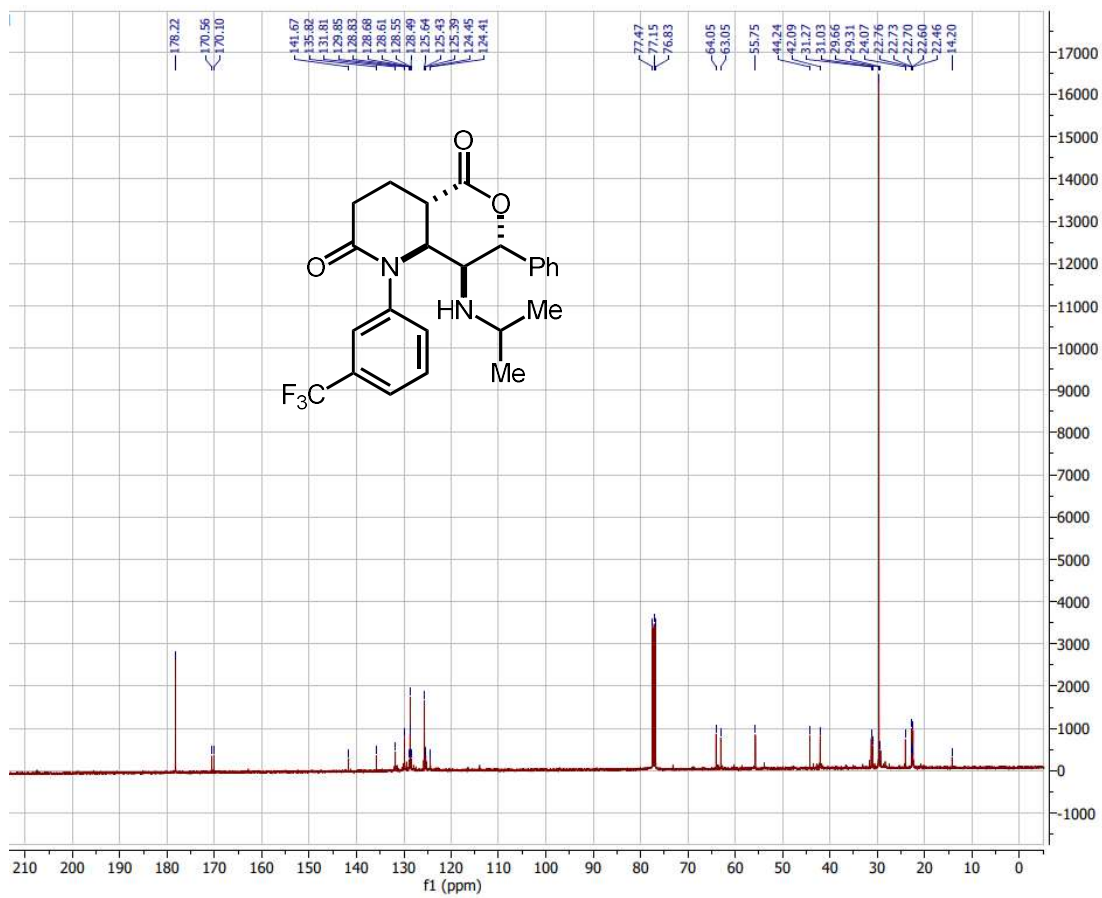
Spectra 3-89. ^{13}C-NMR Spectra of **18b**
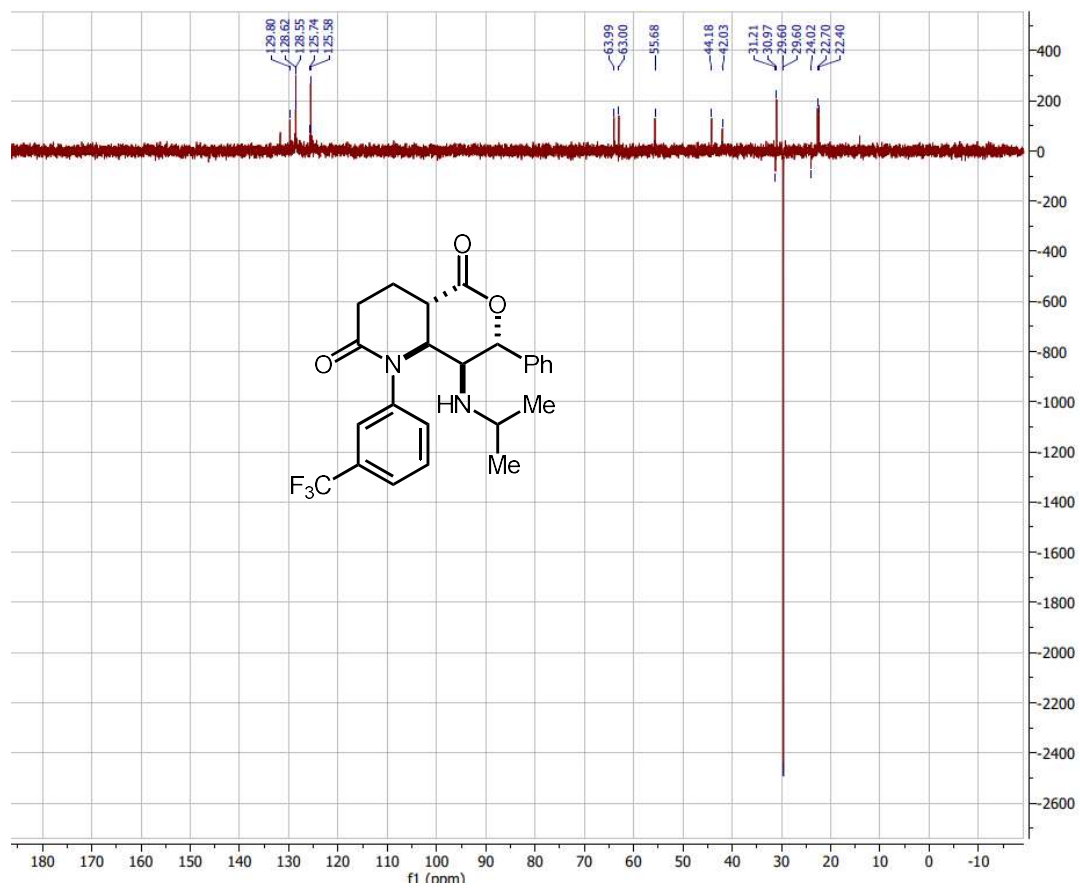
Spectra 3-90. DEPT-135 Spectra of **18b**
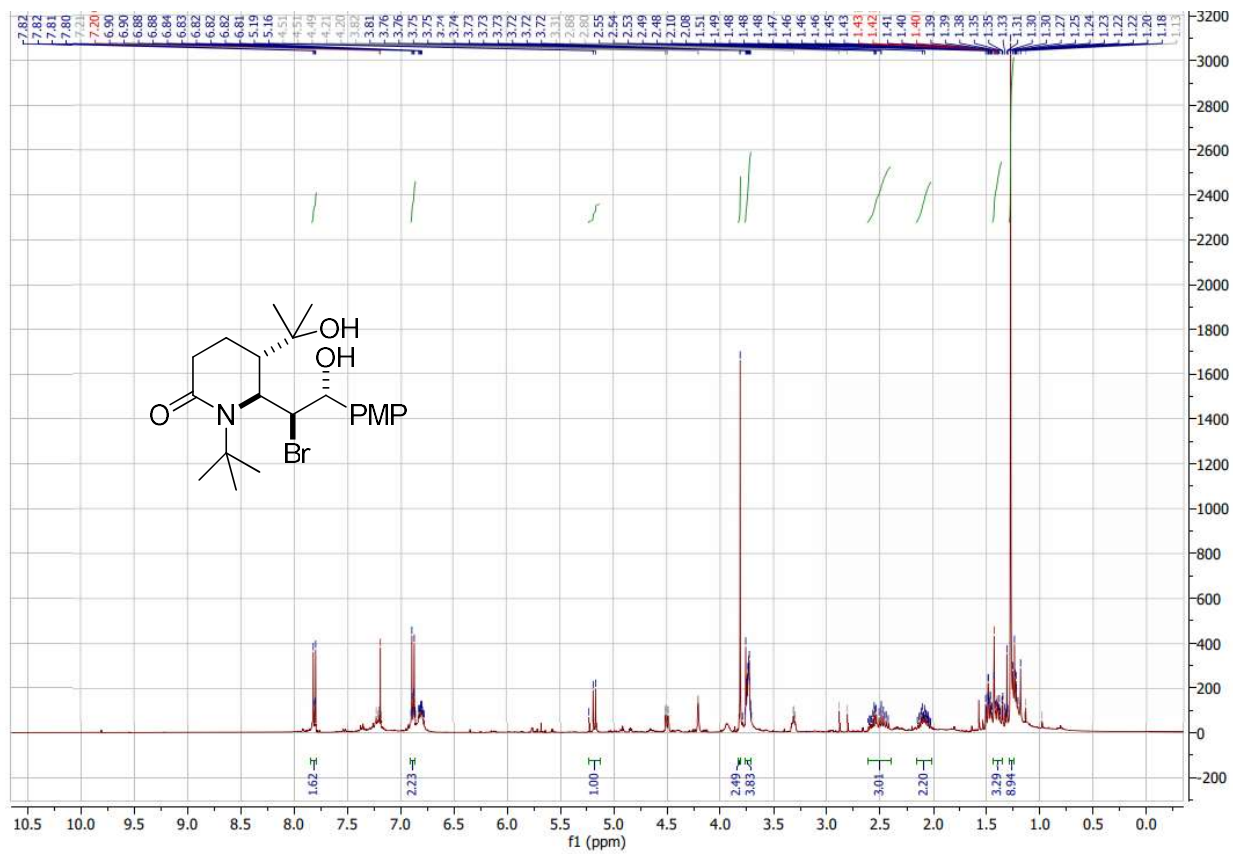
Spectra 3-91. ^{1}H-NMR spectra of **20b**
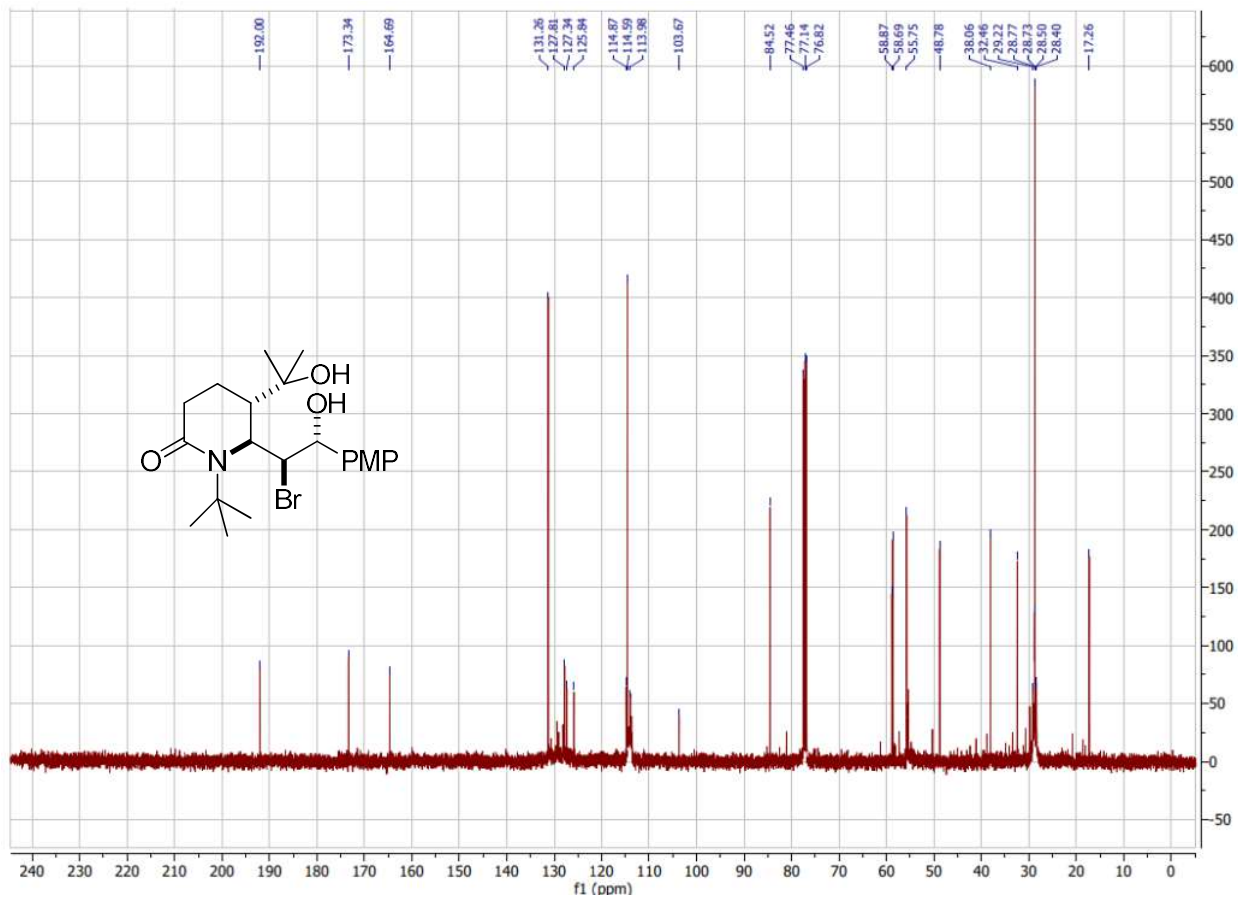
Spectra 3-92. ^{13}C-NMR spectra of **20**
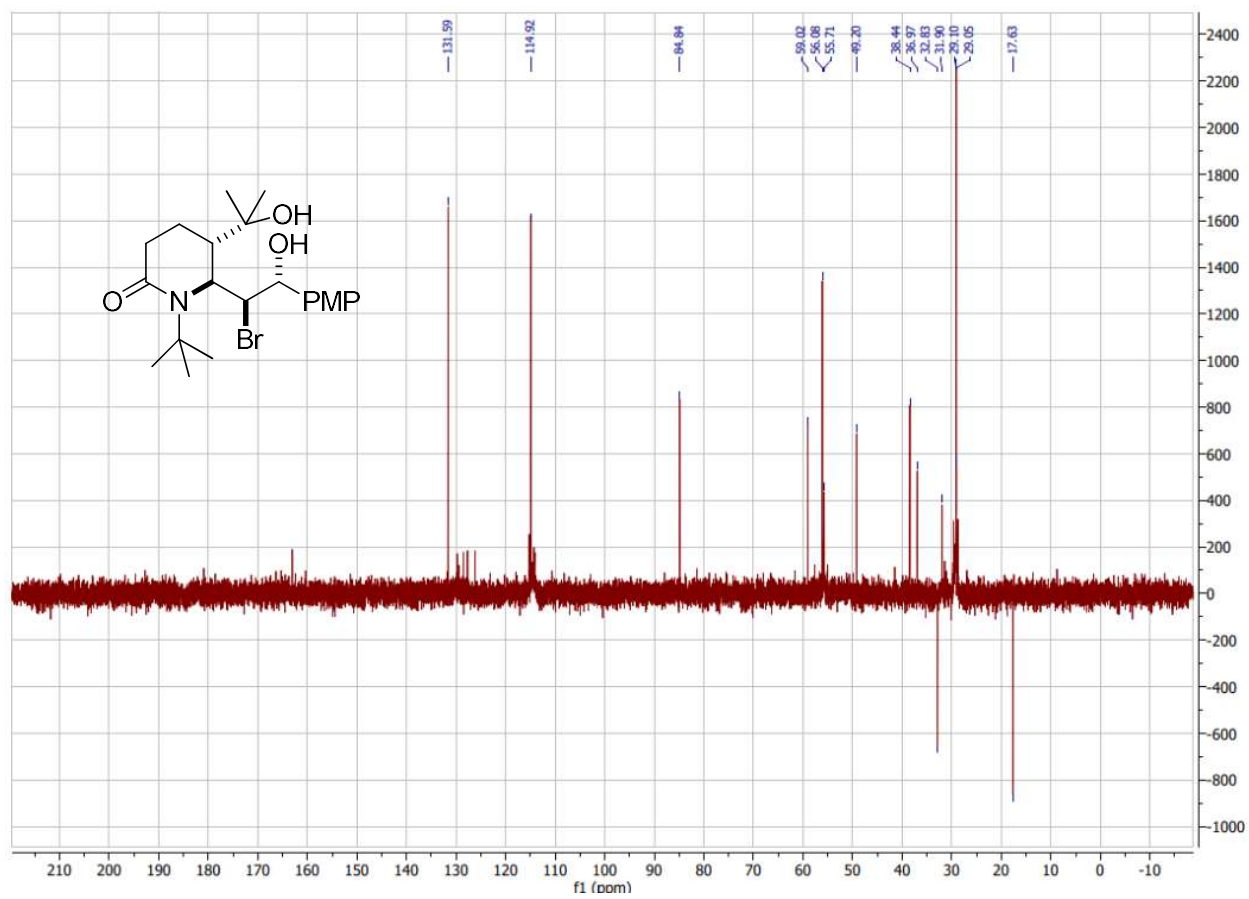
Spectra 3-93. DEPT-135 spectra of **20**